THE OPTICAL IDENTIFICATION AND SPECTRAL ANALYSIS

OF CELESTIAL X-RAY SOURCES

by

Ronald Alan Remillard

A.B. University of California, Berkeley (1974)

A.B. University of California, Berkeley (1976)

S.M. Massachusetts Institute of Technology (1981)

Submitted to the Department of Earth, Atmospheric,
and Planetary Sciences in Partial Fulfillment of the
Requirements of the
Degree of

DOCTORATE IN PHILOSOPHY

at the

MASSACHUSETTS INSTITUTE OF TECHNOLOGY

June, 1985

© Massachusetts Institute of Technology 1985

Signature of Author_____

Certified by_____
Thesis Supervisor

Accepted by_____
Chairman, Departmental Committee

ABSTRACT

A program of optical astronomical observations has been undertaken to identify the faint X-ray sources that were detected in an all-sky survey by the instruments on the HEAO-1 satellite. The optical identifications are necessary if scientific analysis is to proceed from these detections. However, this task had been inhibited by the lack of precise positions from the X-ray instruments. The positions are constrained by the detections of the HEAO-1 Scanning Modulation Collimator, coupled with results from other X-ray experiments. The Modulation Collimator has an unusual beam pattern that creates a multiplicity of relatively precise, allowed positions, one of which contains the position of the X-ray source, to a specified degree of confidence.

The systematic steps in the investigation included a wide-field photographic search for uncataloged ultraviolet objects that are located within the allowed X-ray positions. Catalogs that contain known classes of X-ray emitters were also searched, and bright stars and galaxies were included as candidates. Optical spectra were obtained for all of the optical candidates, and the spectral classifications have led to many X-ray source identifications.

The essential observations were completed for 108 sources, and candidate optical counterparts are suggested in 46 cases. Twenty-six of these are judged to be "very probable" identifications of the X-ray sources. In these cases the object's classification and optical characteristics support the identification, and its position is consistent with the X-ray results of both Modulation Collimator detectors. Another eleven candidates are judged to be "probable" identifications, in which the optical evidence supports the candidate, but the positional constraints from the X-ray detections are not as restrictive. The remaining 9 cases require additional observations, either to confirm tentative classifications, or to obtain additional optical evidence of the X-ray emission.

Among the 37 proposed optical identifications (cases judged as probable or very probable) there are eighteen Seyfert Type 1 galaxies and QSO's, two BL Lac type objects, two clusters of galaxies, an active elliptical galaxy, six Cataclysmic Variables, two Be stars, and six RS CVn type binaries. Twenty-four of these were previously unknown objects. The optical spectra of twenty are examined in detail.

It is found that the new Seyfert galaxies contain six examples that are very strong emitters of FeII lines. Some of them resemble I Zw 1, an unusual Seyfert galaxy known for its strong infrared emission and very high bolometric luminosity. These newly discovered FeII-emitters almost doubles the number of known objects of this type, which is not understood. Other Seyfert galaxies have unusual X-ray properties. One shows evidence of X-ray variability, while another exhibits a very "flat" X-ray spectrum. The flux measures of selected optical emission lines are given for all of the low-redshift Seyfert and QSO types.

Two of the QSO's are high-redshift objects, and they appear to be among the most luminous X-ray emitters known. In addition both have absorption lines in their optical spectra, and the absorption lines are at a different redshift than the emission lines. One is a bright example of a "Broad Absorption Line" quasar, a rare type (5%) of QSO's. The other is probably observed through the gas of an intervening galaxy, and this case has cosmological implications regarding the true distances and luminosities of QSO's.

The two BL Lac objects resemble several others that have been identified as HEAO-1 sources. Since these objects are difficult to identify and since the class is poorly understood, the identifications are an imporant addition to the sample of bright X-ray emitting examples.

Four newly discovered cataclysmic variables are examined. All are relatively bright, and they show strong emission due to HeII. One of them has been confirmed as a magnetic (AM Her type) cataclysmic variable, showing circular polarization that rises to 10% of the optical flux. A tentative orbital period of 2.95 hours was obtained for this object.

The faint detections of the X-ray survey draw attention to some of the brightest available examples of many classes of objects that radiate at high energies. The individual studies begun in this research project are one aspect of the effort to gain a detailed understanding of each class. For many of these classes, the fundamental perceptions of the physical nature of the objects is lacking or is incomplete.

ACKNOWLEDGEMENTS

I am very grateful to the Dept. of Earth, Atmospheric, and Planetary Sciences for the academic support of this research in optical astronomy. I have certainly benefited from the experience of working with Dr. David Jewitt and from the acquisition of my cometary sub-personality. I also appreciate the encouragement I have received from Prof. Jim Elliot.

My interests in optical astronomy and in X-ray sources have been greatly influence by the instruction and example of Dr. Jeff McClintock and Prof. Claude Canizares of the M.I.T. Center for Space Research. I look back on my early training days with some reverence.

This thesis research was accomplished by using many "systems" that worked well because of the sweat and skill of others. I would be morally deficient if I did not clearly express my indebtedness to those persons.

The Modulation Collimator was a proven success long before I became associated with the group. The principal investigators, Prof. Hale Bradt of the M.I.T. Physics Dept. and Dr. Daniel Schwartz of the Harvard-Smithsonian Center for Astrophysics (and Dr. Herbert Gursky before him) have engineered a very exciting and productive probe of the high-energy phenomena of the Universe. I have thoroughly enjoyed working with them, and I hope to continue the research in progress. To the other scientists and architects of the MC experiment, especially Drs. Rodger Doxsey and Mark Johnston and Mr. Mike Garcia, I also extend my gratitude; I could not have continued the project for the fainter X-ray sources without the analysis system that they perfected.

The current cast of MC workers and collaborators, particularly Ms. Wendy Roberts, Dr. Ian Tuohy, Mr. David Buckley, and Dr. Santiago Tapia

TABLE OF CONTENTS

V. Results of the Optical Investigations

VI. Fourteen Broad-Line Active Galactic Nuclei

VII. Two X-ray Emitting BL Lac Objects

9
List of Figures

List of Tables

I. INTRODUCTION

1-1. <u>Development of X-ray Astronomy</u>

Astronomy has rapidly become a science in which observations are made throughout a broad range of the electromagnetic spectrum in an effort to acquire a detailed physical understanding of the astronomical objects. This perspective is the natural consequence of tremendous scientific gains that have resulted from observations at wavelengths far removed from the optical spectrum. As instrumentation technology enters into a "new" spectral regime, new classes of objects are discovered, theoretical models and calculations are advanced and tested, and a variety of new information is obtained that may help to resolve old problems.

During the latter half of this century researchers have conducted the first celestial surveys in several non-optical spectral regions. These have yielded extensive catalogs of sources previously unknown to astronomy. For example, at radio wavelengths the Parkes (Wall <u>et al.</u> 1971) and Cambridge (Bennett 1962; Pilkington and Scott 1965) surveys have brought forth discoveries of QSO's and radio galaxies that have greatly influenced extragalactic science. In addition, radio mapping techniques have imaged a wide range of emission phenomena, from the relativistic beams of hot gases in magnetic fields (see Bridle and Perley 1984) to the cold clouds that extend throughout the Galaxy and in others as well (see Kerr 1969; Zuckerman and Palmer 1974). In the far ultraviolet region, celestial surveys have not been conducted yet, but spectroscopic studies of previously known sources by the International Ultraviolet Explorer have provided new measures from which the

temperatures, densities, and abundances of hot stars and many classes of X-ray sources can be inferred. Furthermore, spectral observations in the UV region are necessary if the physical models of a source's energy balance and ionization structure are to be tested (e.g. Lamb and Masters 1980). In the γ-ray and infrared regions, the first comprehensive surveys are only recently completed (γ-rays: Swanenburg et al. 1981; IR: Kleinmann et al. 1981; Neugebauer et al. 1984), and there are new cosmic mysteries to ponder, such as γ-ray burst sources (Klebesadel, Strong, and Olson 1973) and the infrared "ultrahigh luminosity galaxies" (e.g. Houck et al. 1985). These simplified examples only serve to illustrate the extent of the observational developments during the few decades that represent a Renaissance period in astronomical science.

X-ray astronomy is another recent "photometric" breakthrough. Cosmic X-ray research began in the early 1960's when an X-ray detection from a sounding rocket challenged a prevailing expectation: only the sun could be detected at X-ray wavelengths (photon energies $\gtrsim 1$ keV). This rocket flight (Giacconi et al. 1962) discovered Sco X-1 and the diffuse X-ray background. Subsequent flights continued to bring discoveries of bright X-ray sources (e.g. Friedman et al. 1967; Bradt et al. 1968), and the first optical identification was gained when a lunar occultation showed that an extended X-ray source was centered on the Crab Nebula (Bowyer et al. 1964). Early X-ray observations were also conducted with balloon payloads (e.g. Clark et al. 1965), which extended the spectral coverage to energies as high as 50 keV and achieved observations of longer duration.

The second phase in X-ray observations consisted of satellite missions that surveyed the X-ray sky. These experiments established the

persistent nature of most X-ray sources as well as the dramatic variability of many transient sources. The X-ray positions led to the optical identification of many galactic sources (see Bradt and McClintock 1983) and extragalactic ones (Gursky and Schwartz 1977; Piccinotti et al. 1982). Uhuru, which was launched in 1970, performed the first deep X-ray survey at 2-10 keV; the final catalog (Forman et al. 1978) records 339 sources with a flux density limit of about 1.1 μJy (1 μJy = 10^{-29} erg cm^{-2} s^{-1} Hz^{-1}) at 5.2 keV, for a power-law X-ray spectrum with an energy index of -1.0 (i.e. similar to the X-ray spectrum of the Crab Nebula). A later British satellite, Ariel 5, was launched in 1974 and conducted a similar survey (McHardy et al. 1981; Warwick et al. 1981). Another satellite, SAS-3 (1975-79), employed a Rotating Modulation Collimator that determined precise ($\lesssim$60") positions for the brightest X-ray sources (Bradt, Doxsey, and Jernigan 1979). Its pointing capabilities began the next generation in X-ray astronomy, which emphasized more detailed spectral and temporal studies of individual sources. Finally, the HEAO-1 satellite (1977-79) provided the most complete flux-limited view of the X-ray sky. The HEAO-1 Large Area Sky Survey detected 842 sources with fluxes $>$ 0.22 μJy at 5.2 keV (Wood et al. 1984). Another HEAO-1 experiment, the Scanning Modulation Collimator, provided improved angular resolution that reduces the allowed celestial area of an X-ray source. The data base of the latter experiment and the need to optically identify about half of the HEAO-1 sources constitute the impetus for this thesis research.

Rapid progress in X-ray astronomy has continued in recent times. The Einstein Observatory (HEAO-2; 1978-81) introduced focusing mirrors (at grazing incidence) that achieved spatial resolutions as fine as

several arcsec, although with a relatively small field of view. The
X-ray sensitivity (0.2 to 4.0 keV) was improved over former missions by
more than 2 orders of magnitude, and the spatially extended X-ray sources
were imaged, permitting detailed correlations with optical and radio
images of the emission. Crystal spectrometers and transmission gratings
were also implemented, enabling the measurment of X-ray spectra at
moderate and high resolution. Some of the important results in X-ray
spectroscopy will be reviewed in Chapter 2.

X-ray observations are now continuing with the less powerful EXOSAT
(European Space Agency) and TENMA (Japanese) satellites. The first
permanent, advanced X-ray astronomy facility ("AXAF"), a focusing
telescope with four times more area than the Einstein Observatory, is
planned for shuttle launch by the early 1990's (Clark 1982). The
instruments of AXAF promise to advance high-energy cosmic research by yet
another factor of 100 in sensitivity. AXAF will be complemented by large
aperture, non-focusing missions ("XTE" and "ASTRO-C") that will carry out
detailed studies of temporal phenomena in the brighter X-ray sources.

1-2. Classes of Identified X-ray Sources

Some of the impact of X-ray astronomy can be conveyed by reviewing
the classes of objects identified as X-ray sources. A more detailed
treatment of the physical emission processes will be given in Section
2-3. Generally speaking, X-rays are photons within the energy range of
0.1 to 200 keV. Since X-rays are thermally emitted at temperatures $> 10^6$
K, X-ray measurements are a primary source of information in the study of
celestial objects that contain very hot gases, such as supernova

remnants (e.g. Canizares and Winkler 1981), stellar coronae (Vaiana et al. 1982), the hot component of the interstellar medium (e.g. Marshall and Clark 1984), and the diffuse gas in clusters of galaxies (Forman and Jones 1982). Prior to X-ray observations, the latter two of these examples were unknown, and the coronal luminosities of many types of normal stars had been greatly underestimated. Many of the high energy phenomena revealed by X-ray observations could not have been detected at lower frequencies, even from satellite observatories, because severe photoelectric absorption of UV photons affects any line of sight near the galactic plane.

In some cases the X-ray identifications have led to the recognition of rare or exotic objects. The only firmly established black hole candidates are the massive unseen components in the X-ray binaries Cyg X-1 (Bolton 1975), LMC X-3 (Cowley et al. 1983), and LMC X-1 (Hutchings et al. 1983). There are also very significant X-ray contributions in the study of SS433, a galactic binary with a double, opposing jet that is being ejected at a velocity of 78,000 km sec^{-1} (0.26 times the speed of light) while simultaneously rotating about the central binary at a velocity of 40,000 km sec^{-1} (Margon 1984).

In addition to these special cases, many fields of study have progressed significantly because of the X-ray measurements of class members. The study of Active Galactic Nuclei includes the efforts to define and model the subgroups: QSO's, Seyfert 1, Seyfert 2, other emission line galaxies, and BL Lac type objects. The measurement of X-ray luminosities and spectra have been of crucial importance in the progress gained in the last decade (Osterbrock 1984). Another example is the study of the magnetic confinement of hot gas in mass accreting binary

systems. This work depends on the observations of about a dozen magnetic Cataclysmic Variable systems, many of which are known because of their X-ray emission (Lamb 1983; Mason et al. 1984). Finally, theories regarding the evolution and dynamics of neutron stars are rooted in the observations of X-ray and radio pulsars and X-ray bursters (Lewin and Joss 1981; Joss and Rappaport 1984).

All of these advances depended, at least in part, on the optical identification and subsequent study of the X-ray sources. The X-ray detections have drawn attention to the objects, and they provide coarse information about the high-energy emission spectrum and possible variability characteristics. However, knowledge of the physical nature of the X-ray source has almost always required optical data, and detailed analyses certainly require the analytical powers of optical astronomy and the monitoring opportunity of ground-based observatories.

Figure 1-1 displays the appearance of the X-ray sky, as seen by the Large Area Sky Survey experiment of HEAO-1 (Wood et al. 1984). The subject of this thesis research is the unidentified subset (more than half) of the large number of fainter sources (small dots) in Figure 1-1.

Table 1-1 outlines the classes of X-ray sources that have been identified, emphasizing (as far as possible) the physical nature of the respective classes. Sources observed by the Einstein Observatory are included in the outline. Table 1-1 also gives the typical ranges in L_x/L_{opt}, which is the ratio (distance independent) of the 2-10 keV X-ray luminosity to the optical luminosity in the wavelength range of 3000-7000 Å. The optical and X-ray spectral characteristics of the major classes are discussed in greater detail in Chapter 2.
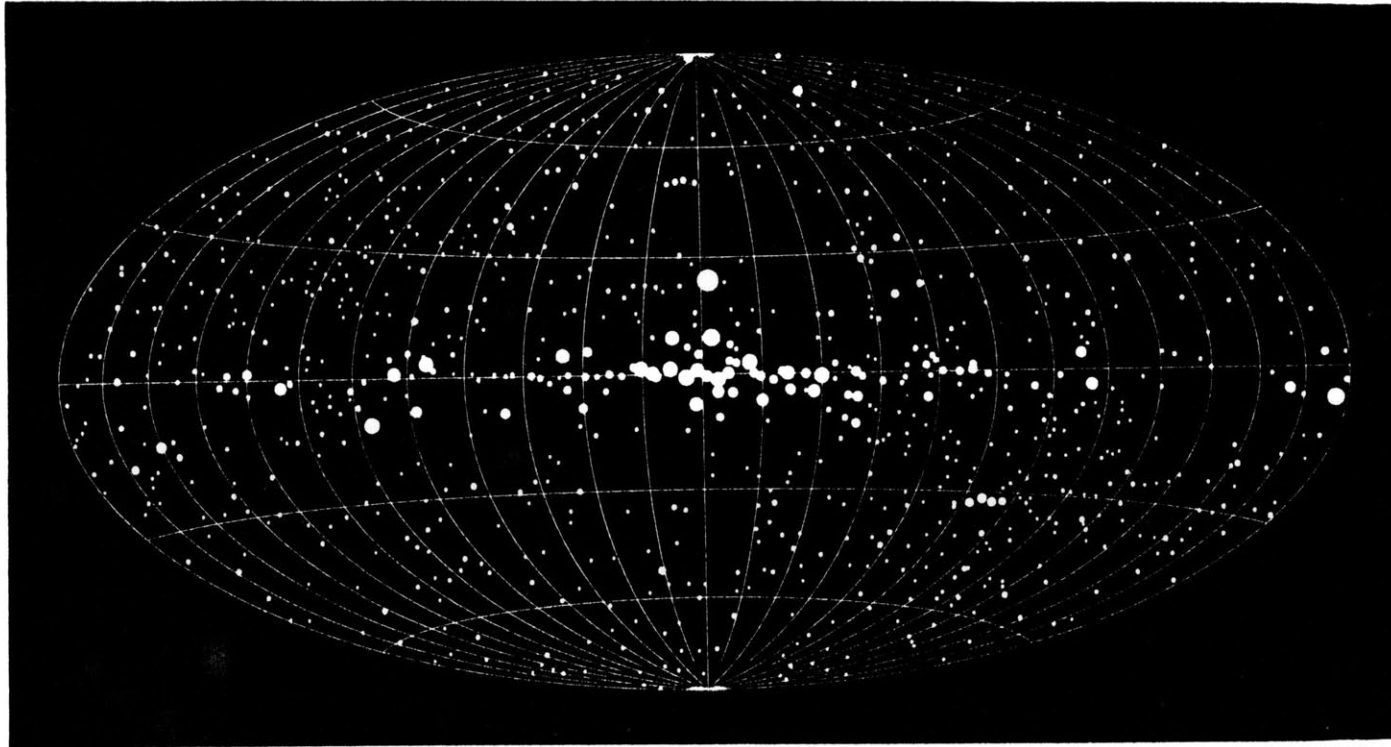
Fig. 1-1. The X-ray sky, as seen by the Large Area Sky Survey of HEAO-1 (Wood et al. 1984). The sources are plotted in galactic coordinates, and the sizes of the dots are scaled to the logarithm of the X-ray flux. Most of the unidentified X-ray sources correspond to the spherically distributed smaller dots.

Table 1-1: Identifications in X-ray Astronomy

A. <u>Galactic Sources</u>

<u>Physical Description</u>	<u>Subclasses</u>	$\underline{L_x/L}_{opt}$
1. Isolated Stars		
Stellar surfaces	White Dwarfs	< 2 keV only
Stellar Coronae	the Sun	10^{-7} to 10^{-6}
	normal stars	10^{-7} to 10^{-3}
	dMe stars, flare stars	10^{-4} to 1.0
	pre main sequence stars (T Tauri and BY Dra types)	10^{-4} to 10^{-6}
? Turbulent Stellar Winds	O,B stars; Wolf-Rayet	$\sim 10^{-7}$
2. Binary Systems		
Active Stellar Coronae	RS CVn stars	10^{-3} to 0.1
? Colliding Stellar Winds	O,B stars; Wolf-Rayet	$\sim 10^{-6}$
Accretion onto a Dwarf	Algol Symbiotic Stars	few, special ?
Accretion onto a Degenerate Dwarf	Cataclysmic Variables; magnetic CV's	10^{-3} to $10.$
Accretion onto Neutron Star	Pulsars, Bursters	10^{-5} to 10^{4}
Accretion onto Black Hole	~ 5 X-ray binaries; X-ray Novae(?)	10^{-1} to 10^{3}
(Special Subsets of Accreting Binary Sources)		
Accretion Disk Coronae	3 examples	~ 50
Globular Clusters (134 total in Galaxy)	8 examples 8 others	$\sim 10^{-3}$ $\sim 10^{-6}$
3. Supernova Remnants	old and young	??
4. Hot Interstellar Medium		not observed optically

Table 1-1 (continued)

B. Extragalactic Sources

Physical Description	Subclasses	L_x/L_{opt}
1. Normal Galactic Sources in Other Galaxies	Accreting Binaries, Globular Clusters, Supernova Remnants	10^{-4} to 10^{-5} (w.r.t galaxy as a whole)
2. Active Galactic Nuclei	QSO's	0.1 to 10.0
	Seyfert Type 1	0.1 to 10.0
	Seyfert Type 2	10^{-3} to 10^{-1}
	other Emission Line (LINER's, HEXELG's, etc.)	10^{-4} to 1.0
	BL Lac objects	10^{-2} to 10.0
3. Groups and Clusters of Galaxies	rich and poor; with and without cD	10^{-3} to 10^{-1}

1-3. <u>Statements of Research Purposes and Thesis Goals</u>

The research task can be summarized as follows. Detailed astrophysical studies of X-ray sources require the identification of the emitting object, and this is most readily achieved by locating and classifying the optical counterpart. A systematic search program has been developed to optically identify the fainter population of X-ray sources detected in an all-sky survey by the HEAO-1 Scanning Modulation Collimator. The goal of the program is to make a coherent statement about the nature and distinguishing properties of the proposed optical counterpart and about the likelihood of the identification.

The program is scientifically productive in two main ways:

(1) An optical identification reveals the nature of the X-ray source and correlates the measurements of the high energy and optical emissions. The identification initiates the effort to explain all of the emission characteristics of the object. HEAO-1 sources are especially suited for individual study, since the survey detects only the brightest X-ray sources, and these may be analyzed in greatest detail.

(2) The optical counterparts of X-ray sources are often previously unknown objects that are of significant astronomical interest. The discovery of new class members is a necessary task in many astronomical fields. Several types of X-ray sources are rare and the discoveries provide important opportunities for observations. In other cases fundamental physical models are uncertain, and studies of large numbers of objects are required to infer statistical relations within the class. This is the only means of gaining a perception of the partial derivatives that relate the emission characteristics and the physical processes which

govern them. Again, the survey objects are especially useful, since they tend to be the nearest or most luminous examples in any given class.

The purposes of this thesis are:

(1) to describe the research program and its goals (Chapters 1-4), and

(2) to present the most important results obtained by the author through a detailed examination of many probable identifications, with an emphasis on objects that were previously unknown (Chapters 5-8). The conclusions gained from this research are given in Chapter 9.

The complete investigation of the (~400) unidentified sources in the HEAO-1 survey would surpass a decade of work, and some practical limits have been set in defining the thesis project. A total of 108 X-ray sources were systematically examined, with at least one iteration through the essential steps of the program to locate the optical counterparts (described in Chapter 4). The 108 sources are listed in Chapter 5, and in 46 cases there are optical candidates. The spectral classifications of the candidates are given, along with judgments of the probability that they are the optical counterparts of the X-ray sources. There are 25 candidates for which the spectral classifications had been previously unknown. Twenty of these are spectroscopically analyzed in detail in Chapters 6 through 8.

1-4. Role of the Author

Collaborations with other researchers are an important aspect of the effort to identify X-ray sources. These cooperations include jointly

conducted observing runs as well as combined individual efforts involving specialized or non-optical observations that are necessary to properly classify objects such as BL Lac types or magnetic cataclysmic variables. Therefore, it seems appropriate to outline the role of the author and acknowledge the valuable contributions of others regarding this research project.

The author coordinated the entire (current) program to identify the faint HEAO-1 X-ray sources and performed the majority of the optical observations required to locate and evaluate the candidate optical counterparts. This included selecting the sources, submitting applications for telescope time, performing the observations with 10 telescopes at 5 observatories, reducing the data at the computing facilities of these observatories, and completing the final spectral and temporal analysis of the data at the computer facility of the M.I.T. Center for Space Research.

Many of the optical observations were made with assistance from Drs. Hale Bradt and Jeffrey McClintock of M.I.T., Ms. Wendy Roberts of the Harvard/Smithsonian Center for Astrophysics, Dr. Joseph Patterson, currently at Columbia University, and Dr. Ian Tuohy and Mr. David Buckley of Mt. Stromlo Observatory, at the Australia National University in Canberra. In some cases the observations were taken by one of these researchers and analyzed by the author. In addition, Dr. Tuohy and Mr. Buckley performed the flux calibrations for all of the spectra taken at the Anglo-Australian Telescope. Moreover, they have conducted independent studies of the southern cataclysmic variables reported in Chapter 8, and they are conducting similar research to identify sources other than those reported in this thesis. Dr. Tuohy and Mr. Buckley are

also responsible for the high-resolution optical spectroscopy (Coude
spectrograph at Mt. Stromlo) that led to the discovery of two RS Cvn type
classifications named in Table 5-1.

Radio measurements of some candidate objects are given in Chapter 7.
They were obtained by a team comprised of Dr. Eric Feigelson and Ms. Joan
Schmelz of Pennsylvania State University and Dr. Daniel A. Schwartz of
the Harvard/Smithsonian Center for Astrophysics. The optical polariza-
tion measurements contributing to the identifications of a BL Lac object
(Chapter 7) and a cataclysmic variable (Chapter 8) were performed and
analyzed by Dr. Santiago Tapia of the University of Arizona.

Additional tasks by the author include the use of the MC data
processing system first to generate data files for many of the fainter
X-ray sources in the HEAO-1 LASS catalog, and subsequently to select the
data subsets that produce the most significant MC detection.

The latter task was also performed by Ms. Wendy Roberts of
Harvard/SAO. Ms. Roberts also measured the celestial positions that are
reported in Chapters 6 through 8. The celestial coordinates were
obtained with the use of the Harvard/Smithsonian measuring engine. In
addition, Ms. Roberts carried out the independent analysis of LASS data
in the attempt to confirm the line of position of the LASS error box by
examining data that were not included in the published LASS catalog (see
Section 3-4).

II. PHYSICAL MODELS OF THE X-RAY AND OPTICAL EMISSIONS

2-1. Sources of Energy

There is widespread belief that gravitational potential energy is the ultimate origin of the luminous power of most of the identified X-ray sources. Mass transfer into the deep potential wells of massive (M) collapsed objects such as a degenerate white dwarf (with radius, R ~ earth size), a neutron star (R ~ 10 km), or a black hole (Schwarzschild radius = $2GM/c^2$) was recognized long ago as a simple and potent source of energy, by the simple relation

$$dE/dt \sim GM/R \times dm/dt,$$

where dm/dt is the rate of mass accretion onto the collapsed object. For example, the most luminous galactic (i.e. within the Galaxy) X-ray sources ($L_x \sim 10^{37}$ erg/s) require a mass sustenance of only 10^{-9} Solar masses per year, if the accreting object is a neutron star and the radiant efficiency is near unity. For extragalactic objects the considerations are the same, although the luminosities (e.g. in a typical QSO, $L_x \sim 10^{43}$ to 10^{46} erg/s) are substantially larger.

Observational support for the gravitational energy hypothesis is gained from optical studies which demonstrate that very many galactic X-ray sources are in close binaries. Detailed studies of the orbital parameters of many systems show that the binaries contain invisible yet massive ($12\ M_o > M > 1\ M_o$) companions to a normal star that may be losing mass either by Roche lobe overflow or through a strong stellar wind (see Bradt and McClintock 1983). Figure 2-1 is an illustration of the physical conditions depicting the concept that X-ray emission arises from mass accretion onto a collapsed object.
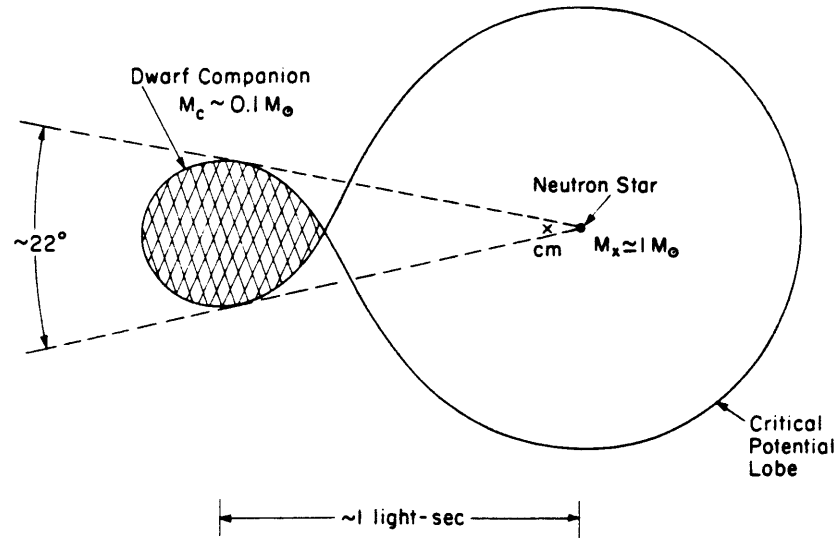
Figure 2-1. An illustration of a low-mass X-ray binary system, drawn to scale (Joss and Rappaport 1984). In this case the collapsed object is a neutron star and the dwarf (~ main sequence star) secondary fills its (gravitational) Roche lobe. The mass entering the inner Langrangian point is believed to spiral into an accretion disk before it reaches the surface of the neutron star.

In the case of active galaxies, the same concept applies, viz. gravitation potential energy is the origin of the X-ray emission, but the mass of the collapsed object is probably much greater, and the details of the accretion process are largely unknown. The evidence for the gravitational origin of the photon emission of this class is more circumstantial. The active nuclei are invariably positioned at the center of the galaxies, and all of the attempts to model the sources seem

to predict the formation of supermassive black holes (Rees 1984).

Nevertheless, there are some clear exceptions to the scenario of X-ray power from mass accretion, as is evident in Table 1-1. Supernova remnants, stellar coronae, and the diffuse hot gases in the interstellar medium and in clusters of galaxies have more complicated and individual origins, some of which will ultimately depend on nuclear reactions in stellar interiors. There is also an isotropic, hard X-ray background which presently is not understood; the observations cannot be explained either in terms of a diffuse thermal source nor with a large number of discrete sources such as distant Seyfert galaxies and QSO's (see discussion in Holt and McCray 1982).

2-2. X-ray Spectra and Emission Mechanisms

X-ray spectroscopy is a rapidly developing field which enables a more detailed analysis of the physical processes governing the high-energy emission. A discussion of the current disposition of observations and theory is presented here to cultivate a deeper understanding of the sources and to explain many of their optical spectral properties.

Low resolution X-ray spectra have been obtained for many of the bright galactic and extragalactic sources, with the principal contributions coming from the HEAO-A2 Experiment (see Section 3-2) and the Solid State Spectrometer of the Einstein Observatory. The resolving powers, $R \equiv E/\Delta E$, were about 6 and 20 for these two instruments, respectively. This field of study continues to progress rapidly as additional data are being reported from EXOSAT, from the Japanese satellites, and from reprocessed observations of the Einstein Monitor Proportional Counter.

High resolution X-ray spectroscopy has been conducted for many of the very brightest sources with two additional instruments of the Einstein Observatory, the Focal Plane Crystal Spectrometer (R = 60 to 700, depending on the dispersive order measured) and the Objective Grating Spectrometer (R = 30).

The most important X-ray spectral features are summarized below. An individual X-ray source may exhibit any sum of these properties.

(1) The spectral continuum of many X-ray sources decreases exponentially or very steeply toward higher X-ray energies. This characterizes the "thermal" X-ray sources, such as Sco X-1 and many other bright galactic sources, stellar coronal sources, most supernova remnants, and clusters of galaxies. The temperature, T, is deduced from thermal bremsstrahlung models, which specify the emitted spectrum from a hot (ionized) plasma that radiates because of collisional accelerations between charged particles. If an optically thin gas is completely ionized, then the high energy radiation emissivity (erg cm^{-3} s^{-1} keV^{-1}), j, will have the spectral form (Tucker 1975)

$$j(E) \propto n_e^2 E^{-0.4} \exp(-E/kT),$$

where E is the photon energy, n_e is the electron density, and k is the Boltzmann constant. Sometimes the X-ray spectrum will decrease sharply, but the data is not consistent with either a unique bremsstrahlung temperature nor the emission from a black body surface. The data may then be modeled by two or more components with a distribution of equilibrium temperatures (e.g. Becker et al. 1980).

(2) Many sources exhibit X-ray emission lines such as the efficient K-flourescence lines of FeI - FeXXIV in the energy range of 6.40 - 6.67

keV. Emissions from K shell transitions of the helium-like and hydro-genic ions of elements such as O, Ne, Mg, Si, S, Ar, and Ca have also been observed (e.g. Becker et al. 1980; Winkler et al. 1981). These emission lines are often seen in combination with the thermal type continua described above. The strength of the lines relative to the continuum is a function of the gas temperature (see Raymond and Smith 1977). The cross section for collisional excitation of the ions by electrons dominates other processes for plasmas in the temperature range of 10^4 to 10^7 K. This causes the ions' emission lines to dominate the spectra at lower X-ray temperatures and to become correspondingly weak at $T > 10^7$ K (see Fig. 2-1).
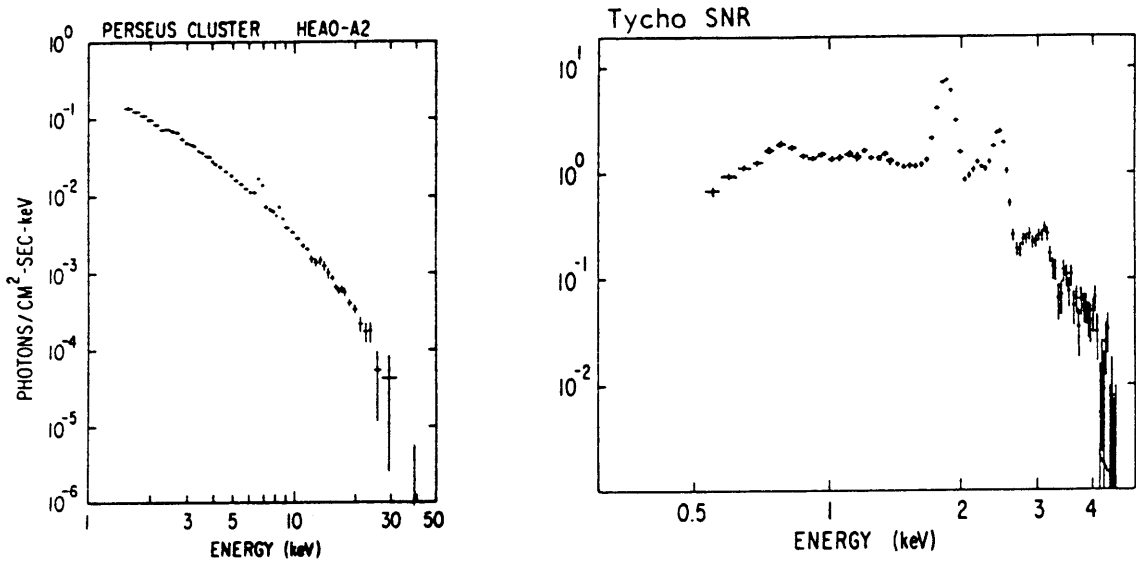
Fig. 2-2. Thermal X-ray spectra. The weak emission lines (Fe) of the Perseus cluster (T ~ 6.8 keV; Holt and McCray 1982) are compared with the stronger emission lines of the cooler gas of Tycho's supernova remnant (T_1 ~ 0.5 keV and T_2 ~ 4.0 keV; Becker et al. 1980).

(3) Other sources exhibit X-ray continua in which the measured flux densities, F(E), are found to be broad power-law functions of the form

$$F(E) \propto E^{-\alpha},$$

where α is a parameter known as the energy spectral index. Special galactic sources such as Cyg X-1, with α ~ 0.5 in the source's "low state" (e.g. Steinle et al. 1982), and the Crab Nebula, a supernova remnant with α ~ 1.0 (Toor and Seward 1974), exhibit X-ray continua of this type. Among the extragalactic sources: QSO's, Seyfert galaxies and some other types of emission line galaxies all have spectral indices near α = 0.67 (Mushotzky et al. 1980; Mushotzky 1982; Maccacaro et al. 1982; Petre et al. 1984), while BL Lac type objects generally have steeper and more variable X-ray spectra, with α ~ 2.0 (Mushotzky et al. 1978; Worrall et al. 1981). Several of these examples are shown in Figure 2-2 below.
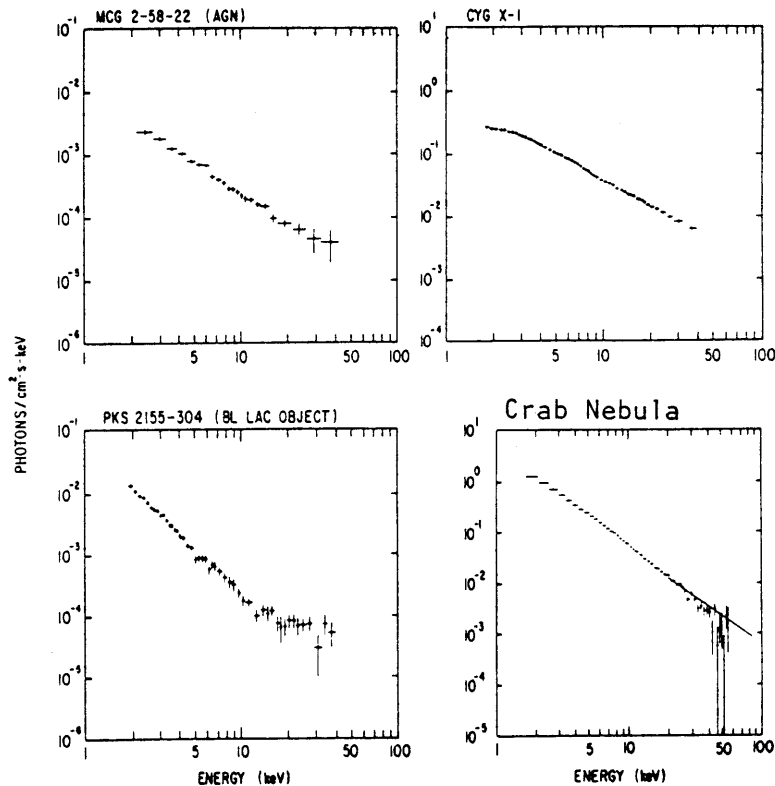
Fig. 2-3. Power-law X-ray spectra of representative extragalactic sources (left column) and galactic sources (right column). The Crab Nebula spectrum is from Pravdo and Serlemitsos (1981), while the other spectra are from White, Fabian, and Mushotzky (1983).

The physical explanations for these simple power-law spectra are a very important goal in theoretical astrophysics; however, the current theories are at best uncertain. The X-ray sources with power-law continua may have electron temperatures in the relativistic or ultra-relativistic domain, because their spectra extend to such high energies. Several of the brighter examples, such as the Crab Nebula and the Active Galactic Nuclei 3C273 and NGC4151, have been observed at energies > 1 MeV in balloon and satellite γ-ray observations (e.g. Swanenburg et al. 1981). In the relativistic domain there are two important non-thermal cooling mechanisms in which gases lose radiant energy from interactions between the electrons and electromagnetic elements in the environment. They are inverse Compton and Synchrotron emission, and they arise from electron interactions with ambient photons and magnetic fields, respectively.

If the electrons are bathed in a large supply of photons, for example from a companion star or near the center of a galaxy, then the electrons can lose energy by transferring momentum to the photons in relativistic collisions. This is the inverse of Compton scattering, in which an energetic photon transfers momentum to an ambient electron.

There are two relatively simple ways in which inverse Compton scattering will produce an emergent power-law spectrum. The first involves energetic but nonrelativistic electrons that have a thermal distribution (temperature = T_e). If soft photons (energies $\ll kT_e$) are Compton scattered by these electrons, then the emerging photons will have a spectrum (in the energy range $E < kT_e$) that is determined by the Comptonization parameter (Rybicki and Lightman 1979),

$$y \cong 4kT_e \, (\tau + 0.5 \, \tau^2) \, / \, m_e c^2,$$

where τ is the scattering optical depth of the electrons, m_e is the

electron rest mass, and c is the speed of light. If $y \lesssim 1$, then the

scattered photon spectrum will have the form:

$$F(E) \propto E^{-\alpha} \quad ; \quad \alpha = -1.5 + (9/4 + 4/y).$$

At energies above kT_e, the spectrum will abruptly fall toward zero

(Rybicki and Lightman 1979).

The second inverse-Compton route to an emerging power-law photon

spectrum is for a non-thermal distribution of relativistic electrons,

where the electron distribution is itself a power law of the form

$$n_e(\gamma) \propto \gamma^{-\Gamma},$$

where γ is the Lorentz factor of an electron $(\gamma = E_e/m_e c^2)$, and Γ is the

index of the electron distribution. In this case inverse Compton

scattering produces a power-law photon spectrum (Tucker 1975):

$$F(E) \propto E^{-\alpha} \quad ; \quad \alpha = (\Gamma-1)/2.$$

The emerging photons will have their energies increased by a factor of

order $\sim\gamma^2$; however, the form of the inverse-Compton spectrum depends

primarily on the energy distribution of the electrons (Tucker 1975).

The other environmentally induced cooling mechanism is Synchrotron

radiation, which is the photon emission of relativistic electrons that

are spiraling around the vector lines of a magnetic field. Since the

electron accelerations are perpendicular to the magnetic field lines, the

electromagnetic vectors of the emitted photons have preferred spatial

orientations, and the radiation is characterized by a significant degree

of polarization. Synchrotron models have been applied to a large number

of non-thermal radio sources which have power-law spectra and are

identified with galaxies (Kellerman and Pauliny-Toth) and Supernova

Remnants (Raymond 1984).

Most of the power of synchrotron radiation (see Tucker 1975) is emitted in a continuum of very high harmonics of the gyrofrequency,

$$\nu_B = eB/2\pi m_e c ,$$

where B is the magnetic field strength, e is the electron charge, and the other symbols are as previously defined. The critical frequency, ν_c, beyond which there is negligible radiation, is determined by the electron's energy:

$$\nu_c = 1.5 \, \gamma^2 \, \nu_B \sin \theta$$
$$\cong 4 \times 10^6 \, \gamma^2 \, B \sin \theta \quad (Hz \, G^{-1}),$$

where γ is again the Lorentz factor and θ is the pitch angle of the electron's spiral motion with respect to the direction of magnetic field. For most astrophysical sources, the magnetic field strength is weak, B < 1 G, and the equation for the critical frequency shows that ultra-relativistic electrons ($\gamma > 10^6$) are required if X-ray ($\nu \sim 10^{18}$ Hz) are to be produced by synchrotron emission in these magnetic environments.

The relevance of synchrotron theories to the study of X-ray sources was strengthened by studies of the Crab Nebula. X-ray polarization at a level of 20% has been demonstrated (Weisskopf et al. 1978), and the electron energies are probably maintained (against radiation energy losses) by magnetic breaking of the rapidly rotating γ-ray, X-ray, optical, and radio pulsar positioned at the center of the nebula.

The link between synchrotron emission and power-law spectra apparently requires, once again, that the ensemble of electrons is characterized by a power law,

$$n_e \propto \gamma^{-p}.$$

In this case the synchrotron emissivity spectrum is (Tucker 1975)

$$j(\nu) \propto \nu^{(1-p)/2}.$$

In the nucleus of a galaxy, the ultrarelativistic electrons will encounter both the local magnetic field and a high density of radio photons from their own synchrotron emission. This will produce a combination of Synchrotron and inverse Compton emissions. The Synchrotron self-Compton ("SSC") model has been applied to the spectra (radio to X-rays) of several BL Lac type objects, in which one or more power-law components (Synchrotron) are followed by a flat X-ray (Compton) tail (e.g. Urry and Mushotzky 1982; Urry et al. 1982).

One final physical issue should be mentioned in this section. Several authors have begun to investigate electron-positron pair production in hot plasmas with a view toward providing new observational tests of the properties of the emitting gas. These studies (e.g. Guilbert, Fabian, and Rees 1983) will influence the interpretation of the next generation of measurements at hard X-ray and γ-ray energies. In addition, a very interesting theory has been put forward by White, Fabian, and Mushotzky (1983) regarding the role of pair production in accounting for the changes in X-ray spectral indices between high and low state X-ray binaries and also between BL Lac's and other types of AGN.

(4) A fourth type of X-ray spectral feature may be observed at the low-energy end of the X-ray spectrum (generally E < 2 keV), where the continuum will sometimes turn over and fall sharply toward lower energies. This turnover usually indicates the absorption of X-rays due to photo-ionization of material along the line of sight to the object. To first order, the effect of photo-ionization can be incorporated into a description of the X-ray continuum by:

$$F(E) = F_o \exp(-E_a/E)^{2.67} f(E),$$

where f(E) is the inherent form of the continuum (thermal, power-law, etc), and E_a is the absorption "cutoff energy", a parameter dependent on an effective cross section (based on Solar abundances) and the column density along the line of sight (Brown and Gould 1970). As the physical models and spectral measurements become more sophisticated, more detailed considerations must be given to the ionization edges of high-Z elements such as O and Fe (Fireman 1974; Morrison and McCammon 1983), and also to the temperature dependence of the cross sections of each element (see Hatchett, Buff, and McCray 1976; Kallman and McCray 1982).

The absorption effect is not an intrinsic X-ray spectral feature, but it may be used to probe the gas surrounding the X-ray source if the absorption is highly variable (e.g. Walter et al. 1982; Remillard and Canizares 1983) or if the deduced column density is much greater than other measures of the amount of interstellar matter through the Galaxy in that direction (e.g. Lawrence and Elvis 1982).

2-3. Optical Emissions of X-ray Source Counterparts

This section outlines the optical properties of X-ray source counterparts and provides some motivations for the optical search techniques given in Chapter 4.

All of the high energy emission mechanisms discussed in section 2-2 predict some level of optical emission by the same process if X-rays are produced. With regard to the identification of the X-ray sources, the first question is whether that optical emission will be the dominant one. Accordingly, the objects may be described in two categories:

(1) those which exhibit continuum and emission line features that are correlated with the X-ray spectral features, and

(2) those in which the optical manifestations of the high-energy emission processes are overpowered by a "normal" optical source, such as the primary (normal) star in a high-mass X-ray binary system or the sum of starlight in a cluster of galaxies.

The physical association between the optical and X-ray emissions for objects in category 1 is supported by several lines of evidence. These sources generally exhibit continuous spectra that extend throughout the X-ray, UV, optical, IR, and radio regions. In the case of Active Galactic Nuclei, it has been shown that the magnitudes of the X-ray and optical continuum fluxes are correlated (e.g. Kriss et al. 1980; Reichert et al. 1982). A strong X-ray/optical link is also indicated by the detections of correlated X-ray/optical variability in low-mass X-ray binaries (e.g. Grindlay et al. 1978; McClintock et al. 1980) and in X-ray novae (e.g. Gull et al. 1976; Canizares et al. 1980).

Sources in the first category tend to show two important spectral characteristics at optical frequencies:

(1-A) The continua are typically flat (plotted in units of energy flux per unit wavelength vs. wavelength) or they resemble power-law functions that rise toward the UV. This applies to the low-mass X-ray binaries (Bradt and McClintock 1983) and to virtually all Active Galactic Nuclei (e.g. see Chapters 6 and 7). These continua may represent either the low-frequency tail of a thermal process or a section of a broad Compton or synchrotron process. Many coordinated X-ray/UV/optical observations have been combined in the effort to model individual sources. It has been claimed that thermal bremsstrahlung emission can explain the optical continuum of Sco X-1 (Willis et al. 1980), although the photons may originate in an accretion disk (Petro et al. 1981), where a radially

distributed temperature profile would be expected. While accretion disk models may be appropriate to most X-ray binaries, there are a few cases where an accretion disk corona and the X-ray heated face of the optical star are needed to explain the X-ray and optical observations (White and Holt 1982).

The optical continua of extragalactic sources in category 1 (AGN, primarily) are basically similar, although a nonthermal origin is implied because the X-ray spectra have power-law continua with no emission lines. The processes are uncertain for QSO's and Seyfert types (see Holt and McCray 1982), while the Synchrotron self-Compton model seems to be favored for BL Lac objects (see Chapter 7).

(1-B) A second important spectral feature exhibited by the optical counterparts in category 1 is the presence of optical emission lines. All Active Galactic Nuclei except BL Lac objects in their bright (normal) states show strong or moderate emission lines from atoms which have a wide range of ionization temperatures (from a few to more than two hundred eV). A large majority of low-mass X-ray binaries also show emission lines, although in some neutron star systems the lines may be very weak (see Bradt and McClintock 1983). Chapters 6 and 8 contain an extensive display of the optical emission lines observed in extragalactic and galactic X-ray sources, respectively.

Physical models of the optical emission lines (e.g. Davidson 1972) favor the explanation that the lines are emitted by recombining ions and electrons that lose their excess energy in a cascade of photon emissions which correspond to changes in quantum energy levels. The ionization structure is assumed to be the result of photo-ionization caused by the

hard (UV and soft X-ray) continuum photons of the X-ray source. In this picture the optical emission lines originate in a cooler gas component that is "lit up" by the bright continuum of the hotter gas. This contrasts with the origin of the X-ray emission lines, which represent a direct cooling mechanism of the hotter gas, as was discussed earlier in this chapter.

The geometries of the gas components are much less certain. There are several proposals concerning the location of the optically emitting gas in X-ray binary systems (see discussion in Bradt and McClintock 1983). The problem is certainly more complicated in the case of AGN, where there are near-relativistic bulk motions of some gas components and a significant variation in the temperatures and densities of the optically emitting components of a single source (see Osterbrock 1984).

Although emission lines are a characteristic of many types of X-ray sources, it should be noted that the presence of emission lines does not imply that the object is an X-ray source. Some classes of objects have emission lines and are not X-ray sources. Other classes have both X-ray emitting and non X-ray members, and in both cases the emission lines are caused by factors unrelated to the production of X-rays. Emission lines without X-rays occur, for example, among Planetary Nebulae, T Tauri stars, Be stars, Wolf-Rayet stars, symbiotics, VV Cepheid stars, and dwarf Me stars. Many of these examples are stars that are surrounded by clouds or shells of gas and (sometimes) dust whose emission lines are powered by the UV and optical continua of the central stars. On a larger scale there are huge clouds called HII regions which are lit up by the UV starlight of hundreds or thousands of early (O and B type) supergiants in star formation regions. Some galaxies are dominated by the emissions of

HII-type regions (e.g. Balzano 1983). The effort to distinguish the optical spectra of narrow-line AGN (X-ray sources) from the nuclear, extragalactic HII regions ("starburst galaxies"; not luminous X-ray sources) requires great care and high-quality spectra (Heckman 1981; Baldwin et al. 1981).

The discussion returns to the second category of optical counterparts, viz. some sources are dominated by the optical spectra of apparently normal stars. The identification of these sources is sometimes difficult to prove; however, for most of the classes of objects that constitute the bright (survey) X-ray sources, there are sufficiently useful means of recognizing the optical counterparts. Globular clusters and clusters of galaxies are optically dominated by the sum of normal stars, but in most cases their identities are easily recognized in an optical photograph of the X-ray field. The massive X-ray binary systems contain stars which are OB-type supergiants or Be stars (B stars with emission lines at $H\alpha$ and sometimes at $H\beta$) which can provide mass transfer over large distances by means of a strong stellar wind (OB types) or by the ejection of photospheric shells (Be types). In each of these spectral classes, the large majority of known examples are not detected as X-ray sources. Therefore, their identifications must be supported by precise X-ray positions or by dynamical evidence of membership in a binary system, particularly if a correlated X-ray/optical periodicity can be demonstrated. Fortunately, these stars are relatively rare and easy to recognize, except when they are located very near the galactic plane.

Other types of X-ray sources appear optically as stars of later spectral type, which are quite common in the Galaxy. However, for the

purposes of this thesis research only a few types need be considered. The distributions in L_x/L_{opt} (Vaiana et al. 1982) insure that most of the known classes of X-ray sources that appear as late-type stars will not be detected above the HEAO-1 threshold unless they are very close to the Solar System. Therefore such identifications will be rare, and they will pertain to extremely bright stars (e.g. apparent visual magnitude, V < 6). The exceptions, i.e. the most luminous X-ray sources appearing as stars of late spectral type, are primarily RS CVn type systems (Walter et al. 1980). These are binaries with primary stars of spectral types F, G, and K, in which the companion-facing hemisphere contains a large number of starspots that create an unusually active and flaring stellar corona. They are classified by high-dispersion spectral observations of strong emissions in the cores of the deep stellar absorption lines of Ca II ("H" and "K" lines) at $\lambda 3933$ and $\lambda 3968$. Several RS CVn stars have been identified as HEAO-1 X-ray sources (e.g. Garcia et al. 1980; Schwartz et al. 1981), and their range in apparent magnitude is typically 9 < V < 5.

III. THE HEAO-1 SCANNING MODULATION COLLIMATOR

3-1. Detectors Used in X-ray Surveys

The X-ray surveys were conducted with non-focusing, mechanically collimated (i.e. baffled) proportional counters (see Rossi and Staub 1949). These detector systems consist of a supply of gas, usually a mixture containing argon or xenon, that is placed in a high-voltage electric field. An X-ray entering the instrument's window ionizes an inner electron of a noble gas atom, and a number of secondary ionizations (outer shell electrons) are produced by collisions with the first electron and with the shower of secondary electrons that are accelerated by the electric field. The sum of electrons are collected at the anode and the event is recorded. Pulse height analysis of the anode signal permits a coarse resolution of the incident photon energy. Typically the instruments were sensitive to 2-12 keV photons and the X-rays were counted in several energy channels. At lower energies the X-ray sensitivity is usually determined by the type and thickness of the detector window, while the limit at high energies depends on the gas composition, the pressure, and the detector depth.

To distinguish the X-ray events from ionizations due to cosmic rays or high-energy particles held in the Earth's magnetic field, there were two types of electronic filters. Pulse shape discriminators rejected events having the longer rise-times of ionizations by energetic particles, and anticoincidence circuitry rejected events that were nearly simultaneously recorded by shielded (windowless) detectors that were planted beneath the active proportional counters.

The survey experiments were placed in low-altitude orbits, and the satellites maintained a low and controlled spin rate. Gyro systems tracked the changes in the satellite's orientation, and the pointing directions were absolutely calibrated with respect to the celestial sphere by means of star camera observations of bright stars. The detector baffles (typically rectangular and sometimes circular) caused the sensitivity to vary as a function (linear in each separate rectangular dimension) of the number of degrees between the detector viewing axis and the line of sight to an object. The full widths at half maximum (FWHM) of these spatial sensitivity functions were most often between 1 and 4 degrees.

For the standard (i.e. non-modulating) collimators, the positions of the X-ray sources were confined in the spin azimuth direction by correlating the time of the maximum detected flux with a corresponding band on the celestial sphere. To confine the position in the direction orthogonal to the spin azimuth (the elevation), the spin axis was usually changed. In the survey of HEAO-1 the spin axis was systematically incremented, and the error boxes could be confined in the elevation direction by matching the envelope of single-scan flux measures with the spatial sensitivity profile of each collimator, after the azimuth line had progressed over the source.

A second type of detector, used for observations at high X-ray energies, was a scintillation counter (Birks 1964), in which the X-ray absorption occurs in a solid crystal lattice, rather than a noble gas. In this case the X-ray's energy excites electrons into the solid state conduction band, and some of the electrons are captured at "active" (doped) sites, leading to the emission of visible light. A photo-

multiplier tube counts these secondary photons and thereby records the
X-ray event. The resolution of energy channels and the use of pulse
shape and anticoincidence discriminators are all conceptually similar to
those used for proportional counters. Scintillation counters were flown
in many rocket and balloon payloads and were used in the HEAO-A4 (hard
X-ray) experiment.

3-2. The HEAO-1 Mission

NASA launched the first High Energy Astronomy Observatory on August
12, 1977. The mission consisted of four experiments, and the detector
areas were of much greater size than any of the other survey experiments
flown with similar purposes.

The satellite orbit was approximately circular at an altitude of 432
km, which determines an earth orbit of ~ 90 min. All of the detectors
faced the y or -y axes, while the z-axis (spin axis, with a spin period
~ 30 min) was always pointed toward the sun. The mission continued until
the satellite began to re-enter the earth's atmosphere during January,
1979. Occasionally the spinning of the satellite was stopped to conduct
pointing observation of sources of interest. This non-surveying mode
accounted for roughly 25% of the mission lifetime, and most of the
pointed observations occurred during the latter half of the mission.

Because the spin axis was pointed toward the sun, the motion of the
earth around the sun caused the detector viewing circle (i.e. the pro-
jection of the spin azimuth on the sky) to slowly rotate about the
ecliptic poles. Since all of the X-ray experiments viewed along the spin
azimuth, each completed a celestial scan every 6 months. Therefore, the

~ 17 month mission produced almost 3 complete scans of the X-ray sky.
The exposure given to a particular position was primarily a function of
the ecliptic latitude.

The four experiments were coded according to the satellite's origi-
nal designation "HEAO-A". The A-1, A-2, and A-4 experiments will be
described briefly here, in order to outline the scope and importance of
the mission. The A-3 instrument is the Scanning Modulation Collimator,
whose detections are the starting points from which this thesis research
proceeds. Its operation and its scientific applications are discussed in
Sections 3-3 and 3-4. Figure 3-1 is a drawing of HEAO-1, which stood
about 10 feet in height.
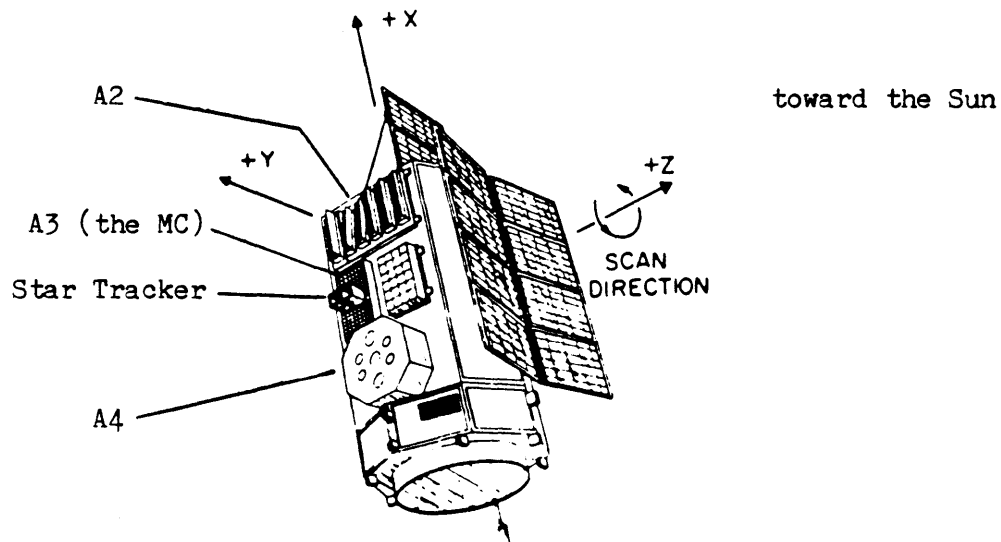
Fig. 3-1. The HEAO-1 satellite. The detector without a label is one of
the A1 (LASS) modules, and the other A1 modules occupied the side of the
satellite that pointed in the -Y direction.

The HEAO A-1 experiment was the Large Area Sky Survey (LASS),
commissioned by the U.S. Naval Research Laboratory. The LASS consisted
of 7 very large proportional counters (1 to 20 keV sensitivity) which
assumed a major fraction of the total detector area of HEAO-1. Serious
hardware problems affected the longevity of the detector modules and the
ability to resolve the X-rays into separate energy channels. However the
LASS catalog (Wood et al. 1984) is easily the prime available survey of
the X-ray sky, detecting 842 sources greater than a flux limit $\sim$0.22 μJy
at 5.2 keV. Furthermore, the LASS X-ray position, with error boxes
ranging in size from 0.01 to about 1 degree^2 depending on the X-ray flux,
are of crucial importance in the use of the Modulation Collimator
positions to identify the fainter population of X-ray sources.

The HEAO A-2 experiment consisted of 6 multilayer proportional
counters which operated with low background noise and observed in a wide
range of X-ray energies, from 0.2 to 60 keV. The experiment was led by
scientists from the Goddard Space Flight Center and the California
Institute of Technology, with collaborators at the Jet Propulsion Labora-
tory and at the University of California at Berkeley. The A-2 project
detected many new X-ray sources and has made major contributions in the
field of low-resolution X-ray spectroscopy. The detections were reported
in two catalogs of hard X-ray sources (3-17 keV) by Marshall et al.
(1979) and by Piccinotti et al. (1982), and in a low-energy survey (two
bandwidths spanning a total range of 0.2 to 2.0 keV) by Nugent et al.
(1983). Among the many additional A-2 research publications are the
measurements of the X-ray spectra of many classes of sources (e.g.
Mushotzky et al. 1980; Worrall et al. 1981; Mushotzky 1982).

The A-4 experiment surveyed the sky at high X-ray and low γ-ray energies. There were 7 NaI/CsI scintillation counters that combined to span the energy range of 13-2300 keV. A-4 was operated by researchers at M.I.T and at the University of California at San Diego. The detector area was small, but a catalog of ~70 sources in the energy range of 13 to 180 keV (Levine et al. 1984) distinguished those bright galactic and Magellanic Cloud sources that radiate at these high X-ray energies. Other A-4 accomplishments include the detection of the periodic behavior of LMC X-4 (Lang et al. 1981), and a nearby active galaxy, Cen A, was observed at energies as up to several hundred keV (Baity et al. 1981).

3-3. Design and Purpose of the Scanning Modulation Collimator

A modulation collimator is basically a standard collimator with the addition of grids of wires that are placed above the detectors. The wires block the transmission of X-rays, and the wire pattern modulates the detected flux of an X-ray source as the detector scans across the field. The phase of the detected signal constrains the allowed position of an X-ray source. Oda (1965) originally suggested that these devices be used in X-ray astronomy to limit the celestial positions of discrete X-ray sources. For a general review of these instruments, see Bradt et al. (1968). A modulation collimator was used to locate the optical counterpart of the brightest persistent X-ray source, Sco X-1 (Gursky et al. 1966). A Rotating Modulation Collimator (z-axis mounted) was flown on SAS-3, and the experiment produced unique, $\lesssim 60$ arcsec error circles for 64 bright X-ray sources in the Galaxy (Bradt, Doxsey, and Jernigan 1979). Another RMC was flown on the British satellite, Ariel 5.

M.I.T. and the Harvard/Smithsonian Center for Astrophysics (whose
investigators were originally at the American Science and Engineering
Co.) jointly developed a Scanning Modulation Collimator (MC) experimment
for the HEAO-1 X-ray survey to produce relatively precise positions of
hard (1-13 keV) X-ray sources (see Gursky et al 1978; Schwartz et al
1978b). The MC (HEAO A-3) consisted of two "banks" of argon-filled
proportional counters, and each bank (MC1 and MC2) was composed of 4
identical detector modules, each with an overall field of view that was
restricted to 4° x 4° FWHM. Four layered grids of parallel wires in
front of each MC bank modulated the detected flux of an X-ray source as
the detectors scanned across the field. The grid pattern of one
collimator is shown in Figure 3-2, with an illustration of sample viewing
angles that produce source transmission or shadow.

FOUR-GRID MODULATION COLLIMATOR
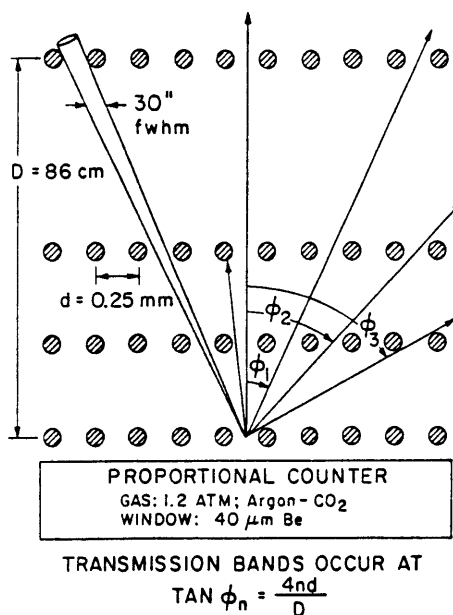
Fig. 3-2. The four-grid modulation collimator, MC1.

As the detector scans across the sky, an X-ray source passes alter-
nately through angles of transmission and shadow, producing a modulation
in each collimator. The net effect resembles what would be seen by a
person who views a large flashlight being carried behind a picket fence.
Figure 3-3 shows the modulation pattern (the raw data) from a single scan
over the position of Sco X-1, the brightest persistent celestial X-ray
source.
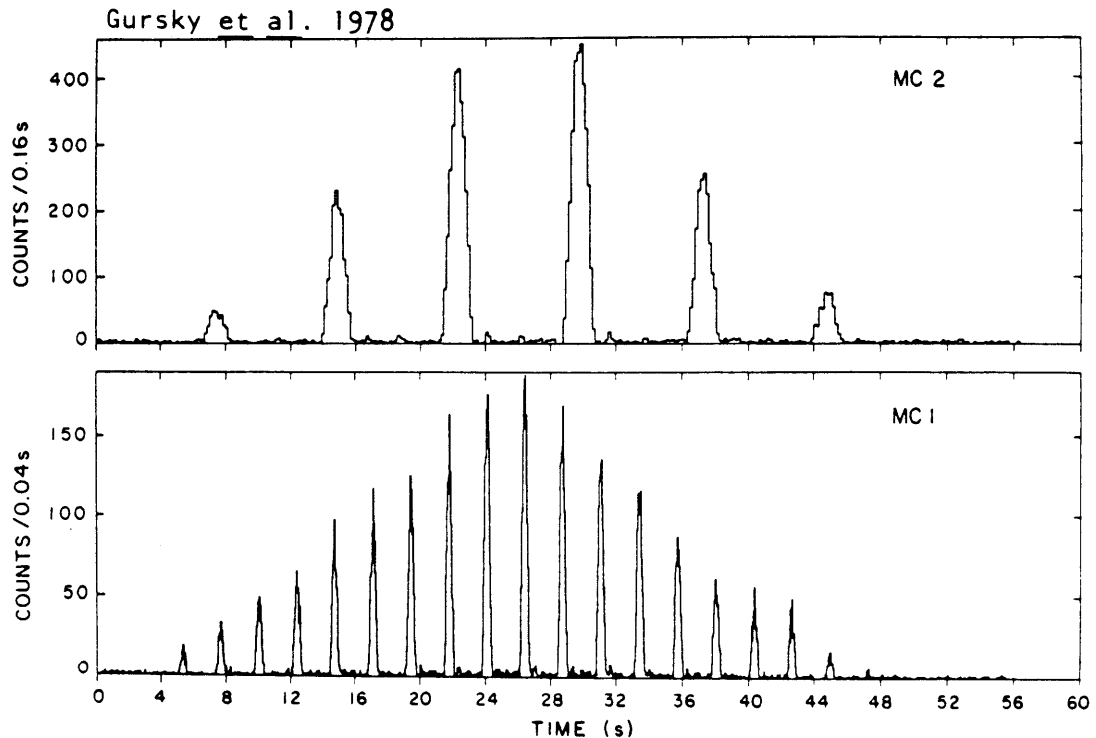
Fig. 3-3. The raw data from a single transit of Sco X-1 shows the
transmission bands of the HEAO-1 Scanning Modulation Collimator.

It can be seen in Figure 3-3 that each collimator had a periodic

response to a point-like X-ray source when the satellite was spinning at

a constant rate. The triangular-shaped envelope of transmission maxima

is the spatial profile of the coarse, $4^{\circ} \times 4^{\circ}$ baffles that restricted the

MC's overall field of view. The frequency and the widths of the trans-
mission peaks in Figure 3-3 demonstrate that one collimator (MC1) is more
finely spaced that the other (MC2). MC1 has 30 arcsec FWHM spatial reso-
lution, with a 4 arcmin periodicity (separation between adjacent trans-
mission bands), while MC2 has 2 arcmin spatial FWHM, with 16 arcmin
periodicity.

The individual transmission peaks can be co-added ("folded"), since
the modulation periodicity, which is determined by the wire spacings and
the satellite spin rate, can be calculated. The _phase_ of a source
detection (above the background rate) in the folded array determines a
set of positional bands on the celestial tangent plane that include the
X-ray source position. Figure 3-4 shows a celestial map of the allowed
bands of position for Sco X-1, determined from the phase of the
transmission peaks shown in Figure 3-3.
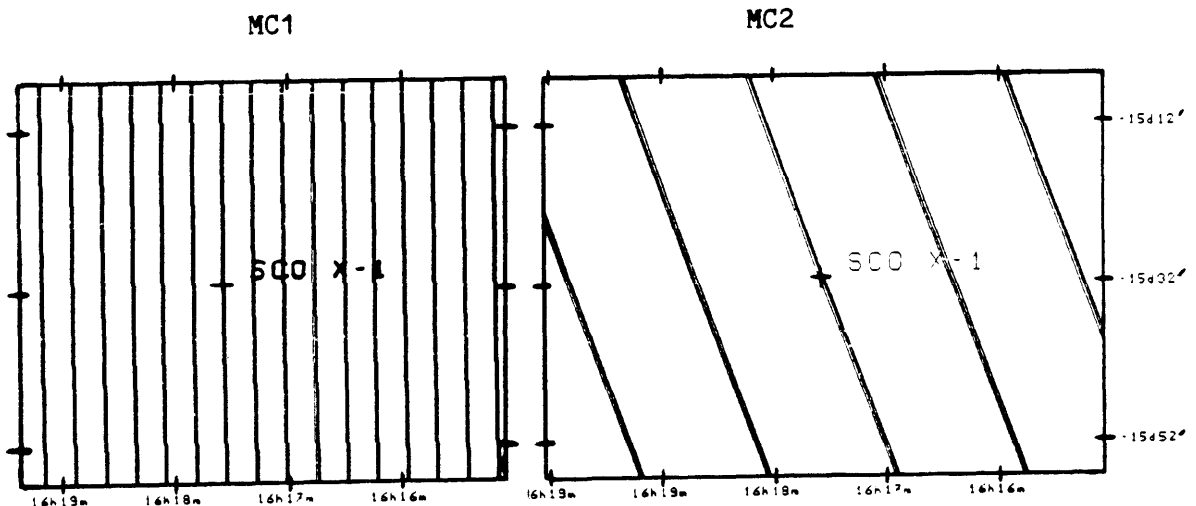
Fig. 3-4. A celestial map of the allowed source bands for Sco X-1. The
bands are determined by the phase of the modulations shown in Fig. 3-3.

The angles of the MC positional bands (see Fig. 3-4) are different

from each other because the wires of one MC are rotated by 20 deg with

respect to the other. The intersection of the bands from the two colli-

mators produces a multiplicity of parallelograms (historically and

hereafter called "diamonds") that are shown in Figure 3-5. The size of a

single diamond depends on the statistical significance of the detected

modulations, with a maximum size for faint sources of about 1 x 4 arcmin,

to 90% confidence. One of the diamonds is expected to contain the X-ray

source.
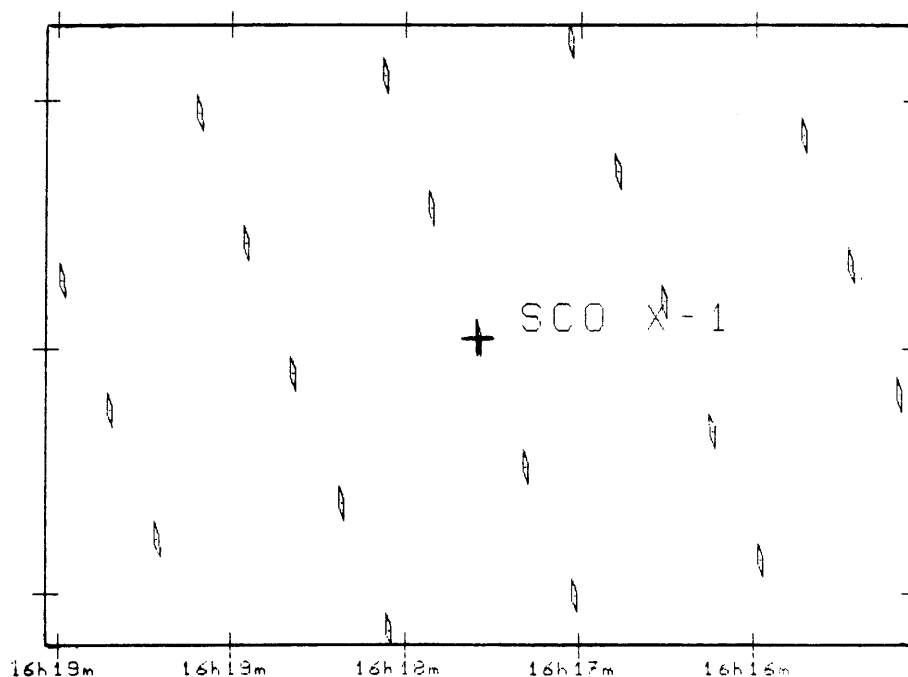
Fig. 3-5. The final positional diamonds for the transit of Sco X-1. The
diamonds are formed by the intersections of the allowed bands of the two
collimators (Fig. 3-4). Ten transits of Sco X-1 would produce a source
detection with a significance > 2000 σ, despite the saturation of the
available counting bits. This response to the extremely bright X-ray
source contrasts sharply with situation for the fainter HEAO-1 sources,
where the sum of the source transits during the satellite lifetime may be
needed to produce diamonds with statistical significances ~ 3 σ.

The MC produces about 20 diamonds per square degree, and the allowed celectial area of an X-ray source is reduced by a factor of ~100 if each MC detects a source with 3.5 σ significance. Since the overall field of view $(4^{\circ} \times 4^{\circ}$ FWHM) is so large, the number of diamonds that must be considered is prohibitive unless the result is used in conjunction with the error box of another experiment. For this purpose the positions of any X-ray experiments may be applied, but the HEAO-1 LASS is the most useful since it was more sensitive than the MC and its observations were contemporaneous (the experiments faced the opposite direction on HEAO-1, which had a spin period of about 30 min).

3-4. The Data Bank and X-ray Positional Analysis

As noted above, the continual pointing of the satellite z-axis toward the sun caused the detector viewing circle (azimuth) to rotate slowly ($\sim 1^{\circ}$ per day) relative to the celestial sphere. During each 6 months of observations, a given source is "scanned" in a series of transits (every ~30 min) for an interval ≥ 4 days (within the trans- mission FWMH of the collimators), depending on its ecliptic latitude. The ecliptic poles are always in the viewing circle.

The analysis of the MC detection of any particular source requires 3 major steps of data processing, in order to extract the MC phase of a particular X-ray source from the continual stream of counts recorded by detectors on a spinning satellite. The analysis is undertaken for each source position that is determined by a standard collimator in an X-ray survey. These positions become the MC "binning positions", which are the nominal starting points for our positional analysis.

Data analysis is carried out for each collimator, independently. In

addition the data from each collimator is recorded in 3 energy channels.
(Channel "A" is the 0.5 to 2.5 keV energy band; channel "B" is the 2.5 to
5.5 keV energy band; and channel "C" is the 5.5 to 13.0 keV energy band.)
Therefore a source transit is really a six-track recording (2 collimators
x 3 energy channels), and the following steps of data analysis apply to
each track:

(1) The star camera data and the satellite gyro readings are analyzed
in order to locate the raw data (cts per time interval) pertaining to
each single transit near the source position. Included are data within
an azimuth window of ± 2 deg whenever the elevation of the transit is
within ± 3 deg, each measured with respect to the binning position. (A
reminder: the azimuth is the angle in the direction of the satellite's
spin motion (30 min period), and the elevation is the orthogonal angle in
the direction of the day-by-day 1° incrementing of the detector viewing
circle.)

(2) The MC data (each collimator, independently) of each source transit
is folded at the (respective) modulation frequency. With regard to
Figure 3-3, this would be described as co-adding the count-rate spikes so
that the transit is converted to a single array containing the collima-
tor's counts as a function of the modulation phase. The number of phase
divisions in the periodicity cycle is arbitrarily set to be 60, and the
nominal binning position defines the location of (arbitrary) zero phase.

(3) The complete set (with respect to the lifetime of HEAO-1) of
phase-binned transits of a given source is accumulated into a single data
file and the analyst must choose a subset that exhibits the most signifi-
cant detection of the X-ray source by both collimators. The parameters
which define the subset are a specific range in the transit elevations,

the MC energy channel(s) (either a single one or sums of 2 or 3), and a combination of celestial scans (i.e. 6 month periods) to be included. To test any defined subset, the constituent phase-binned transits are simply added together, and the array is statistically analyzed to determine the phase location and significance of a source above the background level, assuming the instrument's profile (in phase space) to a point-like X-ray source.

Steps 1 and 2 are performed together for a large number of sources, since the data for any particular source is dispersed throughout a significant fraction of the entire MC raw data set (~1000 magnetic tapes).

The analysis of faint sources requires a special use of step 3. None of the sources within the flux range of 0.5 to 2.0 μJy (at 5.2 keV) can be detected unless approximately one hundred or more transits are grouped together, and the significance of the MC detection may be greatly diminished by the inclusion of transits with elevations $> 2^{\circ}$ from the source. However, only the elevations relative to the nominal binning positions are known until the optical counterpart is actually located. Accordingly we have adopted a practice of systematically testing a large number of permutations among the possible combinations of celestial scans, energy channels, and blocks of 2°, 3°, and 4° ranges in the elevation angle. The goal is to choose the result which combines the strongest statistical significance and the most consistent answer on the surface of permutations. In many cases, as would be expected for the weakest sources and for very extended (angular size > 1 ') X-ray sources such as Supernova Remnants and Clusters of Galaxies, the final judgment

is that the MC does not detect a source.

In some cases a very strong detection is observed with MC2, but there is no significant result in MC1 because the X-ray source is spatially extended with an angular size that is less than the 2 arcmin spatial resolution of the more coarse collimator (MC2). This is the manner in which the MC detects sources such as clusters of galaxies and supernova remnants. Whenever these cases arise, the MC2 result (i.e. the phase-binned sum of the transits) will frequently exhibit a source profile that appears broader than the instrumental response to a discrete X-ray source.

The Modulation Collimator group has also conducted a limited analysis of HEAO-LASS data to confirm the line of position of the X-ray source. (The raw LASS data was given to the MC group in order to determine binning positions that are necessary for the analysis of MC data.) The HEAO-LASS catalog (Wood et al. 1984) is based on the first complete celestial scan (first six months) by HEAO-1. In our analysis, the sum of all the LASS scan modules (1° x 4° FWHM collimators) is inspected for every detector transit over the source position during the entire satellite mission (3 celestial scans in 18 months). The data from each transit are accepted for positional analysis only if the background rate appears uniform; this qualitative judgment is made after viewing a plot of the transit. When reporting the identification of a particular source, we include the results of this analysis only if there is a significant deviation from the catalogued LASS position.

3-5. <u>Previous Identifications of Bright X-Ray Sources</u>

The Modulation Collimator has made major contributions in the identification of bright celestial X-ray sources. From 1978 to 1981 the experiment produced positions that were used to identify about 70 sources. Among the most noteworthy are GX339-4 (Doxsey <u>et al.</u> 1979), a rapidly flickering (10 msec timescales at both optical and X-ray wavelengths) source in the galactic plane, H1538-522 (Schwartz <u>et al.</u> 1978a), a double-line spectroscopic binary and neutron-star system, and 4U2129+47 (Thorstenson <u>et al.</u> 1979) and 4U1822-371 (Griffiths <u>et al.</u> 1978), two of the rare binaries that are explained as accretion-disk corona X-ray sources. In addition, identifications were obtained for several cataclysmic variable systems which led to the clarification of magnetic and intermediate-polar subclasses (Griffiths <u>et al.</u> 1979d; Steiner <u>et al.</u> 1981; Patterson <u>et al.</u> 1981). In the extragalactic domain, the MC group proved that a "poor" cluster of galaxies can be a luminous X-ray source (Schwartz <u>et al.</u> 1980), identified a nearby cluster of galaxies in the galactic plane (Johnston <u>et al.</u> 1981), and discovered a rapidly varying BL Lac object, H0323+022 (Doxsey <u>et al.</u> 1983; Margon and Jacoby 1984). These successes certainly show that the instrument's positions are highly reliable and that the scientific gains have been very significant.

Further indications of the reliability of the MC detectors and the accuracy of the celestial pointing calibrations are provided by studies that combine the temporal and positional aspects of the observations of bright sources in the Large Magellanic Cloud (LMC). The LMC is near the South Ecliptic Pole, and its X-ray sources are almost always within the viewing circle of the HEAO-1 detectors, since the viewing circle pivots

about the ecliptic poles as the survey progresses in time. Therefore, the consistency of the MC positions for the LMC sources provides a continual record of the experiment's stability against systematic errors.

Johnston et al. (1978) used a sequence of MC positions for the bright LMC sources to obtain unique celestial positions that helped to identify the optical counterparts. His work also produced a detection and light curve for a recurrent transient, A0538-66 (Johnston et al. 1979), and its 16.6 day X-ray period was also detected in subsequent observations of the optical counterpart (Skinner 1980).

More recently, the author used the MC observations of LMC X-3 to exclude X-ray eclipses, which helped to constrain the mass ($M > 9$ M_o) of the invisible companion in that system (Cowley et al. 1983). In the X-ray analysis, the flux measures were accepted only if the phase of the LMC X-3 detection was within $\pm$ 20 arcsec of the position of the optical counterpart, in the case of MC1, and within $\pm$ 1 arcmin for the collimator with less spatial resolution, MC2. When the source was in its bright state, only 5% of the single-transit detections (typically having 5σ significance each) failed this requirement.

The conclusion is quite clear: the effectiveness of the Modulation Collimator experiment in the effort to identify the fainter sources of the HEAO-1 survey will be limited by statistics. The essential problems, insofar as the X-ray measurements are concerned, are:

(1) detecting the X-ray signal above the noise due to the X-ray background, and

(2) separating the results if more than one source is detected in a given scanning area ($\pm 2^{\circ}$ x $\pm 3^{\circ}$) of the celestial sphere.

IV. THE SEARCH FOR THE OPTICAL COUNTERPARTS

4-1. The Program

The effort to identify the fainter X-ray sources in the HEAO-1 survey typically requires consideration of between six and thirty MC diamonds in or near the LASS error box. Very many optical objects, to the POSS or ESO B limits, are included within these diamonds, and there is a need for wide-field techniques to distinguish candidates which exhibit characteristics associated with the optical counterparts of X-ray sources. Optical candidates are obtained and evaluated in four systematic steps of investigation:

(1) Once the X-ray data analysis is completed, the X-ray positions are superposed (mapped by computers) on objects in 60 catalogues which contain examples of known classes of X-ray sources. These "Interesting Objects" catalogs include, for example, the New General Catalog of Nonstellar Astronomical Objects, the Uppsala General Catalog of Galaxies, Markarian UV objects, the General Catalog of Variable Stars (Kukarkin), The Ohio Radio Catalog, etc. In most cases this mapping fails to deliver a viable candidate.

(2) The optical search is initiated with an examination of the POSS or ESO Sky Survey Plates. Prominent galaxies, clusters of galaxies, globular clusters, and particularly bright stars (V $\lesssim$ 10.0) become candidates immediately, if their positions are consistent with the X-ray results. This criterion selects the optical counterparts described as category #2 (optical flux dominated by a normal, non X-ray component) in Section 2-3, as applied to the HEAO-1 survey.

(3) Schmidt telescope observations are made of each X-ray source field to recognize objects that have a strong ultraviolet (UV) color. The photographs are made with adjacent U and B filtered images on the same plate, and the exposures reach 17.5 to 18.0 magnitudes in each bandpass. The candidates are obtained from a visual inspection of the plates, and the selection threshold is roughly U-B < -0.1. UV excess is an established optical characteristic of both galactic X-ray sources (Bradt and McClintock 1983) and certain bright extragalactic X-ray sources, such as Seyfert Type 1 galaxies, many BL Lac objects, and QSO's (e.g. Stein and Weedman 1976; Stein et al. 1976). This UV-strong characteristic originates in the flat or power-law optical continuum that characterizes most of the optical counterparts described as category #1 (optical flux analogous to the X-ray emission) in Section 2-3.

A further screening of candidate objects is frequently made from photoelectric photometry (U B V) measurements. The photometry quantifies U-B judgments made from viewing the Schmidt plates, and the color indices (U-B vs. B-V) may reveal significant deviations from the main sequence (see Bradt and McClintock 1983). In a few cases the evidence of photometric variability has promoted candidates that were later identified as cataclysmic variable systems.

(4) After a list of candidates is assembled, the objects are studied spectroscopically to determine their physical nature. Spectral classifications can secure an identification if the object is a member of a well known class of X-ray emitters (with plausible implied luminosity) or if its class is too rare to be located by chance in or near an error diamond. The goal is to make an objective statement about the likelihood of the proposed identification and about the nature and distinguishing

optical properties of the counterpart. The issues which must be judged in evaluating the likelihood of the identification are discussed in greater detail in the next section.

In various special cases we have also carried out objective prism photography and radio observations (e.g. Schmelz et al. 1984) of X-ray source fields. The purpose here is primarily to identify reddened optical counterparts or the rare AGN that exhibit red optical continua (Stocke et al. 1983). The radio detections also provide important information regarding the classification of RS CVn and BL Lac type candidates.

Most of the known classes of X-ray sources detected by HEAO-1 (Wood et al 1984) have optical counterparts that would be recognized by one or more of the above criteria. The exceptions are some very bright X-ray sources that have intrinsically faint optical counterparts (some of the low mass X-ray binaries), and others that are heavily obscured by interstellar matter or lie in severely crowded fields. These exceptions are primarily very near the galactic plane.

4-2. <u>Criteria for a Proposed Identification</u>

To evaluate the probability that a given candidate is the optical counterpart of the X-ray source, one should consider:

(1) the object's position with respect to the allowed X-ray positions,

(2) the statistical significance of the X-ray detections,

(3) the spectral classification or the optical spectral properties of the candidate,

(4) the implied L_x/L_{opt} value in relation to the values for other

members of the particular class of sources, and

(5) the celestial surface density of members of the class that are
brighter than or about equal to the apparent magnitude of the candidate
object. Identification claims must not be blind to chance coincidences
of common types of objects at the allowed X-ray positions.

When all of these factors favor a particular candidate, it is
extremely likely that the candidate is the correct identification. With
few exceptions, the identifications of bright X-ray sources that were
made on the basis of these considerations have been confirmed in subse-
quent X-ray images with spatial resolutions between arcseconds and one
arcminute (see Bradt and McClintock 1983).

The judgment that a candidate is a "probable" or a "very probable"
identification of the X-ray source can be made if several of the criteria
favor the candidate, while the remaining ones do not bear strong evidence
against the candidate, and a systematic effort has been made to locate
and study optical candidate objects. In the early days of X-ray astro-
nomy many identifications were gained from very significant (10-200 σ)
X-ray detections with unique positions from the combined results of
survey experiments. However, the initial optical evidence was often much
less certain (e.g. UV excess only), and constraints from the implied
L_x/L_{opt} values were therefore inapplicable. The effort to identify the
fainter HEAO-1 sources tends to be the converse situation, in which the
optical classification may be very clear and the distribution of L_x/L_{opt}
among the class members may be well known, but the X-ray positions are
spread over a much larger celestial region (as many as 40 diamonds in a
$\sim 1^{\circ} \times 2^{\circ}$ area).

4-3. <u>Observatories and Instruments Used in this Research</u>

The UV-strong candidate objects were obtained from Schmidt telescope photography using the 36"/24" (primary and corrector lens diameters, respectively) Schmidt telescopes at Cerro Tololo Interamerican Observatory (CTIO) and at Kitt Peak National Observatory (KPNO), and also with the 24"/16" Uppsala Schmidt telescope at Siding Spring Observatory in Australia. The photographs were made with standard UGI or UGII (U) and GG385 (B) filters, using IIaO or IIIaJ emulsion-type plates. The exposure times were 45 and 9 min (U and B, respectively) with the 36"/24" telescopes and 90 and 18 min with the Uppsala Schmidt.

The optical spectra were obtained at several observatories, using standard observatory spectrographs and data reduction systems. Many of the spectra shown in Chapters 6-9 were obtained at the 3.9 m Anglo-Australian Telescope with the RGO Spectrograph and the IPCS. This is a two-dimensional, photon-counting system with $\lambda\lambda 3000 - 7500$ Å sensitivity; the AGN observations were conducted with a spectral resolution of ~ 10 Å FWHM. At CTIO the SIT vidicon system (Atwood <u>et al.</u> 1979) and "Big Red" image tube were used on the 1.5 m telescope ($\lambda\lambda$ 3700 - 7500 Å with resolution ~ 15 Å FWHM). Spectra were also obtained with the Mark II system, which is a photon-counting, intensified Reticon scanner ($\lambda\lambda 3700 -$ 7400 Å sensitivity with resolution ~ 15 Å) used on the 1.3 m telescope at the McGraw-Hill Observatory (see Shectman and Hiltner 1976). Data reduction procedures for the Mark II have been described by Canizares, McClintock, and Ricker (1978). The flux calibrations of the spectra were made by observing the standard stars of Oke (1974) or Stone (1977).

Optical photoelectric photometry was performed with the 1.0 m telescope of the Australia National University at Siding Spring Observa-

tory, with the 1.0 m (Yale) Telescope at CTIO, and also with the #2 1.0 m telescope on Kitt Peak. The A.N.U. observations employed a 2-channel photometer (Bessell 1985) with 1P21 and S-20 photomultiplier tubes, while both the CTIO and KPNO photometric observations were made with single channel photometers and RCA 31034 photomulplier tubes. In every case, the measuring diaphragm was 19 or 20 arcsec. All of the photometric observations were made during clear and moonless conditions, with 1-3" seeing. The data were corrected for atmospheric extinction and converted to U,B,V magnitudes by observing photoelectric standards of Landolt (1983) and Graham (1982).

Optical photometry was also performed with the "MASCOT" CCD camera, which was built at the M.I.T. Center for Space Research (Ricker et al. 1981). The MASCOT was used on the 1.3 m telescope at McGraw-Hill Observatory, to record "direct" images at a spatial resolution of about 1.6 arcsec per pixel. Data reduction was performed in the "usual" way (see McClintock et al. 1983). Bias frames and dark frames were subtracted, and the image was normalized by (appropriately filtered) "flat field" observations of the dawn sky. Absolute flux calibration was achieved by observing standard stars of Landolt (1983) and by processing those observations through the same data reduction sequence.

V. RESULTS OF THE OPTICAL INVESTIGATIONS

5-1. Selection of the Unidentified Sources

All of the "unidentified" sources targeted for optical search procedures were detected by both the MC and the LASS experiments. When the program investigations began, the source had not been identified by the MC group or by investigators using the imaging instruments of the Einstein Observatory. Furthermore, the selection categories were:

(1) the source was not listed with a suggested identification in the preliminary (incomplete) LASS catalog that was submitted to the National Data Archive in 1981, or

(2) the MC results were not consistent with the suggested identification given in the preliminary LASS catalog. In most of these cases, the suggested identification was a cluster of galaxies, which are extended X-ray sources, but the MC result indicated a point-like source.

5-2. X-ray Sources and Optical Candidates

The author completed at least one iteration through the four steps of the optical search program (Section 4-1) for 108 X-ray sources. The search procedures have been started for an additional 60 sources, and there are about 150 others for which the MC results are being mapped and Schmidt plates are being taken.

Table 5-1 lists the 108 sources for which all of the candidates were spectroscopically observed on at least one occasion. The optical candidates and their spectral classifications are given, and a summary of the MC result is also included. A detailed presentation is given in Chapters

6 through 8 for 20 (of the 25) newly classified objects. Of these 20
objects, 19 are judged to be "probable" or "very probable" identifica-
tions of the X-ray sources (the distinctions among the ID judgments are
explained below). A summary of the types of candidate objects is given
in Table 5-2, and some general conclusions regarding the program and the
identified sources are given in Chapter 9.

The columns of Table 5-1 are organized as follows:

Col. 1: On the top line of this column is the HEAO-LASS name ("1H") from
the published catalog by Wood et al. (1984). An asterisk appended to
this name indicates that the MC produces two positional results that
appear to be clearly separated in energy channels and/or the ranges in
elevation angle, indicating two sources in the field. There are two such
cases, and each will show two MC detections. Beneath the LASS name is a
list of the other X-ray experiments that apparently detected the same
X-ray source. The code "U" designates the Uhuru survey (Forman et al.
1978); "A" denotes Ariel V (McHardy et al. 1981, Warwick et al. 1981, or
Ricketts 1978); "H" is the HEAO A-2 (Goddard) experiment, with catalogs
referenced in Section 3-2); "M" is the OSO-7 survey (Markert et al.
1979); and finally "E" is used in the two cases in which the detections
by the Einstein IPC instrument helped to locate the object.

Cols. 2 and 3: The Modulation Collimator detections are summarized in
these columns. On the top line is the statistical significance of the
MC detections (i.e. the apparent strength of the source expressed as a
number of standard deviations, σ, where σ is the statistical uncertainty
of the background measurement). The statistical significances for MC1
and MC2 are listed in Col. 2 and Col. 3, respectively. On the lower
line, the first entry (Col. 2) indicates the energy channel(s) which is

common to both collimators' detections. Channel "A" is the 0.9 to 2.5

keV energy band, channel "B" is the range of 2.5 to 5.5 keV, and channel

"C" is 5.5 to 13.0 keV. A multiple entry indicates a detection from a

sum of the listed energy channels, e.g. "ABC" indicates the sum of all

three energy channels (1-13 keV). The next entry (lower line of column

3) is the number of celestial scans that contributed to the MC detection

(each "scan" is a set of transits during a period $\geq$ 4 days, and a scan

was completed by HEAO-1 every 6 months; see Section 3-4).

Col. 4: The galactic latitude of the center of the LASS error box is

listed to correlate the success rate of the program as a function of the

angular diplacement from the galactic plane.

Col. 5: This column lists the candidate optical counterparts for each

X-ray source. Any catalog designations (optical, radio, etc) of the

object are given in this column. If a "$\sqrt{}$" is entered without a catalog

name, then the candidate object was discovered during the optical search.

If a "$\sqrt{}$" is present in conjunction with a catalog entry, then the object

was catalogued, but its distinguishing spectral type was unknown.

Examples in the latter category include a QSO discovered at the position

of an unidentified radio source, and several RS CVn systems that were

cataloged SAO stars listed with normal (typically K0) spectral types.

Col 6: The spectral classification of the candidate is entered in column

6. The classification is appended with a "?" if the judgment is not

completely certain.

Col 7: This column contains the apparent visual magnitude of the candi-

date object. A "v" indicates that the object is known to be variable,

but the precise range cannot be specified.

Col 8: The ID status code assesses the overall probability that the

candidate is the unique optical counterpart of the X-ray source. This judgment is based on the strength of the MC detection and the optical properties of the candidate. The specific issues were given in Section 4-2. The code "A" indicates that the identification is very probable. The object's classification and optical characteristics support the identification, and its position is consistent with the X-ray results, including an MC detection by both collimators. A "B" case is a probable identification, in which the optical evidence supports the candidate, but the positional constraints are not as decisive. Single collimator MC results are included in this category, unless the source is believed to be spatially extended and the detection is by MC2 (see explanation near the end of Section 3-4). Finally, code "C" is a possible identification, requiring more revealing optical information or a confirming X-ray measurement. Suspected bright stars constitute most of the examples.

Table 5-1: X-ray Fields Optically Searched

X-RAY NAMES (1)	MC DETECTION (2)	(3)	GAL. LAT. (4)	OPTICAL CANDIDATES (5)	SPEC. TYPE (6)	V (7)	CODE (8)
HEAO LASS Other X-ray	MC1 Chan.	MC2 #Scans	deg.	CATALOG $\sqrt{=}$ Previously Unknown	Class	mags	ID
1H0025+588 U,A	3.0 ABC	3.9 1	-3.6				
1H0048+250	3.1 BC	3.4 1	-37.6	PG0052+251	QSO	15.0	B
1H0055+753	- ABC	4.2 1	12.7				

X-RAY NAMES (1)	MC DETECTION (2)	(3)	GAL. LAT. (4)	OPTICAL CANDIDATES (5)	SPEC. TYPE (6)	V (7)	CODE (8)
HEAO LASS Other X-ray	MC1 Chan.	MC2 #Scans	deg.	CATALOG √= Previously Unknown	Class	mags	ID
1H0106+324	3.0 ABC	3.0 1	-30.0	√	BL Lac?	15.8	A?
1H0130+473	– ABC	3.9 1	-14.7				
1H0150-535	– BC	3.7 3	-61.5	√	QSO	17.0	B
1H0157+142	4.6 AB	3.2 2	-45.2	TT Ari	CV	~15	A
1H0201-029	3.3 BC	4.8 2	-60.1	√	QSO	16.9	A
1H0258+443 H	2.9 C	2.9 2	-12.4				
1H0307-722	3.1 ABC	2.6 3	-41.4	√	Sy 1	14.9	A
1H0310+576	4.1 BC	4.0 1	0.1				
1H0350-735 U	3.4 AB	4.7 3	-38.1				
1H0350+472 U	3.1 B	2.8 2	-4.9				
1H0413-116	2.7 B	4.0 1	-39.6				
1H0414-551 U	3.1 A	2.9 2	-43.9				
1H0422-086 U	3.1 ABC	3.1 3	-36.3				
1H0433-088	3.2 A	3.1 1	-34.0				
1H0435-274	3.0 AB	3.1 3	-40.3				

X-RAY NAMES (1)	MC DETECTION		GAL. LAT. (4)	OPTICAL CANDIDATES (5)	SPEC. TYPE (6)	V (7)	CODE (8)
HEAO LASS Other X-ray	MC1 Chan.	MC2 #Scans	deg.	CATALOG √= Previously Unknown	Class	mags	ID
1H0435-531	3.0 AB	3.0 2	-41.4				
1H0437+206	3.1 C	3.5 2	-16.8				
1H0441-207*	4.2 AB	3.9 1	-37.0				
"	3.2 BC	3.0 2	"				
1H0443+836	5.1 B	3.0 1	24.0				
1H0455+518	3.7 ABC	3.1 2	5.8				
1H0456+304	5.0 BC	3.4 3	-7.3	Dark Cloud?			C
1H0458-326	4.2 AB	3.9 1	-36.6				
1H0458-367 U	- ABC	4.3 3	-37.3				
1H0459+230 A?	3.5 C	3.1 1	-11.4				
1H0459+248 A?,E	2.7 ABC	4.4 2	-10.3	√	CV	15.6	A
1H0502-755	3.2 AB	3.3 3	-33.0	HD32918	RS CVn	8.14	A
1H0506-039 U	3.0 B	4.6 2	-24.6	SAO131838	B9	7.7	C
1H0509+166 U,H,E	3.0 B	2.9 2	-13.1	√	Sy 1	~15	A
1H0523-118	2.4 AB	4.0 3	-24.2	√	Sy 1	15.0	A

X-RAY NAMES (1)	MC DETECTION (2) (3)		GAL. LAT. (4)	OPTICAL CANDIDATES (5)	SPEC. TYPE (6)	V (7)	CODE (8)
HEAO LASS Other X-ray	MC1 Chan.	MC2 #Scans	deg.	CATALOG √= Previously Unknown	Class	mags	ID
1H0533+607 U	3.5 BC	4.4 2	15.2	√	CV	14.4-15.5	A
1H0538-577 H	3.5 BC	5.2 3	-32.2	√	CV	14.8v	A
1H0538+401	3.9 B	3.1 2	5.3				
1H0539-226	3.2 ABC	3.4 2	-25.0				
1H0542-407	2.4 AB	4.0 3	-29.4	√	CV	15.9v	A
1H0543-289	3.0 ABC	3.1 2	-26.2	SA0170915 √	RS Cvn	8.5	A
1H0547-575 U	3.2 AB	3.1 2	-31.0	√	Sy2?	∼15	B?
1H0556+286 U	3.1 ABC	3.3 3	2.6	HD249179	Be	9.87	A
1H0557-503	3.4 ABC	– 3	-28.7	PKS0559-504 √	QSO	15.0	B
1H0613+479 A	3.5 C	2.8 2	14.5				
1H0620-646 H	– BC	5.7 3	-27.6	SC0620-646	Cluster		A
1H0633-752 A?	2.9 ABC	2.9 2	-27.4	PKS0633-75	QSO	∼16	B
1H0635-431	3.3 C	3.2 3	-20.7	SA0218071	B8	3.2	C
1H0659-494 U	3.0 BC	3.4 3	-18.8	√	Sy 1	15.7	A
1H0706-567* U,H	3.7 A	3.1 3	-20.3				

X-RAY NAMES (1)	MC DETECTION (2) (3)		GAL. LAT. (4)	OPTICAL CANDIDATES (5)	SPEC. TYPE (6)	V (7)	CODE (8)
HEAO LASS Other X-ray	MC1 Chan.	MC2 #Scans	deg.	CATALOG √= Previously Unknown	Class	mags	ID
"	3.6 AB	3.5 2	"				
1H0707+443 A	3.6 ABC	3.3 2	21.9				
1H0709-360 A,U,M	2.4 B	4.6 1	11.9				
1H0713-112 H	4.3 B	4.0 2	0.1				
1H0714-630	3.6 BC	2.9 1	-21.5				
1H0737-668	- B	4.4 2	-20.5				
1H0741+289	3.0 A	3.3 2	23.5	Sigma Gem	RS CVn	4.3	A
1H0745-191 U,A	- B	4.1 2	3.0				
1H0759-490 U	2.8 B	3.1 2	-9.9				
1H0806-545 U	3.0 ABC	3.4 2	-11.8				
1H0809+796	2.8 A	4.0 2	30.5				
1H0815-571 U,A	3.7 ABC	4.4 2	-12.0				
1H0846-534 H	3.9 2	4.3	-6.3				
1H0900-482 U	4.0 ABC	3.2 1	-1.3				
1H0921+633 U	3.2 B	4.2 2	41.0				

X-RAY NAMES (1)	MC DETECTION (2)	(3)	GAL. LAT. (4)	OPTICAL CANDIDATES (5)	SPEC. TYPE (6)	V (7)	CODE (8)
HEAO LASS Other X-ray	MC1 Chan.	MC2 #Scans	deg.	CATALOG √= Previously Unknown	Class	mags	ID
1H1005-365	3.5 AB	3.7 1	15.4				
1H1012-574 A	3.8 C	3.5 1	-1.1	SAO238130	Be	6.9	A
1H1012-399 U	3.2 BC	3.7 3	13.4				
1H1013+498 A,H	3.2 A	3.3 3	52.9				
1H1023+513 H	3.2 B	3.2 3	53.7	Mkn 142	Sy 1	~15	B
1H1027-351 A?	- C	4.3 3	19.1	Group of NGC Galaxies			A
1H1100-230 U,A	3.0 B	2.9 2	33.2	√	BL Lac Obj.	16.5	A
1H1142-178 A	2.6 AB	3.1 2	42.0	√	Sy 1	14.6	A
1H1244-588 H,U	7.3 AB	4.1 2	3.8				
1H1303-047	2.7 A	3.8 1	57.7	SAO139157 √	RS CVn	8.4	A
1H1312+393	3.2 A	3.1 1	77.1				
1H1313+363 A,H	3.2 A	3.0 1	79.6				
1H1325-246	- AB	3.2 2	37.2	√	Sy 1	15.7	B
1H1332-233	3.3 AB	4.7 2	38.2	SAO181689	KO	9.1	C
1H1348-633 M	3.5 AB	4.2 3	-1.5				

X-RAY NAMES (1)	MC DETECTION (2) (3)		GAL. LAT. (4)	OPTICAL CANDIDATES (5)	SPEC. TYPE (6)	V (7)	CODE (8)
HEAO LASS Other X-ray	MC1 Chan.	MC2 #Scans	deg.	CATALOG √= Previously Unknown	Class	mags	ID
1H1400-478	3.2 ABC	4.3 1	13.1				
1H1424+350	3.8 A	3.4 2	68.2				
1H1430+423 A,U?	3.0 B	3.8 2	64.6	√	BL Lac Obj.	16.4	A
1H1444-553 U	3.8 BC	4.0 2	3.7				
1H1539-323	3.3 ABC	4.1 2	17.9				
1H1535-445 U	3.0 ABC	3.5 1	8.6				
1H1600-757	3.7 ABC	3.5 1	-17.4				
1H1613-060	3.9 ABC	3.3 1	30.4				
1H1625-333 U	3.5 B	3.1 2	10.5				
1H1645-596 U,H	3.3 B	3.0 2	-9.6				
1H1646+152	4.4 ABC	4.1 3	34.0				
1H1758-482	3.8 AB	3.0 3	-12.4	SA0228707	RS CVn	7.1	B
1H1832-076 A,H	5.5 BC	6.3 1	0.1				
1H1836-786 H,M	4.0 BC	2.9 3	-26.2	√	Sy 1	15.6	B
1H1907+074 A,U	8.9 BC	7.1 3	-0.6				

X-RAY NAMES (1)	MC DETECTION		GAL. LAT. (4)	OPTICAL CANDIDATES (5)	SPEC. TYPE (6)	V (7)	CODE (8)
	(2)	(3)					
HEAO LASS Other X-ray	MC1 Chan.	MC2 #Scans	deg.	CATALOG √= Previously Unknown	Class	mags	ID
1H1927-516	3.5 A	3.8 3	-27.0	√	Sy 1	15.2	B
1H1929+509 H	3.4 AB	3.9 2	15.1	√	CV		B
1H1934-063	3.3 AB	3.1 2	13.0	√	Sy 1	15.3	A
1H2010-697 U	4.2 BC	3.1 3	-32.6	√ BL Lac Obj. ?		16-18	B?
1H2032-358	3.3 A	3.1 2	-35.7				
1H2107-097	3.1 BC	4.7 1	-35.1	√	Sy 1	14.3	A
1H2129-624	- C	3.1 3	-42.3	√	Sy 1	15.1	B
1H2158-602 A,M	3.5 AB	3.4 2	-46.4				
1H2207+455	5.0 AB	2.4 1	-8.3	AR Lac (=SAO051684)	RS CVn	6.9-7.7	A
1H2226-269 A	3.0 A	3.2 2	-58.4	NGC 7313	?	~15	C
1H2236-372 A,H	3.6 B	3.4 3	-60.4				
1H2251+450	4.1 B	4.0 1	-12.8				
1H2303+039	3.6 AB	4.3 3	-49.6	PG2303+039	Sy 1	~15.5	A
1H2313+783	- A	5.4 1	16.7				
1H2322-269 A	- BC	4.4 2	-70.8				

X-RAY NAMES (1)	MC DETECTION (2)	(3)	GAL. LAT. (4)	OPTICAL CANDIDATES (5)		SPEC. TYPE (6)	V (7)	CODE (8)
HEAO LASS Other X-ray	MC1 Chan.	MC2 #Scans	deg.	CATALOG √= Previously Unknown		Class	mags	ID
1H2351-315	3.3 BC	2.9 3	-76.9	√ √	BL	Lac Obj.? Sy 1	17.5 15.9	A? C
1H2355-350 U	– BC	5.0 1	-76.3	PKS2354-35	√	Active Elliptical	14.0	A

Table 5-2: Types of Candidates

Total Number of Sources Investigated   108

Total Number of Sources with Candidates   46 (43%)

Candidates by ID Status:	Status	ID Code
	"A"	26
	"B"	11
	"C"	5
	"?"	4

Candidates by Spectral Type:

Spec. Type	Number Codes A and B	(# Cataloged, #Prev. Unknown)		Number Codes C and ?
Seyfert Type 1	13	(2,	11)	0
QSO	5	(2,	3)	0
BL Lac Objects	2	(0,	2)	3
Cluster of Galaxies	2	(2,	0)	0
Other Extragalactic	1	(0,	1)	2
Cataclysmic Variable	6	(1,	5)	0
Be Star	2	(2,	0)	0
RS CVn Type	6	(4,	2)	1
Very Bright Stars	0			2
Other Galactic	0			1
Totals:	37	(13,	24)	9

VI. FOURTEEN BROAD-LINE ACTIVE GALACTIC NUCLEI

6-1. Introduction

This chapter presents a detailed spectral analysis of fourteen active galactic nuclei (AGN) that were discovered by the author in the effort to optically identify the X-ray sources of the HEAO-1 survey. Eleven are Seyfert Type 1 (Sy 1) galaxies and the other three are quasi-stellar objects (QSO's). The only essential difference between these classifications is the visibility of the host galaxy of Sy 1 types in the photographs of the Palomar or ESO sky surveys. All but one of the fourteen AGN exhibit the spectral and positional requirements necessary to identify the X-ray sources. A fifteenth newly discovered AGN is listed in Table 5-1 (1H1325-246), but the quality of the available spectrum does not warrant detailed analysis.

Twelve of the fourteen AGN are nearby objects (low redshifts), and their optical spectra are described in detail in Section 6-2. The optical and X-ray fluxes of this group place them among the ~ 100 brightest known Sy 1 galaxies and QSO's. Furthermore, many of the discoveries exhibit unusual spectral characteristics that will motivate additional studies. The remaining two are distant QSO's, and they show strong absorption lines in addition to their emission spectra. They will be reported separately in Section 6-4. The remaining part of Section 6-1 is an introduction to AGN classifications, redshifts, and emission properties. The definitions of additional spectral measurement terms that are used throughout Chapters 6-8, such as line fluxes, line widths, and equivalent widths, are given in the Appendix.

AGN are defined as galaxies that contain bright, stellar-appearing

(i.e. having small angular size) sources of radiation that show spectral characteristics distinctly different from any summed distribution of normal stars, HII regions, and supernova remnants, which are the usual luminous ingredients of a galaxy (Balick and Heckman 1982). The category is composed of QSO's, Seyfert galaxies, some other variously labeled narrow emission-line galaxies (a complicated topic), some radio galaxies, and BL Lac type objects. The bright AGN constitute about 1-3 % of giant spiral galaxies (Simkin et al. 1980); however, low-level nuclear activity may be quite common (Phillips et al. 1983).

With the exception of BL Lac objects (see Chapter 7), AGN show broadened optical emission lines covering a wide range of ionizations (see Osterbrock 1984). Sy 1 and QSO's have very broad permitted lines (e.g. transitions of H, He, Fe, Mg, and C), that have "full widths at zero intensity" (FWZI, see the Appendix) that are greater than about 3500 km s^{-1}. They also have forbidden lines (e.g. low-probability transitions of O, N, Ne, and S), which are much narrower (FWZI < 2000 km s^{-1}). Seyfert Type 2 galaxies are different, in that the permitted and forbidden lines are both narrow, with FWZI in the range of 500 to 3000 km s^{-1} (Khachikian and Weedman 1974; see FWZI tabulation in Steiner 1981).

The distance (d) to an emission-line AGN is determined by measuring the Doppler redshift of the emission lines and then applying Hubble's law. The redshift parameter, z, is a normalized measure of the changes in wavelength: $z = (\lambda - \lambda_o) / \lambda_o$, where λ is the observed (apparent) wavelength of an emission feature that is identified with a quantum transition having a wavelength of λ_o in the rest frame (laboratory). To first order, all of the emission features of an individual object will have the same value of z. This research

employs a commonly used form of Hubble's law, which assumes "big bang" cosmology with a deceleration parameter, q_o = 0 (see Allen 1976). In that case:
$$d = c \, z \, (1 + z/2) \, / \, H_o,$$
where c is the speed of light and H_o is the Hubble constant, here assumed to be 50 km s^{-1} Mpc^{-1}.

AGN are a firmly established class of X-ray sources (Elvis et al 1978; Tananbaum et al. 1978), and the MC has been used to identify the X-ray emission from many known examples of Sy 1 and other types of emission-line galaxies (Griffiths et al 1979a,b; Dower et al 1980). The Einstein Observatory (1979-81) has further extended the AGN sample by discovering many AGN from serendipitous detections in X-ray images of fields at high galactic latitude (e.g., Grindlay et al. 1980; Chanan et al. 1981; Reichert et al. 1982; Kriss and Canizares 1982; Stocke et al. 1983; and Pravdo and Marshall 1984). Most of the galaxies presented here are a factor of 10 to 100 brighter at both X-ray and optical wavelengths than most of the serendipitous Einstein AGN.

Many of the current studies of AGN require accurate measurements of the emission line fluxes so that (1) the observations can be compared to the predictions of various physical models, and (2) correlations may be tested with the hope of extracting diagnostic relations among the various types of measurements (optical, radio, X-ray, infrared, etc). Model calculations of the emitted spectra of a gas that is photoionized by a power-law UV continuum have reproduced many of the observed spectral characteristics (Davidson and Netzer 1979; Koski 1978). However, many more details regarding these diverse objects are not understood, and a basic comprehension of their structure and evolution is not available (see Osterbrock 1984). To facilitate this research, the flux measures

and line widths of selected emission lines will be reported for the
twelve nearby AGN, which are observed at the optical and near-UV
wavelengths that are most useful to theoreticians.

6-2. Twelve Nearby AGN

In Figs. 6-1 and 6-2 the positions of the twelve AGN are shown in
comparison with HEAO-1 and other X-ray positions. The statistical
significance of the X-ray detections are discussed for each source later
in this section. Apologies are given for the order in which the AGN are
described. There is an order of right ascension, but there are two
sequences because the graphic work was organized for articles submitted
or in preparation for publication.

The MC results for each of the AGN include data from two or three
celestial scans by HEAO-1, except for H2106-099, which shows evidence of
X-ray variability. In addition, all of the MC detections appear spatial-
ly unresolved, which indicates that the angular sizes of the X-ray
sources are $\lesssim$ 1 arcmin. In the next section it is shown that the proba-
bility of a spurious identification is small.

The X-ray fluxes reported below are derived from the cataloged LASS
counting rates, assuming a 2-10 keV conversion factor of 2.0×10^{-3} LASS
cts cm^{-2} s^{-1} per 1.0×10^{-11} erg cm^{-2} s^{-1}. This factor was determined
from a comparison of LASS count rates and the HEAO A-2 flux measurements
of bright Sy 1 galaxies (Mushotzky et al. 1980). This result is within
10% of the nominal 2-10 keV conversion factor given by Wood et al. (1984)
for a Crab-like spectrum. The r.m.s. statistical error in the LASS
counting rates for the fourteen X-ray sources is $\pm$ 14%.

Fig. 6-1. Maps containing eight positions of low-redshift AGN (heavy plus) and the allowed X-ray positions from the HEAO-MC (diamonds or bands, depending on whether both or a single collimator produces a detection). The X-ray error boxes are from the HEAO-LASS ("1H"; Wood et al. 1984), the GSFC (HEAO A-2) Survey ("H"; Marshall et al. 1979), Uhuru ("U"; Forman et al. 1978), and the Ariel 5 Sky Survey Instrument ("A"; Ricketts 1978). The dashed lines indicate the LASS line of position that is obtained from the independent analysis of the LASS data by the MC group (see the end of Sectio 3-4).

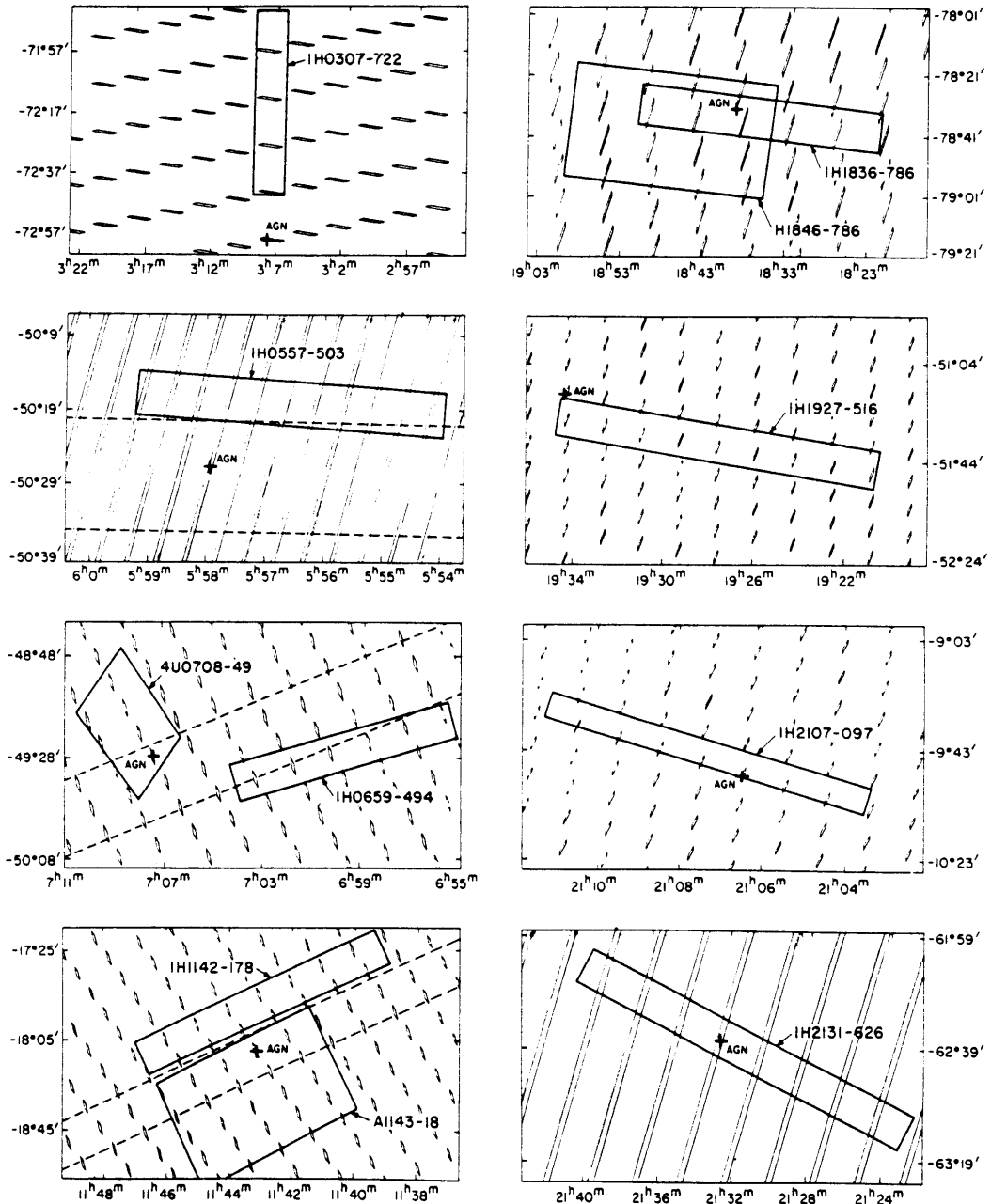Fig. 6-2. Maps containing the positions of four low-redshift AGN (heavy plus) and the allowed X-ray positions from the HEAO-MC (diamonds). The X-ray error boxes are from the HEAO-LASS ("1H"; Wood et al. 1984) and the GSFC (HEAO A-2) Survey ("H"; Marshall et al. 1979). For H0508+164 there is also an Uhuru position with a large uncertainty area (4U0517+17; Forman et al. 1978) that includes the position of the AGN.
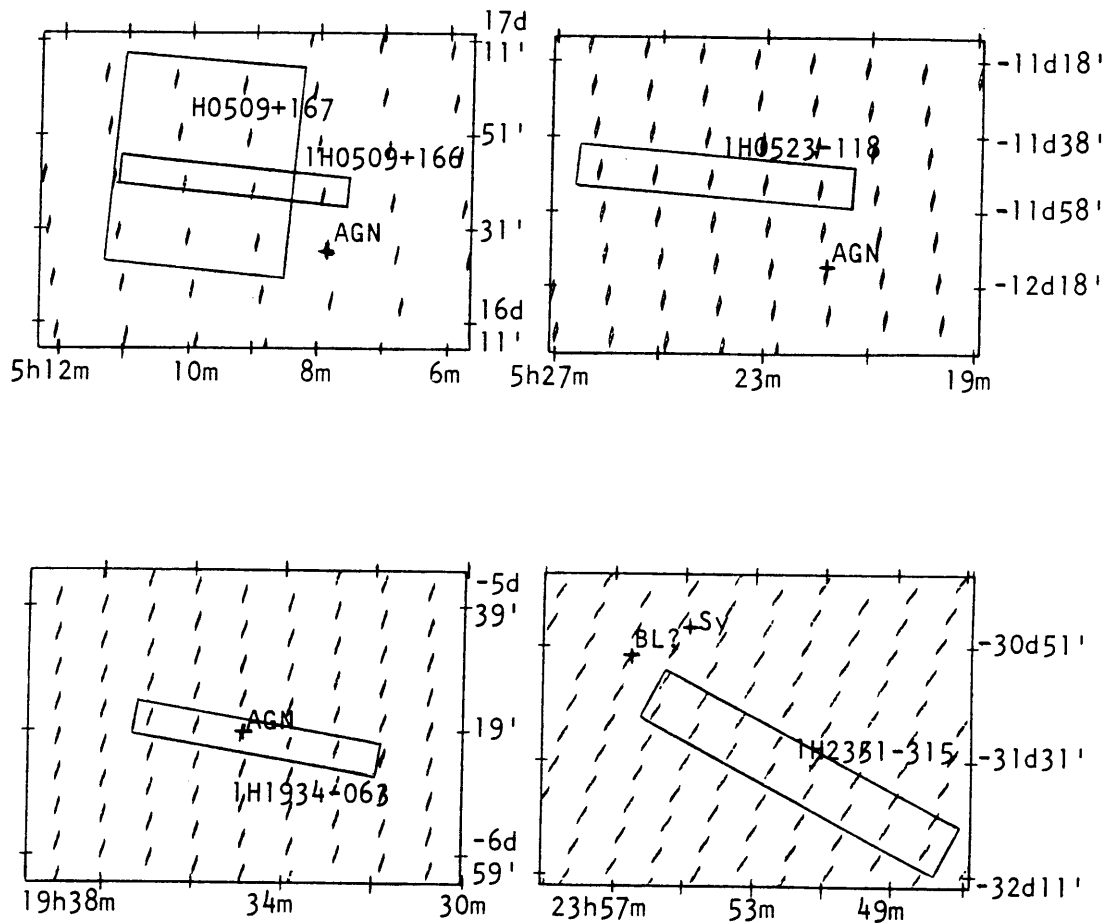
Table 6-1 contains the celestial positions, redshifts, photometric magnitudes, and X-ray and optical luminosities for each of the twelve nearby AGN. The astrometry was performed by Ms. Wendy Roberts at the Harvard measuring engine, and the results are typically accurate to 1". Table 6-1 also contains the optical/X-ray energy index, β_{ox}, that connects the optical continuum flux at $\lambda_o 4000$ Å with the X-ray flux at 2 keV (i.e. $F_\nu \propto \nu^{-\beta}$) in the rest frame of the AGN (see the Appendix). The continuum flux at $\lambda_o 4000$ is corrected for galactic extinction by estimating $A_V = 0.18$ csc b (e.g. Schmidt 1968) and then applying the E(λ-V) results of Bless and Savage (1972). Light loss at the spectrograph aperture is checked by comparing the integrated flux densities with the photometric results, using the photometric bandpasses and normalizations of Allen (1976). The calculations of β_{ox} and the absolute emission flux of Hβ include a scaling factor that brings the spectral and photometric magnitudes into agreement, unless the deviation can be attributed to the contribution of the host galaxy in the 20" aperture, as in the case of H0307-730. The X-ray flux density at 2 keV is calculated from the 2-10 keV flux by assuming an X-ray energy index of 0.7 (Mushotzky et al. 1980; Petre et al. 1984).

The eleven Seyfert galaxies show slightly extended optical images, and, as was mentioned above, this is the only distinction between the Sy 1 and QSO classifications. The stellar nuclei strongly dominate the optical emission for all of the Sy 1 galaxies except H0307-730.

The optical spectra of the AGN are shown in Figures 6-3, 6-4, and 6-5. The flux measurements of selected emission lines and the equivalent widths and FWZI of Hβ emission are given in Table 6-2. All of the AGN show hydrogen emission lines that are much broader than the forbidden

Table 6-1: Twelve Low-Redshift AGN

Name	Other X-ray Names	AGN Positions (1950.0) R.A.	DEC.	z (±.001)	V[a]	B-V	U-B	Mv[b]	ID[c] Status	Lx[d]	βox[e]
H0307-730	1H0307-722	03 07 40.1	-73 01 29	.0280	14.90	+0.58	-0.28	-21.5	A	43.75	1.03
H0508+164	4U0517+17 H0509+167 1H0509+166	05 07 52.6	16 26 16	.0169	~15.0	+0.90:	-	-	A	43.71	-
H0522-122	1H0523-108	05 21 47.4	-12 12 51	.0491	14.98:	+0.70:	-0.60:	-22.9	A	44.38	1.07
PKS0558-504	1H0557-503	05 58 34.6	-50 26 55	.1372	14.97	+0.21	-0.89	-25.1	B +	45.39	1.08
H0707-495	4U0708-49 1H0659-494	07 07 22.6	-49 28 13	.0411	15.70	+0.32	-0.71	-21.9*	A	44.24	1.06
H1143-182	A1143-18 1H1142-189	11 43 08.3	-18 10 37	.0330	14.58	+0.45	-0.56	-22.2	A	43.83	1.18
H1839-786	H1846-786 1H1836-786 1H1849-77	18 39 03.5	-78 35 06	.0743	15.55	+0.59	-0.77	-23.2	B +	44.86	0.95
H1934-513	H1928-520 1H1927-516	19 34 14.8	-51 16 35	.0403	15.20	+0.47	-0.81	-22.1	B	44.18	1.09
H1935-063	1H1934-063	19 34 52.7	-06 19 54	.0101	15.35:	+0.77:	-0.01:	-19.4*	A	43.13	0.98
H2106-099	1H2107-097	21 06 28.2	-09 52 29	.0268	14.32	+0.48	-0.63	-22.0	A	43.84	1.22
H2132-626	1H2129-624	21 32 33.2	-62 37 27	.0588	15.15	+0.53	-0.89	-22.9	B	44.53	1.04
H2353-307	?4U0009-33 1H2351-315	23 54 52.2	-30 44 16	.0310	15.94:	+0.65:	-0.71:	-20.6	C	<43.7	>1.03

[a] Optical photometry was performed with a 20" apertures. The 1σ errors are 0.04 in V and 0.05 in the color indices. A colon is used if the magnitudes or colors are calculated from the spectral flux densities (Allen 1976) rather than by photoelectric photometry. In those cases the uncertainties are about 50% larger.

[b] M_v was calculated from V with the assumptions H = 50km/s-Mpc and q_0 = 0, and with a correction for galactic absorption, A_v = 0.18 cosec b (Schmidt 1968). AGN at galactic latitudes < 20 deg. are marked with a "*", to indicate uncertainty in the use of a generalized extinction correction at those galactic latitudes.

[c] "A" objects are very probable identifications of the X-ray source. "B" objects are probable identifications, with less certain detections by the Modulation Collimator. "C" candidates are possible identifications. The "+" symbol is used if the identification has been subsequently confirmed by an imaging X-ray observation.

[d] L_x is the 2-10 keV X-ray luminosity if the AGN emits the measured HEAO-LASS flux (expressed as an upper limit in the case of H2353-307). The units are log (ergs cm^{-2} s^{-1}). In the case of H2106-099, the value pertains to the first HEAO-1 scan (see text).

[e] $β_{ox}$ is the power law index connecting the optical flux density at λ4000 Å with the X-ray flux density at 2 keV in the AGN rest frame. The flux density at λ4000 has been corrected for extinction in the galaxy and for light loss at the spectrograph aperture, and the flux density at 2 keV is calculated from the 2-10 keV flux by assuming an X-ray energy index of 0.7 (see text).

Table 6-2: Optical Spectral Measurements

				RELATIVE LINE FLUXES (Hβ ≡ 1.0)[c]									
Name	FWZI (Hβ) (km/s)	E.W. Hβ[a]	LINE FLUX of Hβ[b]	Hα λ6562	Hγ λ4340	Hδ λ4101	HeI λ5876	HeII λ4686	FeII sum[d]	OIII λ5007	OII λ3727	NeIII λ3868	NeV λ3426
H0307-730	9400	36.9	1.08	2.95:	.33	.15:	...	...	1.47	0.24	.030	.024	.050
H0508+164	9700	121.0	-	6.55	.17	.04:	...	.19	...	2.20	.03:	.02:	xx
H0522-122	>20000	129.7:	3.52:	3.67:	.36:	.10:	.08:	.14:	0.59:	1.32:	.11:	.070:	.075:
PKS0558-504	6400	48.7	1.58	xx	.24	.16	.12	...	1.56	0.12:	.027	...	...
H0707-495	6300	60.7	1.04	2.22	.25	.16	.09	...	2.77	0.14:	.010	...	...
H1143-182	8000	119.2	4.86	3.76	.44	.22	.10	.30	...	1.21	.168	.083	xx
H1839-786	12000	151.7	2.46	3.87:	.30	.11	.12	...	0.77	0.30	.025	.032	.011
H1934-513	12600	155.5	3.77	2.45	.45	.19	.14	.25:	0.35:	0.22	.021	.021	.056
H1935-063	7300	89.0	1.86	5.29	.38	.10	.05	.17:	1.64	1.32	.099	.053	.064
H2106-099	10700	96.2	5.54	4.68	.41	.31	.42	...	1.05	0.29	.039	.091:	xx
H2132-626	10200	157.2	3.61	3.01:	.38	.19	.15	.10:	0.54:	0.56	.025	.043	.057
H2353-307	9500	49.9	0.70	3.19	.42	.18	.16	.17:	1.38	0.15	.039	...	...

[a] The equivalent width of Hβ in Å.

[b] The integrated flux of the Hβ emission line in units of 10^{-13} erg/cm^2-sec.

[c] Columns 5-14 contain the integrated line fluxes of selected emission lines normalized to Hβ emission, which is given in flux units in column 3. An "xx" indicates that the line was outside of the observed spectral range, and "..." used if the lines are not detected with significance > 3.5σ. A colon indicates uncertainty in the listed value. For Hα, HeII, FeII, and OIII, the uncertainty arises from blended lines of NII, FeII, HeII, and FeII, respectively; in the other cases the uncertainty is statistical. In the case of H0522-122, all of the values are somewhat uncertain, because the permitted lines (H, He, and Fe II) are so broad.

[d] The FeII flux is summed over two broad intervals to include the multiplets near λλ4570, 5190, and 5320, as labeled in Figures 6-3 to 6-5.

83

Fig. 6-3. Optical spectra of four AGN. H0307-730 and PKS0558-504 were observed at the AAT on (UT) Feb. 8, 1984, while H0707-495 was observed at the AAT on May 17, 1983. The spectrum of H1143-182 was obtained at the McGraw-Hill Observatory on March 15, 1983.
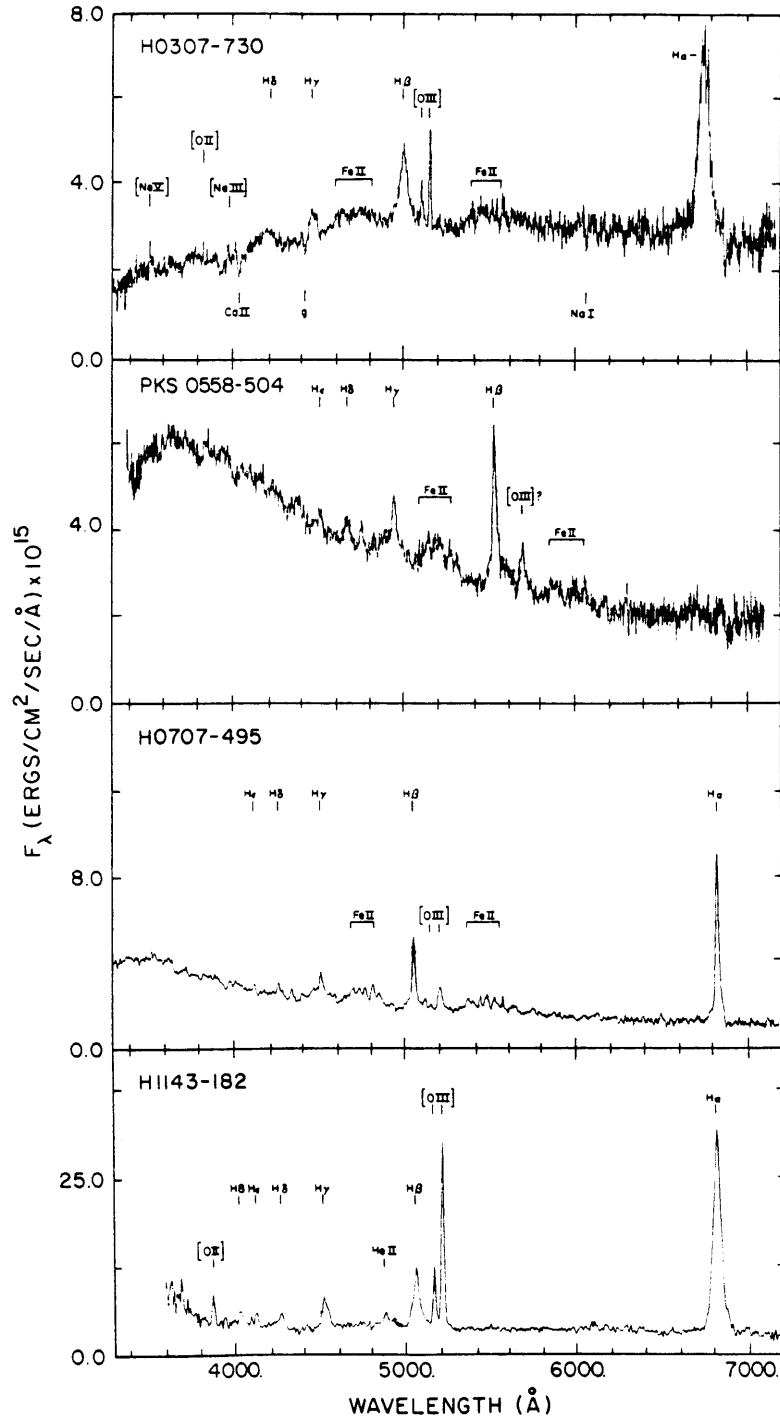
Fig. 6-4. Optical spectra of four AGN. The spectrum of H2106-099 was obtained at CTIO on (UT) Oct. 25, 1982, and the other three AGN were observed at the AAT on May 17, 1983.
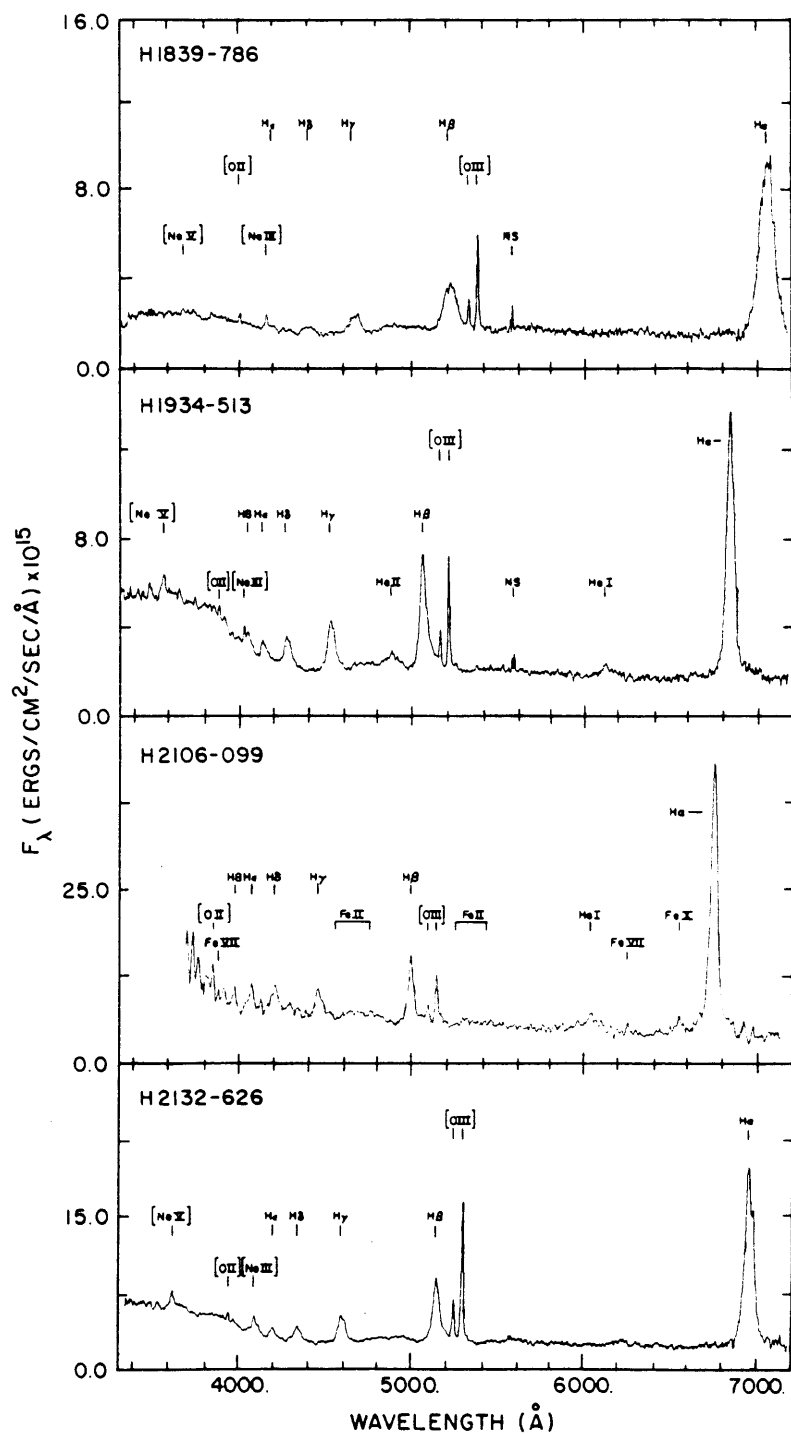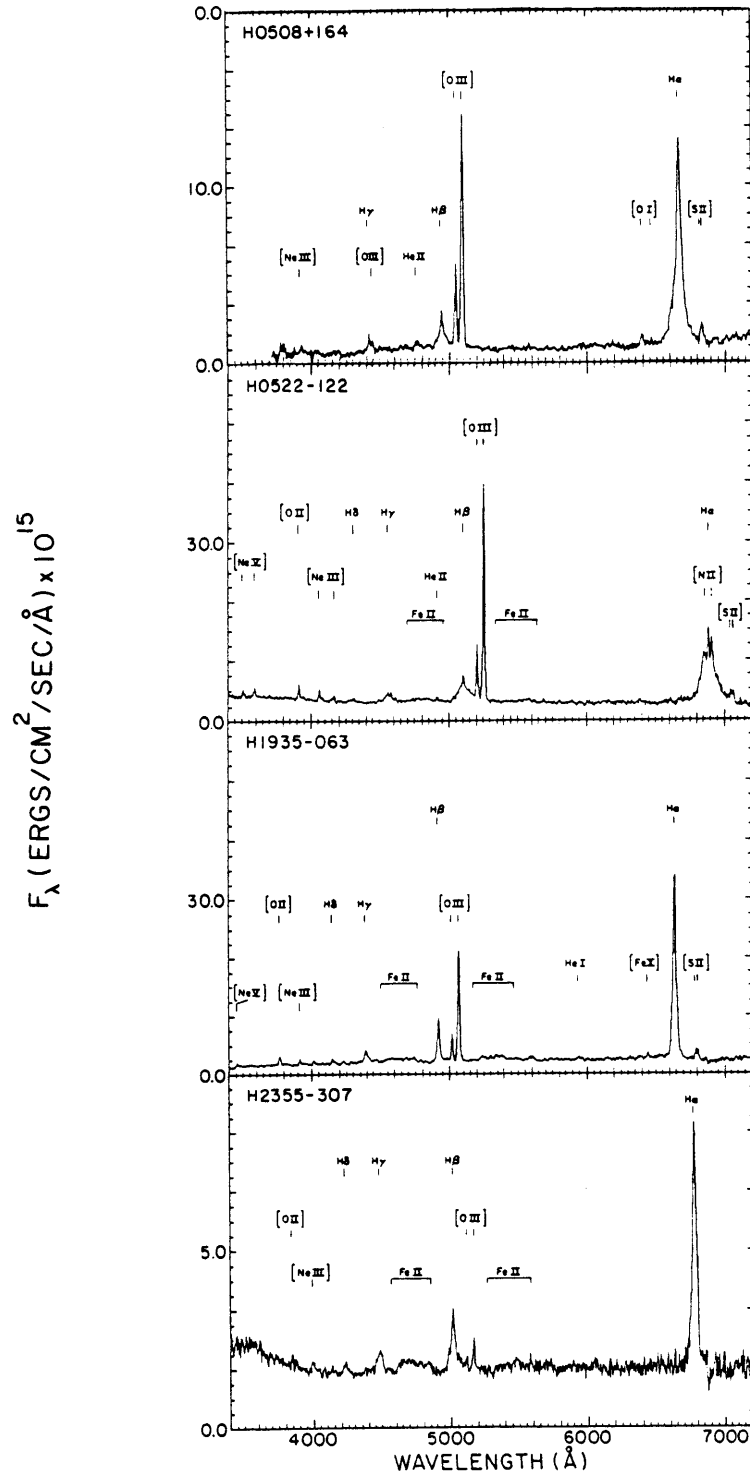
Fig. 6-5. Optical spectra of four AGN. The spectrum of H0508+164 was obtained at the McGraw-Hill Observatory on (UT) Dec. 23, 1982. The other AGN were observed at the AAT on Oct. 18, 1984.

lines, and this is known to select AGN of high X-ray luminosity (Kriss et al. 1980). Further important characteristics are discussed below.

H0307-730 (Sy 1)

This Seyfert type 1 nucleus is found in a host galaxy which contributes a significant fraction of the total optical flux. The galaxy reddens the photometric U-B value (20" aperture) and the spectral continuum (Fig. 6-3), and it produces weak absorption lines (CaII, the g-band, and NaI at the same redshift as the emission lines) that are typical of early Hubble type spirals. The emission spectrum exhibits high excitation forbidden lines of OIII, NeIII, and NeV as well as broad, permitted lines of H and FeII, all of which are common Sy 1 features.

The AGN is contained within a HEAO-MC error diamond, but the detection is not strong (significances of 3.1σ in MC1 and 2.6σ in MC2, both in the range of 1-13 keV; see Fig. 6-1). The X-ray flux is 1.6 x 10^{-11} erg cm^{-2} s^{-1} at 2-10 keV. The HEAO-LASS catalog (Wood et al 1984) lists a cluster of galaxies, STR0308-723 (Duus and Newell 1977) as the likely X-ray source identification. Although the cluster is within the HEAO-LASS error box, its characteristics (open; N = 20; 0.1 < z < 0.15) do not support the identification. Furthermore the cluster identification is not consistent with the spatially unresolved MC result. The AGN is nearby (z = 0.028), and the implied X-ray luminosity of 43.7 (log units, ergs s^{-1}) is very plausible (e.g. Elvis et al. 1978). It is therefore proposed that the AGN is the correct identification.

PKS0558-504 (QSO)

A Schmidt photograph revealed a bright (V = 14.97) and very UV

stellar image near the HEAO-LASS error box, and the object's position was found to be within 9" of the unidentified radio source PKS0558-504 (Wright, Savage, and Bolton 1977). The spectrum (Fig. 6-3) shows a very strong FeII-emitting QSO (Z = 0.137), with very weak forbidden lines and very narrow cores of H emission. This object is an extreme example of the type of Fe-emitting AGN represented by I Zw 1 and PKS1510-08 (see Phillips 1977, 1978). The optical luminosity is high (M_v = -25.1); however, the FWZI (Hβ), as judged from the blueward wing, is only 6400 km s^{-1}, and the full width at half maximum (FWHM) of Hβ is only 1500 km s^{-1}. Emission lines of Fe II complicate the resolution of the redward profile of Hβ and of the OIII lines, although the latter must be very weak since the OIII line at λ_o4959 is not evident. There are additional FeII lines blended with and blueward of HΥ (see Phillips 1978). The strength of the FeII emission is usually measured by the ratio of FeII to Hβ emission, r(FeII/Hβ), where the FeII flux is summed over two broad intervals to include the multiplets near λ_o4570 and those near λ_o5190 and λ_o5320 (Osterbrock 1977; Steiner 1981), as labeled in Figures 6-3 through 6-5. For PKS0558-504 r(FeII/Hβ) = 1.56, which is exceeded by only 5 of the 147 AGN reviewed by Steiner (1981).

Some of the strong FeII emitters, particularly I Zw 1 and PKS1510-08, also show very weak forbidden line spectra, and several AGN, such as I Zw 1 and Mkn 478, also exhibit relatively narrow H emission lines (Phillips 1977). PKS0558-504 occupies a special position with regard to these, since it is both a high-luminosity and very narrow-line example among these very strong FeII-emitting AGN. FeII emission was found to be uncommon in moderate redshift QSO's (Phillips 1977). Narrow-line QSO's may be even more unusual; one was observed at higher redshift

by Uomoto (1984), but its weak FeII and MgII emission suggest that it is
not related to AGN like PKS0558-504. Stocke et al. (1982) have also
presented an X-ray discovered narrow-line quasar with no indication of
FeII emission.

The HEAO-MC detection of PKS0558-504 is limited to a single colli-
mator (3.4 σ in MC1 for the 1-13 keV channels; see Fig. 6-1). However,
the identification was recently confirmed through an observation by
EXOSAT, the X-ray observatory operated by the European Space Agency. The
automatic analysis of the LE detector (0.04 to 2.0 keV) shows a single
bright source that is 2 ± 10 arcsec from PKS0558-504, in an X-ray image
that was centered on the QSO with a field of view of 2.2° diameter. The
LE flux of 0.108 ± 0.003 counts s^{-1} is fully consistent with the HEAO-
LASS flux (3.0×10^{-11} erg cm^{-2} s^{-1} in the range of 2-10 keV) for an
X-ray energy index of ~0.7 and a column density of ~10^{20} N_H cm^{-2}. The
complete analysis of the X-ray spectrum must await the receipt of the
data from the other EXOSAT detectors.

H0707-495 (Sy 1)

This object is clearly a fainter (V = 15.70) and closer (z = 0.041)
relative of PKS0558-504. The FeII lines are very strong, the forbidden
lines are weak, and the hydrogen cores are again very narrow (see Fig.
6-3). The measured value of r(FeII/Hβ) is 2.77, which is nearly equal to
the value for I Zw 1, the strongest FeII emitter (relative to Hβ)
reviewed by Steiner (1981), although a value of 4.71 is given for the
very unusual AGN Mkn 231 (Phillips 1978; see also Boksenberg et al.
1977). Compared to PKS0558-504 the forbidden lines are stronger, as OIII
$\lambda_0 4959$ is clearly visible. The H lines appear asymmetric, and the FWZI

of Hβ is estimated to be ~6300 km s^{-1}, while the FWHM of Hβ is only 1000 km s^{-1}. The very narrow cores of the permitted emission lines is also exhibited in the profiles of the FeII multiplets.

This X-ray source was detected by both Uhuru and HEAO-LASS (2.4 x 10^{-11} erg cm^{-2} s^{-1}), and the MC error diamonds (Fig. 6-1; MC1 has 3.0σ significance and MC2 has 3.4σ significance, both for the 2.5-13 keV energy channels) contain the AGN position. The galaxy is 2 arcmin outside of the field of view of an Einstein HRI observation targeted at the center of the 4U error box. The HRI detected a source, but only at its threshold (9 counts in 1845 s), in an optically blank field, and it is most unlikey that this weak source, if real, is the same as the LASS source. The Monitor Proportional Counter (MPC) gave a possible detection of 0.18 ± 0.06 counts s^{-1} from the same observation, which would correspond to 0.84 ± 0.26 x 10^{-11} erg cm^{-2} s^{-1} if from the Sy galaxy.

H1143-182 (Sy 1)

This Sy 1 galaxy is one of a pair, both of which have redshifts of 0.033 ±0.001. Their separation orthogonal to the line of sight is about 20 kpc. The galaxy that is a companion to the Sy 1 shows normal absorption features without signs of nuclear activity or HII-type emission. The AGN spectrum (Fig. 6-3) shows broad H lines and strong HeII $\lambda_0$4686 emission, and FeII is absent.

The AGN lies within a HEAO-MC error diamond (2.6σ in MC1 and 3.1σ in MC2, both for the 0.9-5.5 keV channels). The X-ray source was originally detected in a search for emission from Abell clusters with data from the Ariel V Sky Survey Instrument (Ricketts 1978). The source is also detected by the HEAO-LASS (1.4 x 10^{-11} erg cm^{-2} s^{-1} at 2-10 keV).

H1839-786 (Sy 1)

Fig. 6-4 contains the spectrum of another Sy 1 nucleus, showing broad hydrogen emission lines with a FWZI(Hβ) ~ 12,000 km s^{-1}. The host galaxy is the largest of this group, projecting an observable diameter of >35 kpc. at z = 0.074. The optical luminosity (M_v = -23.2) is large for a Sy galaxy (e.g. Schmidt and Green 1983).

This X-ray source was one of the few remaining unidentified sources in the HEAO A-2 (Goddard) high galactic latitude survey (Piccinotti et al 1982). The AGN is within the HEAO-LASS error box for this source (3.0 x 10^{-11} erg cm^{-2} s^{-1} at 2-10 keV), as is a cluster of galaxies, STR1839-787 (medium compact, N = 20, extremely distant; Duus and Newell 1977). The MC detection has significance of 4.0σ (MC1) and 2.9σ (MC2), both in the 2.5-13 keV energy channels. The AGN is included within the MC1 result, but it is slightly outside of the less significant MC2 band (see Fig. 6-1). Since the MC detection is spatially unresolved, unlike X-ray emission from clusters of galaxies (Schwartz et al. 1979), the AGN candidate is favored.

After the Seyfert galaxy was located, the MC group became aware of an Einstein IPC guest observation by Wood et al. targeted at the center of the LASS error box. The original processing did not make an X-ray image because the star camera was not locked on the guide stars. In addition, the IPC high-voltage supply was turned off for most of the observation. The Einstein data bank was used to construct an IPC image using the "map mode" aspect solution. In 281 s of useable data, the IPC detects a single source that is only 40 arcsec from the position of the Seyfert galaxy. This confirms the identification, marking another success for a candidate listed as "probable" in Table 5-1.

In this same Einstein pointing, the MPC detected a flux of 4.8 ± 0.3 x 10^{-11} erg cm^{-2} s^{-1}, and the X-ray spectrum was fit by a power law with an energy index of 0.1. The is an unusually flat ("hard") X-ray spectrum, which challenges the notion of "universal tendency" for AGN to exhibit an X-ray spectral index of 0.7 (Mushotzky et al. 1980; Petre et al. 1984).

H1934-513 (Sy 1)

This Sy I nucleus is found in a barred spiral galaxy which has a distinct ring on its outer edge. The phenomenon is a common tidal resonance, and it is not unusual among AGN (Balick and Heckman 1982). The spectrum (Fig. 6-4) shows broadened emission of hydrogen, HeI, and HeII, and relatively strong forbidden lines of NeIII and NeV. The hydrogen lines are very asymmetric, with much broader profiles on the redward wings. The "UV bump" appears very strong in this spectrum (see Malkan and Sargent 1982; Malkan 1983).

The AGN is positioned just outside of a HEAO-MC error diamond (MC1 detection at 3.5σ and MC2 at 3.8σ, both in the 0.9-2.5 keV energy channels), near the edge of the HEAO-LASS error box (2.2×10^{-11} erg cm^{-2} s^{-1} at 2-10 keV). The identification is regarded therefore as probable.

H2106-099 (Sy 1)

This is the brightest (V = 14.3) of the AGN presented here. Unlike the others described in this chapter, this Sy 1 galaxy appears to be a variable X-ray source. The AGN is contained within an MC error diamond (MC1 detection at 3.1σ and MC2 at 4.7σ, both in the 2.5-13 keV channels), derived from the first HEAO-1 scan of the source (1977 November 5-11).

The source is not detected by the MC during the second or third scans by HEAO-1 (1978 May 3-9 and 1978 November 6-12), and the sum of all three scans gives a poor result, compared with the detection for the first scan alone. Similarly, our analysis of HEAO-LASS data indicates an 8.1σ detection during the first scan ($2.25 \pm 0.39 \times 10^{-11}$ erg cm^{-2} s^{-1} at 2-10 keV), while the second scan detection has only 2.3σ significance, with a flux of $0.75 \pm 0.47 \times 10^{-11}$ erg cm^{-2} s^{-1}. The third LASS scan contains data of poor quality.

The optical spectrum of this Sy 1 galaxy (Fig. 6-4) shows many typical AGN emission features, including FeII emission and H emission with broad wings. Additionally, He I appears to be unusually strong, and there are very high-excitation forbidden lines of FeX $\lambda_o 6374$, and of FeVII at $\lambda_o 3760$ and $\lambda_o 6086$. The FeX line has been observed with similar relative intensity in several galaxies, such as NGC4151 (Oke and Sargent 1968), 3C390.3, and NGC3783 (Cooke et al. 1976), all of which are variable X-ray sources (Charles et al.1975; Mushotzky et al. 1980). Thus, optical spectral features give circumstantial evidence which supports the identification of this X-ray source. H2106-099 appears to be a member of a select group of Sy 1 galaxies that are characterized by extremely hot gas components and a high degree of X-ray variability.

H2132-626 (Sy 1)

This Sy I galaxy exhibits broadened H emission and strong forbidden lines of NeIII and NeV. This is the third case in which an AGN and a cluster of galaxies both lie within or near the HEAO-LASS error box. The cluster is STR2131-623 (medium compact, N = 30, estimated 0.1 < z < 0.15; Duus and Newell 1977), and there is a possibility that the X-ray flux

$(2.2 \times 10^{-11}$ erg cm^{-2} s^{-1} at 2-10 keV) is shared between these objects.
The AGN $(z = 0.059)$ is detected in only one of the HEAO-MC detectors (by
MC2 at 3.1σ in the 6-13 keV channel). However, the implied X-ray lumino-
sity of 44.6 (log erg cm^{-2} s^{-1}) is a typical value of Sy 1 types. The
AGN is judged to be the "probable" identification of the X-ray source.

HO508+164 (Sy 1)

This is a nearby $(z = 0.017)$ Seyfert galaxy that was found in a
crowded field at a galactic latitude of 13°. The discovery is unlike the
other, UV-selected counterparts, since the search was led by the coinci-
dence of an Einstein IPC detection and an MC error diamond (a 3.0 σ
detection in MC1 and a 2.9 σ detection in MC2 in the 2.5 to 5.5 keV
energy band for 2 celestial scans). The LASS X-ray flux $(4.1 \times 10^{-11}$ erg
cm^{-2} s^{-1} at 2-10 keV) can be reconciled with the weaker IPC flux ($\tilde{~}0.8 \times$
10^{-11} erg cm^{-2} s^{-1} at 0.5 to 4.5 keV) if the spectrum is hard and some of
the soft X-rays are attenuated by absorption in our Galaxy.

The optical spectrum shows an exceptionally steep Balmer decrement,
with HeII emission but very little or no lines of FeII. OIII is very
strong, and this is the only one of the fourteen AGN which clearly shows
emission by OI. The strength of OI and OIII, combined with the weakness
of OII, illustrates the diversity of ionization structures that can be
found in the same AGN.

Photoelectric photometry has not been performed for HO508+164, and
the absolute calibration of the spectral flux density is uncertain, due
to the presence of cirrus clouds during the observation. Therefore the
values of some parameters are omitted for this AGN in Table 6-1.

H0522-122 (Sy 1)

This Seyfert nucleus exhibits a very interesting optical spectrum. The emission line profiles are a combination of extremely broad permitted lines and very strong emission from the narrow lines as well. Hβ does appear to have a two-component (narrow + broad) discontinuity that is usually classified as Seyfert type 1.5 (see Osterbrock 1984). Even HeII exhibits this narrow emission component. The narrow forbidden lines of OIII, NeIII, NeV, NII, and SII are also very strong, compared to the optical continuum. At the same time the hydrogen wings expand to a FWZI of about 24,000 km s^{-1}, which can only be judged at Hα since FeII and OIII lines are located in either of the wings of Hβ. Line widths of this magnitude are seen in only a handful of galaxies (Steiner 1981), most of which are very luminous AGN initially detected as strong radio sources (e.g. 3C382). Since the purpose of the Sy 1.5 classification is to designate the galaxies that are intermediate between Sy 1 and Sy 2 line profiles, it seems more sensible to classify this galaxy as a Sy 1 with a strong narrow-line component, rather than as a Sy 1.5 with emission lines that are broader than 95% of normal Sy 1 emission features. This AGN is bright (V = 15.0) and would be an excellent subject for high-resolution studies of AGN with extreme velocity fields. Just how close to the speed of light do these wings go?

This galaxy was detected by the MC (2.4 σ and 4.0 σ, respectively) for the sum of three celestial scans in the 0.9 to 5.5 keV energy band. The LASS flux (2.2 x 10^{-11} erg cm^{-2} s^{-1}) implies a log X-ray luminosity of 44.4, which is very plausible.

<u>H1935-063</u> (Sy 1)

This is the third (and last) discovery of a member of the "rare" I
Zw 1 family of AGN that show very strong FeII emission with relatively
narrow emission lines of hydrogen. Compared to the other FeII-emitters
presented in this chapter, the optical spectrum (shown in Fig. 6-6) is
different in two ways. The spectrum basically resembles that of
H0706-495, except that the forbidden lines are much stronger in the
present galaxy. In fact, all of the common AGN forbidden lines are
clearly exhibited by H1935-063. In addition there is forbidden FeX
emission (redshifted from $\lambda_o 6374$), the significance of which was
discussed with respect to H2106-099. However, in this case there is no
evidence that the X-ray source is highly variable.

The galaxy is positioned within an MC error diamond resulting from a
sum of the three celestial scans, with significances of 3.1 σ and 3.3 σ,
respectively, in the 0.9 - 5.5 keV band. The implied X-ray luminosity is
43.2 (log units at 2-10 keV), and the identification appears to be very
secure.

The absolute visual magnitude, M_v, of H1935-063 is -19.4 (see Table
6-1). Compared to the other values of M_v and L_x, this AGN appears to be
almost as faint (intrinsically) as PKS0558-504 is luminous. The two AGN
are both very strong FeII-emitters with rather narrow H lines, but the
measures of the absolute optical and X-ray luminosities differ by factors
of 190 and 180, respectively. The calculations of the absolute visual
magnitude included a crude estimate of the visual extinction at that
galactic latitude, A_v = .18 csc b (Schmidt 1968; see Table 6-1). For
H1935-063 (which is at a galactic latitude of only 13°), the value is A_v
is 0.8. At low latitudes such as this, an accurate measurement of M_v

requires a study of the extinction indicators in the specific direction of the object. However, the comparison between H1935-063 and PKS0558-054 in X-ray luminosity (differing by a factor of 180) is not as uncertain. There does not appear to be significant X-ray extinction (by absorption) in the case of H1935-063 in the energy range of the HEAO-1 instruments. The MC detection of H1935-063 is strong in the lowest energy channel (0.9 to 2.5 keV), where photo-ionization would have its greatest effect. The conclusion is that the strong FeII emitters presented in this Chapter range by a factor of ~200 in luminosity.

H2353-307 (Sy 1)

The last Seyfert galaxy is clearly in the same league as the other eleven nearby AGN, insofar as the distance ($z = .031$), optical magnitude ($V = 15.9$), and the spectral characteristics are concerned. However, in this case there is another optical object, an unconfirmed BL Lac object (see Table 5-1), which appears to emit the major fraction of the X-ray flux in the region near the LASS X-ray source position. The Seyfert galaxy is consistent with a weak detection in a single collimator (3.0 σ by MC2 for the sum of 2 scans in the 0.9 - 5.5 keV energy channel), whereas the best MC result (MC1 at 3.6 σ and MC2 at 3.2σ for the sum of 3 scans in the energy range of 2.5 to 13 keV) include the position of the BL Lac candidate but not the Sy galaxy. The BL Lac candidate shows no spectral features in an AAT spectrum, and its optical color indices are distinctly non-stellar (U-B = -0.61; B-V = 0.55). The object is targeted for further study by radio observations, optical polarimetry, and deep imaging with a CCD camera.

The Seyfert galaxy is presented here because it remains a candidate object, and because its optical discovery and description are certainly of interest to the astronomical community. The weak MC1 result that is consistent with the position of the Seyfert galaxy may not be spurious; this object is surely expected to show X-ray emission at some level. If one were to estimate (albeit crudely) from the MC detection that the Sy galaxy emits one-third of the LASS flux, then a log L_x of 43.23 is implied.

The optical spectrum shows strong FeII emission, normally broadened permitted lines, and very weak forbidden lines. This is the fifth example showing very strong FeII and the third case in which the forbidden lines are unusually weak.

6-3. Discussion of the Low Redshift AGN

The newly discovered AGN exhibit some spectral characteristics that are typical of Sy 1 nuclei. The Balmer decrements are generally steeper than that predicted for radiative recombination (Osterbrock 1977), although H1934-513 and H2132-626 are near the recombination values. FeII emission is often present and He I is always observed, with values that tend to cluster around 10% of H (see also Osterbrock 1977). However, there are also unusual properties among several of these AGN. The FeII lines of H0706-495, H1935-063, PKS0558-504, and H0307-730 are comparable to the 6 strongest FeII emitters in a sample of 147 AGN reviewed by Steiner (1981), and H2353-307 is not far behind. FeII lines are the most puzzling optical emision lines found in AGN. They are the least correlated with the optical continuum flux, and one investigator proposed

to classify AGN on the basis of FeII characteristics (Steiner 1981),
although the physical conditions which regulate the various FeII types
are not understood.

The strongest Fe-emitters, I Zw 1 and Mkn 231, are of further
interest because they are known to be great sources of infrared emission.
Their bolometric luminosities are easily the highest among Seyfert
galaxies (Reike 1978), but the nature of this emission is not understood.
The AGN presented in this chapter will almost double the opportunity to
observe the strong Fe-emitters, and several of the AGN bear a distinct
resemblance to I Zw 1. PKS0558-504 would be a particularly interesting
target for infrared observation, since it is already more luminous
optically and in X-rays than I Zw 1.

The emission line profiles of PKS0558-504, H0707-495, and H1935-063
are very narrow for AGN of high X-ray luminosity, but they do not resem-
ble either the emission lines of Sy 2 galaxies nor the more discontinu-
ous, two-component profiles that characterize the classifications in the
range of Sy 1.5-1.9. The FWZI measures for Hβ are complicated by nearby
FeII lines; however the values do not appear to be underestimated, since
in both cases the FWZI of Hα are 10-15% _less_ than the values given for Hβ
(Hα of PKS0558-504 was observed in an earlier spectrum obtained at
C.T.I.O.). The line profiles might indicate a pole-on view of the
emitting regions of these galaxies; however, this hypothesis is highly
speculative. Another galaxy, H0522-122, does show a Sy 1.5 type of
discontinuity, but its emission lines subsequently expand to as large an
FWZI as is observed. Since there is a tendency to describe Sy 1.5
spectra as showing weakness in the broad-line region, the spectrum of
H0522-122 appears more like a contradiction than a source of information.

Two additional AGN show noteworthy X-ray properties. H2106-099
appears to belong to a small group of FeVII and FeX emitting Sy galaxies
that are highly variable X-ray sources, while H1839-786 emits an X-ray
spectrum that is considerably harder than the others which have been
measured. These AGN are obvious choices for further study.

A lower limit can be estimated for the probability that the identi-
fications are correct. From Huchra and Sargent (1973) the surface
density of 0.05 deg^{-2} is derived for Seyfert galaxies (defined as M_p >
-23) which apppear brighter than m_p = 16. Although there are as few as
four to six diamonds inside the LASS error box, a more realistic view
would consider 10 to 40 diamonds "near" or along the length extensions as
possible source locations. Forty diamonds of the maximum 4 $arcmin^2$ size
would occupy 4.8 deg^2 for all of the 108 X-ray sources investigated in
this research, giving an expectation value of 0.24 coincident Seyfert
galaxies and a (Poisson) probability of 79% that none of the 13 proposed
identifications (Table 5-1) are spurious. For bright QSO's (e.g.
PKS0558-504), a similar argument could be made using the density analysis
of Schmidt and Green (1983), but the issue is superceded by the EXOSAT
measurement of a single, bright source at the position of the AGN.

The 11 AGN identifications presented here have an average L_x of 44.3
(log X-ray luminosity in erg s^{-1}). This is very similar to the mean of
44.2 for the broad line AGN in the compilation of Seyferts and low
redshift QSO's by Steiner (1981). Although this comparison involves
different X-ray spectral ranges, the integrated fluxes in 2 to 10 keV vs.
the 0.5 to 4.5 keV band are virtually equal for a typical Seyfert X-ray
energy index of 0.7 with little or no energy cutoff due to absorption

(Mushotzky et al. 1980; Petre et al. 1984). The optical/X-ray spectral index has a mean β_{ox} of 1.07 ± 0.03 for these 8 AGN, and the mean is flatter (3σ) than the mean index of 1.19 ± 0.03 for the X-ray selected sample of Kriss et al. (1982). However none of the 8 AGN have β_{ox} values outside of the range of the larger sample of Kriss et al. (1982), and the differences in the mean values may be due to different redshifts or to selection effects regarding the identification sequence (i.e. the optically brightest are first) of HEAO-1 X-ray sources. X-ray fluxes are least certain for H1934-513, H2132-626, and H2353-307, as judged from the significance of the MC results.

The optical identification of the fainter sources in the HEAO-1 survey promises to increase significantly the numbers of bright examples of several classes of X-ray sources. Increasing the sample of bright objects is particularly important in the study of Active Galactic Nuclei. AGN optical properties have proven to be complex and diverse, and progress in understanding the physical conditions and dynamics of the various emitting regions is crucially dependent on the detailed analysis of significant numbers of objects in the various subgroups, which is most readily achieved for the brighter objects. The occasional discovery of extreme or unusual spectral characteristics in an AGN may encourage studies directed toward this end.

6-4. Two Distant Absorption-Line QSO's

Two distant QSO's have been discovered, and they have redshifts of 0.50 and 1.56, respectively. At these redshifts the optical observations correspond to ultraviolet spectral ranges in the rest frames of those

objects. The common emission features of AGN at UV wavelengths are well documented (see Strittmatter and Williams 1976), since hundreds of faint (20 > V > 17) QSO's have been observed out to a redshift of almost 3.8 (see Kuhr et al. 1983).

The distant quasars frequently show absorption lines in addition to their emission spectra, and this phenomenon becomes the norm at z > 1.9 Major reviews on this topic have been written by Strittmatter and Williams (1976) and by Weymann, Carswell, and Smith (1981). An absorption line redshift, z_a, is often significantly different from the object's emission redshift, z_e. There are even cases in which $z_a > z_e$, and one study offered a model for the latter case whereby the emitting gas is being driven outward toward the observer, while the absorbing gas is located in filaments bound in clusters of galaxies that contain the QSO (Weymann et al. 1977).

The locations and the profiles of absorption lines in QSO spectra can be extremely complicated. Spectral features may split into multiple, narrow components when re-observed at higher resolution, and there are many cases in which a large number of absorption features remain unidentified, even when high-resolution spectra are analyzed to the tedium limit. Weymann, Carswell, and Smith (1981) proposed a classification scheme that distinguishes QSO absorption features in 4 categories. Type "A" are broad, metallic absorption lines (full widths $\gtrsim 2000$ km s^{-1}) that are less redshifted than (i.e. found blueward of) an emission line of the same atom (often CIV at $\lambda_0 = 1550$ Å). The broad absorption lines are always due to atoms in high ionization states (e.g. CIII ionizes at 48 eV), and type A lines are estimated to occur in ~5% of QSO's. Type B absorption lines are narrow lines with only slight differences between

the absorption and emission redshifts, with the absolute value of

$(z_e - z_a)/(1 + z_e)$ being less than 0.01. Type "C" and "D" are similar,

narrow lines with larger absorption/emission differences in redshift,

i.e. the normalized separation is greater than 0.01. Type C lines are

metallic absorptions, and type D are the "L^α forest", a large complex of

absorption features blueward of the strong emission of hydrogen at the

Lyman α transition (λ_o = 1216 Å).

Type A and B absorption lines are suspected of being intrinsic to

the QSO's. The broad absorption lines (type A) may arise from shells of

gas that are being driven out of the continuum-emitting region, whereas

the narrow absorption lines that appear with $z_a \cong z_b$ (type B) may be

caused by ambient gas or filaments that are local to the QSO. The origin

of types C and D lines are highly controversial, and many researchers

favor the interpretation that these absorptions are caused by intervening

matter that is extrinsic to the QSO (Weymann, Carswell, and Smith 1981).

Both of the distant QSO's being reported in this chapter show

absorption lines in their spectra. Their interpretations are quite

different, and the details can be explained within the framework of this

introductory discussion. The X-ray detections are shown in Figure 6-6,

and the spectra are shown in Figure 6-7.

The QSO positions, magnitudes, and luminosities are listed in Table

6-3. The optical/X-ray spectral index, β_{ox}, (see Section 6-1 and the

Appendix) is also given. Here, β_{ox} is calculated for two choices of the

assumed X-ray spectral index, α_x, that is used to calculate the flux

density at 2 keV from the broad-band (1-20 keV) X-ray flux measured by

the LASS. The purpose of this choice will become apparent in the

discussion (Section 6-5) that follows the description of the QSO's.

Fig. 6-6. Maps containing the positions of the two distant QSO's (heavy plus) and the allowed X-ray positions from the HEAO-MC (diamonds or bands, depending on whether both or a single collimator produces a detection). The X-ray error box is from the HEAO-LASS ("1H"; Wood et al. 1984).
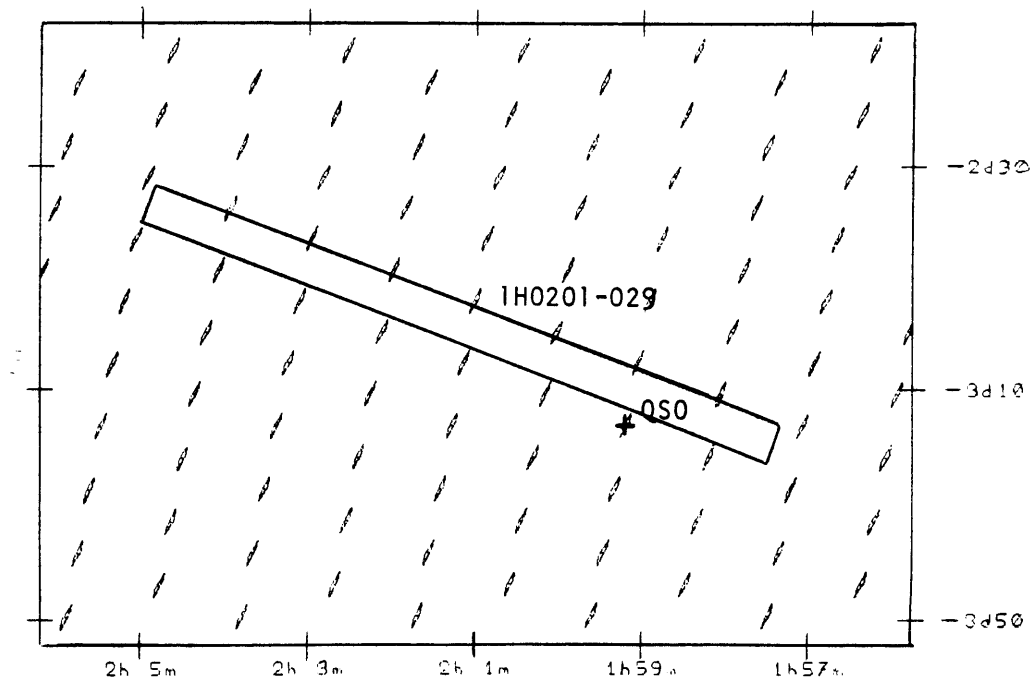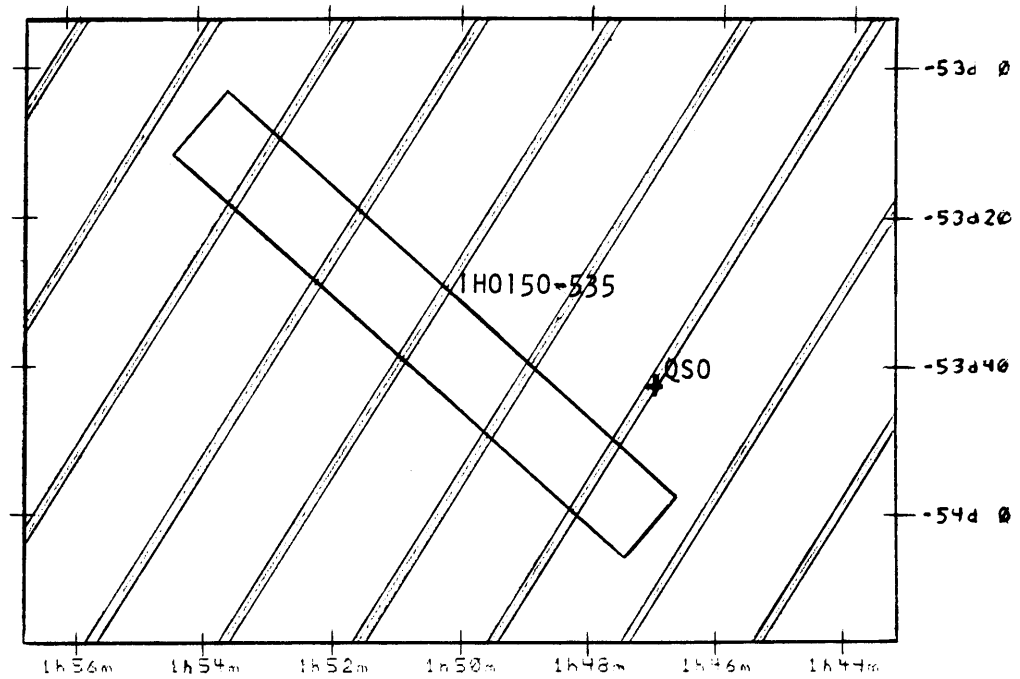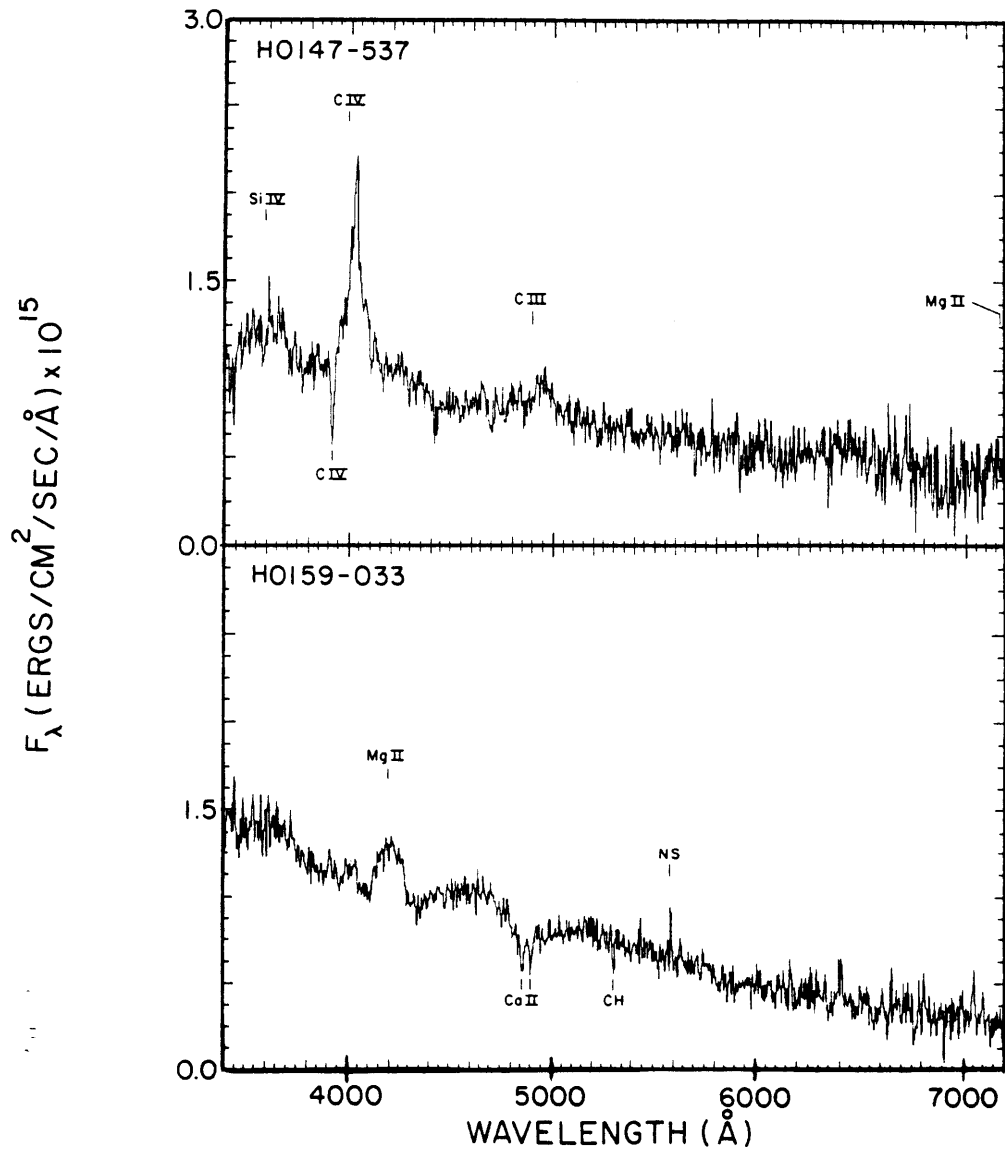
Fig. 6-7. Optical spectra of two distant QSO's. Both were observed at the AAT on (UT) Oct. 19, 1984.

HO147-537 (BAL QSO, z = 1.56)

A redshift (z_e) of 1.56 consistently explains all of the broad emission features in this spectrum (see Fig. 6-7). The SiIV line $(\lambda_o =$ 1398 Å) is the clearest emission feature that is not distorted by an absorption line, and it is observed with a redshift of 1.56 ± 0.01. Weaker, broad emission features are then satisfactorily explained as due to CIII $\lambda_o 1909$ and MgII $\lambda_o 2798$, if it is assumed that all of these permitted emission lines will show the same normalized widths (FWZI). Following this interpretation one step further, the strongest emission line is CIV $\lambda_o 1550$, but a broad absorption feature has distorted the profile of the emission line. The position of CIV with a redshift of 1.56 is indicated in Figure 6-7.

The full width of the CIV absorption feature is about 2000 km s^{-1}. This value is obtained after the real width and the instrumental resolution (~10 Å) are deconvolved, assuming that the observed width is the resultant (hypotenuse) of the real and instrumental widths. The absorption width of 2000 km s^{-1} barely qualifies as a type A feature. Technically, according to Weyman, Carswell, and Smith (1981), all broad absorption line (BAL) QSO's (i.e. those having type A features) must be observed at high spectral resolution before they are so classified. However, the BAL QSO classification is adopted here, considering: (1) the depth of the absorption feature (at 10 Å resolution), (2) the degree that the strong CIV emission line is displaced, and (3) the fact that several known BAL QSO's show the same type of simple absorption/emission profile (called a "P Cygni" profile) of CIV as does HO147-537 (Strittmatter and Williams 1976).

To the author's knowledge, the only BAL QSO that is closer and

brighter than H0147-537 (z = 1.56; V = 16.97) is PG0946+301 (z = 1.216;

V $\cong$ 16.0), which was recently classified by Wilkes (1985).

H0147-537 is the most distant object ever considered as an MC X-ray

source. Its candidacy is limited by the fact that only one collimator

(MC2, with 3.7 σ significance in the 2.5-13.0 keV energy band for the sum

of all three celestial scans) detected an X-ray source (see Fig. 6-6).

On the other hand, the QSO is within the MC2 band, and there are no other

optical candidates. The absolute visual magnitude of this QSO (M_V =

-29.3) is surpassed by many luminous QSO's that have been observed; Kuhr

et al. (1983) show 31 examples within the range -33 < M_V < -30. However,

the implied log X-ray luminosity (47.9) is several times larger than the

most luminous QSO's detected by the Einstein Observatory (Zamorani et al.

1981; Marscher and Broderick 1981). It must be noted, however, that the

optical sample is far larger than the number of QSO's measured by X-ray

instruments.

H0159-033 (QSO, z = 0.50)

This QSO also shows emission and absorption lines, but their inter-

pretation is quite different from that of the previous QSO. The emission

line near 4200 Å in Figure 6-7 is due to MgII, with a redshift of 0.501 $\pm$

0.003. If a QSO exhibits a single emission line in a high-quality

spectrum with broad wavelength coverage, the line is always presumed to

arise from MgII λ_o2798 Å (see e.g. Strittmatter and Williams 1976).

There is only one wavelength interval ($\lambda\lambda$ 2000 - 4000 Å in the rest frame

of the emitter) that is sparse in strong emission lines, for all of the

relevant redshits (0.0 < z < 4.0) that may enter the optical range of the

spectrum.

A redshift of ~0.5 also gives meaning to the curved continuum shape that is observed to the right of 4400 Å. This is the "UV bump" that is frequently observed in QSO's and Seyfert galaxies (e.g. H1934-513 earlier in this chapter). In the spectrum of H0159-033 (Fig. 6-7), the UV bump rises above the continuum throughout the wavelength range of 4400 - 5850 Å.

Malkan and Sargent (1982) model the UV bump as a combination of high-order Balmer (hydrogen) emission lines and an independent thermal component that locally change the profile of the optical power-law continuum. It has been claimed that the thermal component originates in an accretion disk (Malkan 1983). In the spectrum of H0159-033 (Figure 6-7), the UV bump extends even further blueward of the Balmer limit (λ_o = 3634 Å in the rest frame) than does the unusual UV bump of 3C273 (ibid.), and there should be strong interest in modeling the optical continuum of this QSO on that basis alone.

The QSO's position is within an MC diamond which has strong statistical signficance (3.3 σ and 4.8 σ, respectively) in the 2.5-13.0 keV energy range. Both of the available celestial scans were used to determine the MC position; this X-ray source is within the narrow celestial strips (1-2 hours and 13-14 hours of right ascension at the celestial equator) for which the third celestial scan was not completed by HEAO-1. The implied X-ray luminosity of 46.7 (log L_x) is again very high, but it is less than the L_x values for the most luminous QSO's measured by the Einstein Observatory (Zamorani et al. 1981; Marscher and Broderick 1981).

Carved into the UV bump is a pair of deep absorption lines. Their location and separation are consistent with absorption by CaII (H and K lines) at a redshift of 0.2325 ± 0.001. The next most significant

absorption feature can be attributed to CH $\lambda_o 4300$ (a narrow molecular feature) at the same redshift (0.233; see Fig. 6-7). Within the observed wavelength range, these three lines are the strongest absorption features that appear in many spectra of stars that are viewed through cold interstellar clouds in the Galaxy (Allen 1976; McNally 1971).

The spectral characteristics of H0159-033 lead to predictions concerning the red spectrum beyond the range of coverage of the AAT observation (Figure 6-7). $H\beta$ emission is expected (with a redshift of z = 0.50) at ~7290 Å (possibly with nearby OIII emission), and a very deep (and possibly broadened) absorption feature, the NaI doublet, should be observed near $\lambda 7263$ Å (being redshifted by 0.233). This odd profile will not signify a BAL QSO.

The absorption features in this spectrum are clearly type C, as $(z_e - z_a) / (1 + z_e) = .179 >> .01$. Furthermore, since the absorbing material appears to be similar to the cold interstellar matter in the Galaxy (but at a redshift of 0.233), there is encouragement for the interpretation that the absorbing gas is intervening material that is not associated with the AGN. This evidence has strong cosmological implications regarding the true distances and luminosities of QSO's.

Most studies comfortably assume (as this one does) that Hubble's law applies to QSO emission lines just as it does to galaxies with absorption lines. The case is not proven, however, and the analysis of QSO absorption lines may eventually decide this issue (see discussion in Strittmatter and Williams 1976). One alternative notion about the nature of QSO's, for example, is the hypothesis that they are only moderately luminous objects expelled by nearby galaxies (Arp 1983). H0159-033 has absorption lines that may be at just at the right place to constrain the

QSO's distance and luminosity with meaningful lower limits. If the QSO is "forced" to have a Hubble redshift (as a lower limit) of z = .233, then the luminosity of the object would still be $M_V = -24.3$, which is a factor of 33 times greater than the visual luminosity of a large spiral galaxy (like the Galaxy).

Table 6-3: The High-Redshift QSO's

		H0147-537	H0159-033
Other X-ray Names		1H0150-537	1H0159-033
QSO Position (1950)		01 47 00.2 -53 43 21	01 59 11.7 -03 16 25
Redshift (z ± 0.01)		1.56	0.50
Spectral Magnitudes	V	16.97	16.88
(Allen 1976)	B-V	0.20	0.17
	U-B	-0.65	-0.71
M_V		-29.3	-26.2
L_x		47.92	46.69
ID Status		B	A
β_{ox} ($\alpha_x = 0.7$)		0.58	0.68
β_{ox} ($\alpha_x = 0.0$)		0.79	0.83

6-5. Discussion of the High Redshift QSO's

The two QSO's offer an exciting opportunity to study bright ($V < 17$) examples of very luminous members of that class of objects. The implied X-ray luminosities are in the range of the highest values measured. The X-ray properties of BAL QSO's are not established; many of the ~33 known examples have been discovered recently (see Wilkes 1985).

The surface density of faint QSO's on the celestial sphere is higher than that of Seyfert galaxies, but the two objects are sufficiently bright that they are not likely to be found, by chance, within the MC positions for the X-ray source. It can be extrapolated from Schmidt and Green (1983) that the density of QSO's with B magnitudes brighter than 17.0 is 0.036 deg^{-2}. For the 108 sources, the number of "chance" QSO's ($V \lesssim 17$) within the 40 diamonds nearest to the LASS error box is 0.17, which implies an 84% Poisson probability that none of the "A" status QSO's are spurious identifications. The probability of a chance discovery of H0147-537 (the BAL QSO) and the other "B" status QSO's is slightly higher. If an area three times greater than the LASS error box is reduced by a factor of 8 by the detection of a single MC collimator, then the expectation value for a "chance" QSO from the 108 program sources is 0.37. However, the probability of finding no QSO's (i.e. no spurious identifications) in this case is still 69%.

A comparison of the LASS X-ray survey (Wood et al. 1984) and a list of bright Seyfert Type 1 galaxies (e.g. Weedman 1977) leads to a simple conclusion that most of the nearby broad-line AGN are detected as X-ray sources by HEAO-1. However, the emission properties of QSO's that are detected by HEAO-1 are not yet clear. Certainly most QSO's appear too

faint in X-rays to be detected by the HEAO-1 survey (e.g. Zamorani et al. 1981). In addition, two factors seem to be important:

(1) The redshifted spectra of QSO's create a bias against their detectability, as compared to Seyfert galaxies, because the X-ray spectral indices tend to be negative. The observed flux densities are actually "harder" X-rays in the inertial frame of the QSO, and the redshift "fading" factor for a power-law spectrum is $(1 + z)^{\alpha}$, where α is the X-ray spectral index.

(2) Several studies show that the X-ray luminosities of QSO's do not keep pace with the optical luminosities (both redshift-corrected) as the absolute values of the luminosities increase (Reichert et al. 1982; Tucker 1983), i.e. the ratio L_x/L_{opt} decreases as L_{opt} increases.

On the other hand, the values of α_x and L_x/L_{opt} (which is a parameter that is basically similar to β_{ox}) will be distributed with some range among individual QSO's. There are objects with very low β_{ox} values (equivalent to high L_x/L_{opt}) such as NRAO 140 (Marscher and Broderick 1981), and other AGN may have "flat" X-ray spectra ($\alpha_x \sim 0$), such as H1839-786, seen in Section 6-2. The QSO's with large redshifts (e.g. z > 0.3) that are detected in the HEAO-1 survey are likely to be somewhat exceptional examples for both of these parameters, unless they are optically bright (e.g. v < 15). In Table 6-3, β_{ox} was calculated for the case of $\alpha_x = 0$, and the resulting values ($\beta_{ox} \sim 0.8$) are similar to the exceptional cases among the QSO's in the "medium sensitivity" sample measured by the Einstein Observatory (Stocke et al. 1983). Therefore, the X-ray/optical emission properties of the two QSO's, while certainly extreme, need not be considered unique. They may have flat X-ray spectra and a high value of the X-ray/optical luminosity ratio, which are the

properties of QSO's that HEAO-1 was apt to select.

The rest of this discussion concerns the cosmological implications of the absorption lines of H0159-033, a momentary digression from the assumption that the large redshifts of QSO's are equivalent to large distances.

One of the important goals in the study of QSO absorption lines is to learn whether the frequency and redshifts of the absorption features are consistent with the expectations of great cosmological distances (Bahcall and Peebles 1969; Bahcall 1971). The efforts to prove the distances (and therefore the luminosities) of QSO's have encountered difficulties (see Strittmatter and Willimas 1976; Weymann, Carswell, and Smith 1981). Some QSO's with very large redshifts appear to have absorption lines with $z_a \ll z_e$ (types C and D). These are the absorptions that are likely to be caused by intervening matter. The fact that there are so many faint absorption features in many of these cases limits the certainty with which line identifications can be claimed. In addition the identified species with $z_a \ll z_e$ are sometimes highly ionized, and this indication of energetic activity makes it more difficult to prove that the gas is intervening material.

A much more simple case is reported by Boksenberg and Sargent (1978) and Haschick and Burke (1975). The two studies demonstrate that the QSO 3C232 ($z_e = 0.53$) exhibits absorption features due to CaII H and K lines and due to neutral hydrogen at 21 cm. Both types of absorptions are at the same redshift as NGC3067 ($z = 0.005$), which lies ~2 arcmin away from the QSO on the plane of the sky. These observations have implications concerning the nature of QSO absorption lines in general. However the

intervening galaxy (NGC3067) is near our own galaxy (low redshift) and cannot force a lower limit on the QSO luminosity that is above the range of a normal galaxy. The devil's advocate (see Arp 1983) would use the same case to argue that NGC3067 has expelled 3C232.

Similar cases whereby QSO absorptions are attributed to nearby NGC galaxies or nearby clusters of galaxies have been reported by Blades et al. (1981) and by Boksenberg et al. 1980. As in the previous case, the Ca lines are relatively weak, NaI is not observed, and the intervening object is not very distant from our Galaxy.

The case of H0159-033 is different in two respects. First, the absorption lines appear to be far stronger than any of the previous detection of Ca H and K lines in a QSO. Secondly, the absorption lines have almost half of the redshift of the QSO. If the NaI lines are detected and if a faint nebulosity can be imaged near the QSO position, then there will be strong pressure to accept Hubble's law for the galaxy that is causing the "cold" absorption lines, and lower limits of M_V = -24.3 and log L_x = 45.9 may be established for the QSO.

If the absorbing material is contained within a galaxy similar to our own (M_V = -20.5), then the apparent magnitudes of the galaxy at z = 0.233 would be approximately V ~ 21 and R ~ 20.5, with an angular extent of about 4 arcsec. This is certainly within the imaging capability of a CCD camera on a 4 m telescope, and the Space Telescope could measure such a galaxy rather easily.

VII. TWO X-RAY EMITTING BL LAC OBJECTS

7-1. Introduction

BL Lac objects are a class of active galaxies that are named after the prototype example, BL Lacertae, which was first noticed by Kukarkin in his General Catalogue of Variable Stars. BL Lac objects are a recently defined (or semi-defined) class (Strittmatter et al. 1972), and much of their behavior is still regarded with awe. The classification of these objects is more difficult than most types, although they all exhibit most of the following characteristics (see Stein, O'Dell, and Strittmatter 1976; Angel and Stockman 1980):

(1) The optical spectrum is dominated by a featureless continuum that is much broader (i.e. typically more UV and more infrared) than the thermal continua of stars.

(2) They are compact radio sources.

(3) The optical flux is linearly polarized by an amount that can vary from a few percent to as much as thirty percent, while the radio flux typically shows polarization of a few percent or less.

(4) The source luminosity is highly variable at all observed wavelengths. Variability at timescales of months or days is common, and there are a few reports of variations with timescales of a minute or less.

Sometimes the classification of BL Lac objects is assisted by evidence that the stellar-appearing nucleus is surrouded by a faint optical nebulosity with an extent of several to tens of arcsec. The nebulosity is interpreted as an image of the host galaxy (e.g. Ulrich et al. 1975), just as in the case of deep photographs of emission-line

QSO's (e.g. Wyckoff, Wehringer, and Gehren 1981). The relation between QSO's and BL Lac objects is further established by two other lines of evidence. Spectroscopic observations have revealed that several individual objects show class-crossing behavior. In a few cases, for example 3C446 (Barbieri et al. 1984), a "violently variable" quasar has been observed to brighten into a state in which the optical spectrum loses its emission lines and resembles a BL Lac object. A second link between BL Lac objects and QSO's is obtained from the discovery of a class of highly-polarized quasars that also exhibit radio properties similar to BL Lac objects (Moore and Stockman 1981).

Many BL Lac objects have been detected at X-ray wavelengths. The MC played an important role in establishing their X-ray emission as a class (Schwartz et al. 1979a). The nearest ones, Mkn 501 and Mkn 421, are among the brightest extragalactic X-ray sources in the sky (Wood et al. 1984); other examples observed by HEAO-1, such as H0414+009 amd H0323+022 (Ulmer et al. 1983; Doxsey et al. 1983) were discovered because of their X-ray emission. The radio-selected objects also show X-ray emission, although at somewhat weaker flux levels (Maccagni and Tarenghi 1981).

The X-ray spectra of these objects are generally steep power laws, with an energy index of ~ 2.0 (Worrall et al. 1981). However, their X-ray spectral shape can change very significantly and may even appear "flat" (see Mushotzky et al. 1978; 1979). As described in Section 2-3, the emission is frequently modeled in terms of synchrotron and Compton processes, although the simplest application of these models is not sufficient to predict the X-ray flux densities (Madejski and Schwartz 1983).

Worse than the problems of simple emission models is the inability

to explain their physical nature. The most successful explanation of BL Lac objects is the hypothesis that an otherwise "normal" active galactic nucleus happens to be beaming a relativistic jet of plasma toward our Galaxy (e.g. Lovelace 1976; Rees 1978). There are direct observations of superluminal radio jets in extragalactic objects (see Bridle and Perley 1984). In addition, relativistic beaming and bulk motions appear necessary to make the Synchrotron/Compton model work in the case of BL Lac objects (Urry and Mushotzky 1982; Madejski and Schwartz 1983). The beaming model also has the ability to accomodate the large changes in the polarization angle and source luminosity that are observed in BL Lac objects (e.g. Blandford and Rees 1978). However, the full picture is far from coherent.

Superimposed on these ideas are two observed correlations which seem to convey different notions about the origin of these objects. An association has been established between nearby BL Lac objects and elliptical host galaxies (Ulrich et al. 1975; Weistrop et al. 1979; Weistrop et al. 1981). On the other hand, Seyfert galaxies are strongly associated with spiral galaxies (see Balick and Heckman 1982). However, jets are observed in all types of galaxies and QSO's, and therefore, the beaming model is not easily correlated to an elliptical morphology.

The other correlation is newly reported and somewhat controversial, and it concerns the space density of BL Lac objects. The bright X-ray emitting BL Lac objects appear to be almost as numerous as bright Seyfert galaxies, which statistically argues against the beam-orientation hypothesis (Schwartz and Ku 1983). In addition, serendipitous discoveries of faint X-ray sources in high-latitude Einstein observations are not identifying additional BL Lac objects (Stocke et al. 1983). This

contrasts sharply with the numerous X-ray discoveries of distant QSO's, as the references in Section 6-1 attest. These statistics convey strong implications reqarding the cosmic evolution of BL Lac objects, as compared with QSO's. This evidence motivates another theoretical plane that seems to be askew of the beaming hypothesis.

7-2. The Two BL Lac Objects

In Table 5-1 there are 5 sources for which the optical candidate is a newly classified (or tentative) BL Lac object. In two of these cases there is currently enough evidence to insure that the classification is correct, and they are presented in this chapter. The other objects show featureless continua, but the measurements of radio flux, polarization, and the extent of the optical image have not been performed yet.

Celestial maps showing the X-ray detections and the positions of the two BL Lac objects are shown in Fig. 7-1. The optical, radio, and X-ray flux measurements of the two objects are compiled in Table 7-1. For these sources β'_{ox} is the optical/X-ray spectral index, as was defined in Chapter 6 (see also the Appendix), but with two modifications. First, β_{ox} is calculated for two choices of the assumed X-ray spectral index (α_x), as was done for the distant QSO's, since the X-ray spectra of these objects may vary substantially (references above). The choices for α_x (see Table 7-1) are 2.0 and 0.0. In addition, the primed symbol serves as a reminder that the spectral index must be given in the observer's rest frame, since the redshifts of these BL Lac objects are unknown.

Fig. 7-1. Celestial maps showing the positions of the BL Lac objects and the X-ray positions of the MC (diamonds), the HEAO-LASS ("1H"; Wood et al. 1984), Uhuru ("U"; Forman et al. 1978), and Ariel V ("3A"; McHardy et al. 1981). Note the widely different scales.
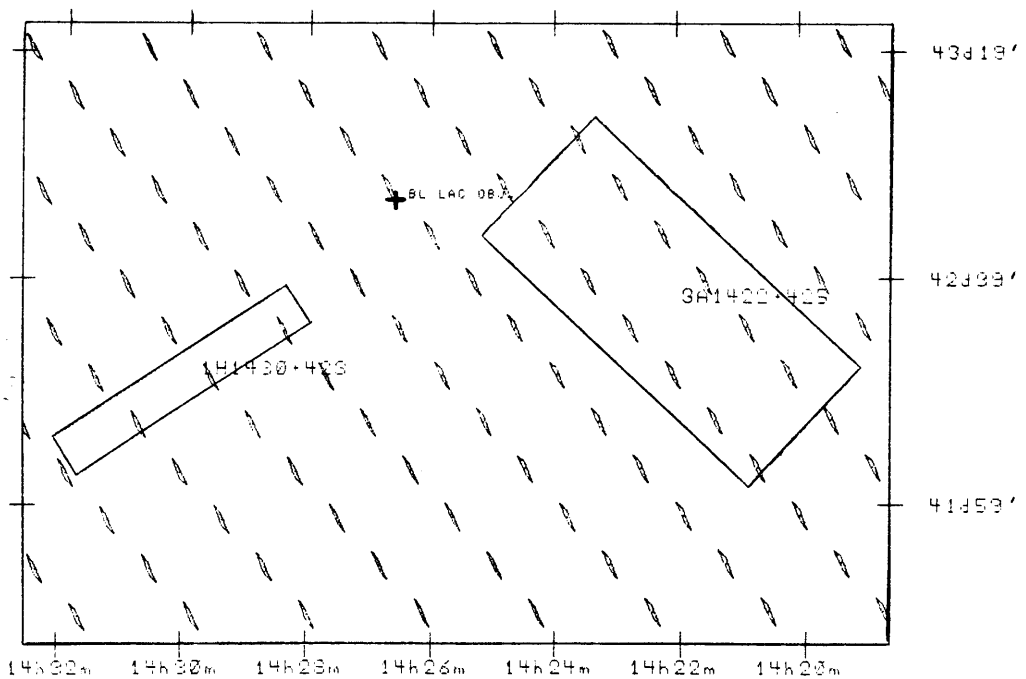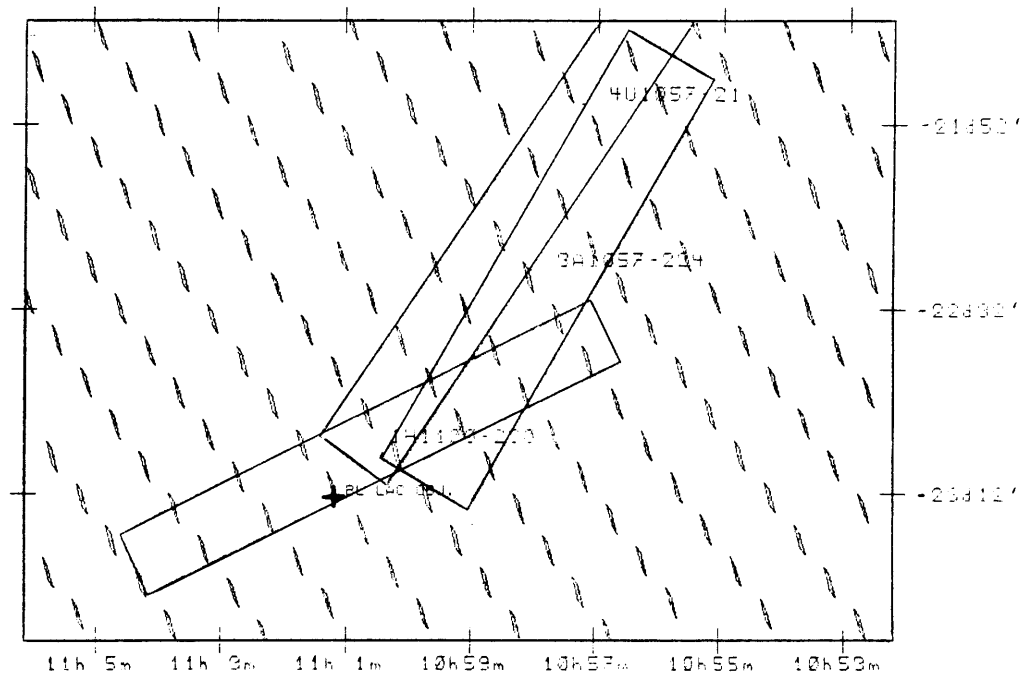
H1101-232 (BL Lac Object)

This object exhibits all of the common BL Lac properties except for variability, which has not been seriously tested. The object first became an important candidate after the radio survey of MC positions (see Section 1-4) using the Very Large Array. A compact radio source with a flux of 83 mJy at 1.4 GHz was found to be positionally coincident ($<$ 1 arcsec displacement) with a ~16th magnitude UV object. The optical spectrum taken at the AAT (Fig. 7-2) showed no significant spectral features except for some residual flux at the location of the strongest emission line of the night sky ("NS").

The BL Lac classification received further support when a CCD image in the R band ($\lambda\lambda$ 5800-8000 Å) using the "MASCOT" instrument (see Section 4-3) showed that the UV object is the nucleus of a ~ 15 arcsec nebulosity, which accounts for ~ 25% of the total number of (red) photons from the object. Finally, a broad-band optical polarization of 2.7% $\pm$ 0.3% was recently measured by Tapia (private communication). The classification of H1101-232 as a BL Lac object is certain.

The X-ray source was detected by several survey experiments (LASS, Ariel V, and Uhuru), as shown in Fig. 7-1. The BL Lac object is within an MC error diamond which has 3.0 σ significance in MC1 and 2.9 σ in MC2, both of which include data from two celestial scans in the 2.5 - 5.5 keV energy channel.

H1427+429 (BL Lac Object)

A UV candidate with non-stellar optical colors was found just prior to the VLA survey of MC positions, and the object was subsequently detected at 1.4 GHz as a compact source with a flux of 33.7 mJy. A

spectrum was obtained through a service proposal to the Multi Mirror Telescope at the MMT Observatory near Tucson, Arizona. The raw data showed a featureless optical continuum ($\lambda\lambda$4000-7000 $\overset{\circ}{A}$ coverage with ~15$\overset{\circ}{A}$ resolution), except for a marginally significant feature near the rest wavelength of Hβ (λ4861). An opportunity arose to observe the object again using the 4 m KPNO telescope with the IIDS spectrograph. A 40 min exposure in the wavelength range of 4600 - 5600 $\overset{\circ}{A}$, displayed in Fig. 7-3, shows that the optical spectrum is truly featureless.

The BL Lac object is contained within an MC error diamond. The significance of the detection is 3.0 σ in MC1 and 3.8 σ in MC2, for the sum of three celestial scans in the 2.5 to 5.5 keV energy channel. Fig. 7-1 shows the X-ray error positions for H1427+429. The BL Lac's position is consistent with the extensions of the LASS and Ariel V error boxes along their narrow dimension. This is the spin-azimuth dimension, which is much less susceptible to dislocations caused by source variability. In addition, there is a very large Uhuru box ~2° to the northeast of the object, and its narrow dimension also points toward the position of the BL Lac object. The simplest explanation for all of these results is that the BL Lac is a variable X-ray source that was detected by all of those instruments. The optical investigations of this X-ray source covered the regions around the LASS and Ariel error boxes in addition to the convergence area in which the BL Lac object is located.

CCD camera images of H1427+429 in the W ($\lambda\lambda$ 4000-6400 $\overset{\circ}{A}$) and R bands ($\lambda\lambda$ 5800-8000 $\overset{\circ}{A}$) both show that this UV object is also the nucleus of a substantial (~16 arcsec) nebulosity of low surface brightness. The shape and apparent uniformity of the nebulosity are consistent with the morphology of an elliptical galaxy, although further observations are

needed to establish the type of host galaxy conclusively. The galaxy

contributes about 24% of the total flux in the W-filtered image and 27%

of the total flux in the R-filtered image.

Fig. 7-2. Optical spectra of the two BL Lac objects. H1101-232 was observed at the AAT on Feb. 8, 1984, while H1427+429 was observed with the 4 m telescope at Kitt Peak National Observatory on Jan. 17, 1985.
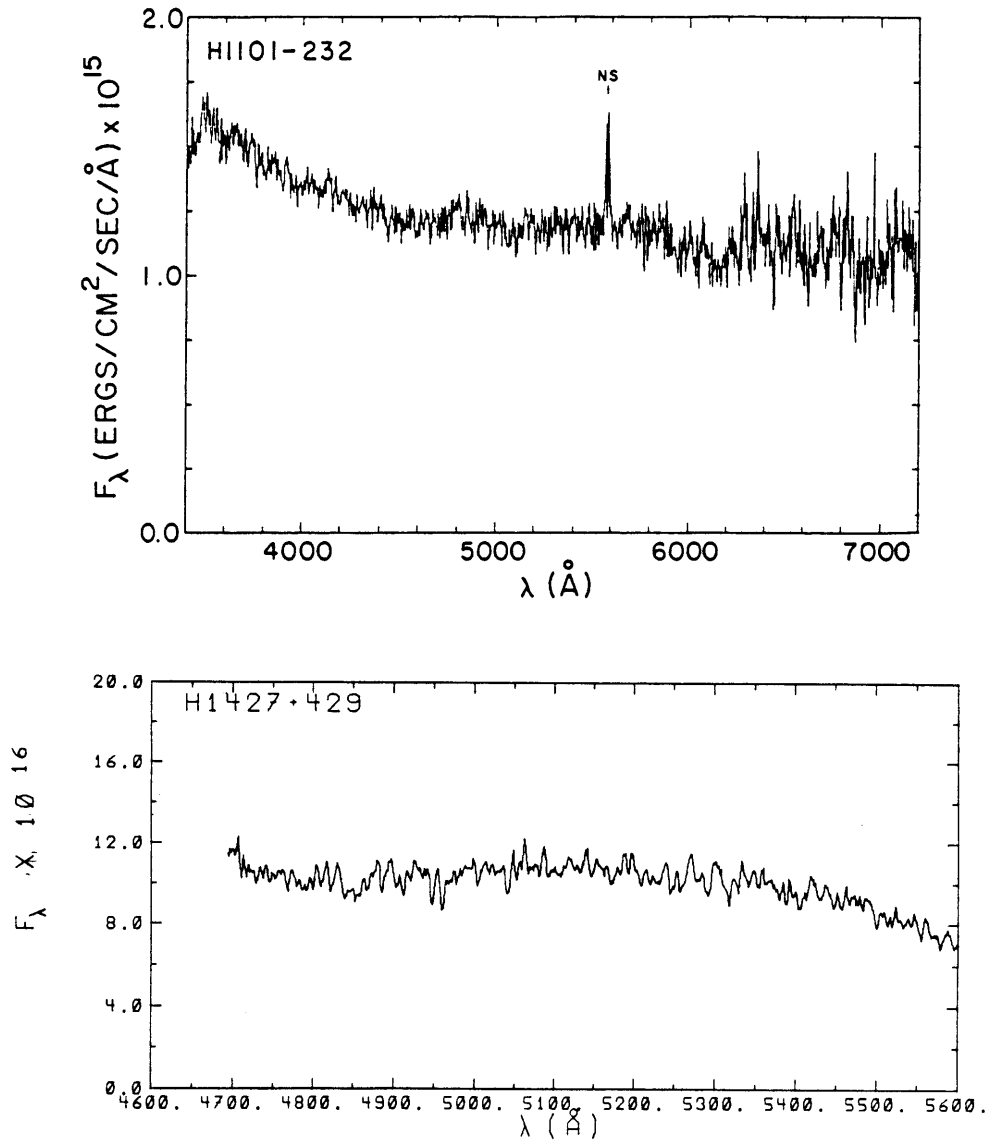
Table 7-1: The BL Lac Objects

		H1101-232	H1427+429
X-ray Names		4U1057-21	?4U1444+43
		3A1057-224	3A1422+425
		1H1100-230	1H1430+423
BL Lac Position	R.A.	11 01 11.1	14 26 35.9
(1950.0)	Dec.	-23 13 20	42 53 44
ID Status		A	A
Photometric	V	16.55	16.42
Magnitudes	B-V	+0.45	+0.50
	U-B	-0.61	-0.55
Optical Polarization (% linear)		2.7 (0.3)	?
Radio Flux Density (mJy at 1.4 GHz)		83.0 (2.0)	33.7 (2.0)
β'_{ox} (α = 2.0)		0.72	0.65
β'_{ox} (α = 0.0)		0.97	0.89
L_x (log erg cm^{-2} s^{-1}) (if z = 0.10)		45.10	45.30

7-3. <u>Discussion</u>

About fourteen BL Lac objects are known to be HEAO-1 X-ray sources
(see Wood <u>et al</u>. 1984; Ulmer <u>et al</u>. 1983; Doxsey <u>et al</u>. 1983). There-
fore, the addition of even two new examples significantly increases the
available sample of bright X-ray emitters among that class of objects.
If the "missing" BL Lacs at large distances is proven to be a real
effect, then the BL Lacs among the unidentified HEAO-1 sources are
especially important cases.

Since both of the objects are contained in MC error diamonds, it is
very probable that they are the correct identifications of the X-ray
sources. If the space density of Seyfert galaxies is taken as an upper
limit to the BL Lac distribution (Schwartz and Ku 1983), then the chance
coincidence of the BL Lac positions within an MC error diamond is ruled
out by the same arguments given for the Sy 1 galaxies in Section 6-3.

The luminosities of these objects are unknown, since the redshifts
cannot be obtained from the spectra of the nuclei. However, the red-
shifts may be estimated by comparing the angular extent of the underlying
galaxies (16 arcsec) with the elliptical galaxy images (~50 arcsec) of
the three bright X-ray BL Lac objects with redshifts ~ 0.032 (Ulrich <u>et
al</u>. 1975). The estimated redshifts are then $z = 0.10$ for both H1101-232
and H1427+429. The X-ray luminosities implied by this redshift (see Table
7-1) are similar to other examples of bright BL Lac objects (see Schwartz
and Ku 1983). The underlying galaxies are sufficiently bright (V ~ 17)
that spectroscopic observations with large apertures (16 arcsec) should
reveal the precise redshifts by observing the galaxies' absorption
features.

There is a remarkable overall resemblance in the characteristics of

these BL Lac objects and the previous BL Lac identifications gained with
the help of MC detections, H0323+022 (Doxsey et al. 1983) and H0414+009
(Ulmer et al. 1983). The four objects have very similar optical
magnitudes, modest radio fluxes (70 ± 30 mJy at 1.4 GHz), low (2-3 %)
optical polarization, and relatively low β_{ox} values (high L_x/L_{opt}). In
addition, at least 3 of the 4 have host galaxies with the same angular
size (see Margon and Jacoby 1984). The similarities are unexpected,
given the erratic variability that characterizes the class and the widely
different luminosity values that are observed when X-ray selected and
radio selected samples are combined (see Biermann et al. 1981; Schwartz
and Ku 1983). The similarities raise the question whether BL Lac objects
may occur in a bimodal rather than a broad distribution.

Chapter VIII: FOUR CATACLYSMIC VARIABLES

8-1. Introduction

Cataclysmic Variables are close binary systems (periods < 16 hours) that contain a white dwarf (the "primary" star) and a normal, main-sequence star (the "secondary") with a spectral type later than or equal to G0 (see Robinson 1976; Patterson 1984). The observed orbital parameters support the hypothesis that the secondary star fills the surface of gravitational equipartition between the two stars (i.e. its "Roche lobe"), and matter is being transferred from the secondary star onto the white dwarf. Dynamical considerations predict the formation of an accretion disk (Pringle 1981) around the white dwarf (or any other accreting compact object), and the material will reside in this disk until angular momentum losses permit the descent onto the surface of the white dwarf.

The optical spectrum of both stars are usually overpowered by a UV continuum and an asortment of emission lines due to hydrogen and helium (see Williams 1983). This spectrum is attributed to the hot gases that are descending onto the white dwarf (Williams and Ferguson 1982). Although the accretion material is comparatively bright, the absolute luminosities of Cataclysmic Variables are rather low (except during classical novae), with M_V (disk) generally in the range of 2-10 (see Patterson 1984). Therefore, the observable objects are at distances between several hundred pc and one kpc, and their apparent distribution is roughly spherical.

As the name implies, a cataclysmic variable (CV) is also likely to

exhibit dramatic photometric variations, such as occasional outbursts, flaring, and short-timescale (1 to 10 s) flickering (e.g. Tuohy et al. 1981). This behavior is sometimes interspersed with periodic modulations on timescales between minutes and one day (Patterson 1984).

CV's are generally divided into four groups, depending on the type of eruptions observed (Robinson 1976). The divisions are classical novae (7 to 15 magnitude outbursts), recurrent novae (more than one classical nova episode), dwarf novae (frequent mini-novae of 2 to 6 magnitudes), and nova-like (no novae). Within these divisions are many subgroups that are usually named after prototype examples (U Gem, Z Cam, AM Her, DQ Her, SU Uma, etc.) from Kukarkin's General Catalogue of Variable Stars. The organization of these phenomenological subgroups is rather complicated (e.g. one type is prone to "superhumps"), and such classifications can only be made after the objects are monitored for a long term.

A more physical distinction among CV's concerns the magnetic character of the white dwarf, and this topic has attracted great interest over the last several years. About 10% of CV's (11 of 124 CV's in a comprehensive review by Patterson 1984) show a significant degree of circular polarization (5-30%) that is indicative of a very strong magnetic field (Angel 1978). During quiescent periods, the absorption features of the white dwarfs in these systems exhibit Zeeman splitting that implies a magnetic field strengths of 10^7 to 10^8 gauss (Wickramasinghe, Visvanathan, and Tuohy 1984). These CV's ("AM Her types") have short orbital periods (1 to 4 h) in which the photometric and polarization modulations are locked in phase. This is interpreted as magnetic confinement of the accretion flow, and the "accretion column" may contain all of the matter being transferred to the white dwarf (no disk; see Angel 1978).

A second type of magnetic CV, known as "DQ Her type" or "intermedi-
ate polars" do not show optical polarization; however they exhibit rapid
and stable photometric periods (1 to 15 m timescales) that are believed
to be caused by the rotation of a magnetic white dwarf (Angel 1978;
Patterson and Price 1981). The lack of optical polarization in this type
of CV probably signifies that the magnetic fields are not strong enough
to completely control the accretion path between the secondary star and
the magnetic poles of the white dwarf. Still, the majority of CV's do
not show evidence of either of these magnetic types.

CV's are a major subclass of the X-ray binaries (see Table 2-1).
Some of the brightest X-ray sources at high galactic latitude are
magnetic CV's or nearby dwarf novae (Wood et al. 1984). Many were
discovered because of their X-ray emission, and the Modulation Collimator
has played an important role in these discoveries (e.g. Griffiths et al.
1979d; Griffiths et al. 1980; Steiner et al. 1981). Their X-ray spectra
are often characterized by an excess of soft X-rays when compared to the
predictions of thermal bremsstrahlung models (Rothschild et al. 1981).
However, their spectra cannot be generalized as easily as other types of
X-ray sources. Two of the CV's reported in this chapter are detected in
the higher energy channels (2.5 to 13.0 keV) of the MC.

The great interest in studying these objects is not limited to the
thrill of tracking their light curves. First of all, CV's may not be as
esoteric a class as might seem at first glance. The correlations between
CV orbital periods and the spectral types of the secondary stars suggests
an evolutionary process that is more general than the "accidental"
formation of a particularly close binary system (see Patterson 1984).
The latter author sees the descent of a white dwarf binary into a CV

"phase" as a natural consequence of the loss of angular momentum by magnetic braking of the stellar wind emitted by the secondary star. The CV phenomenon may occupy a position in the latter stages of evolution in binary systems just as planetary nebulae are a phase related to the formation of white dwarfs. Secondly, science (and civilization) has much to gain by mastering a detailed, predictive understanding of the behavior of plasma flows in high magnetic fields. The effort to model the magnetic CV systems and compute their emission spectra is one test of that scientific capability.

8-2. The Four Cataclysmic Variables

This research program has actually produced five discoveries of Cataclysmic Variables (see Table 5-1). However, the data reductions for 1H1926+503 are at an early stage; the other four are presented in this section. Figure 8-1 shows the positions of the CV's and the X-ray positions of the MC and other experiments. The optical spectra are shown in Figures 8-2 and 8-3, and the celestial coordinates and selected flux measurements are compiled in Table 8-1.

The 2-10 keV X-ray fluxes for these objects are calculated from the LASS count rates, as was done for the AGN, but the empirical conversion factor is different for these objects. A comparison of LASS count rates with the Goddard (HEAO A-2) 2-10 keV flux measurements of 6 identified X-ray emitting CV's determines that 1.16×10^{-3} LASS cts cm^{-2} $s^{-1} = 10^{-11}$ erg cm^{-2} s^{-1}. Cataclysmic Variables apparently do not produce as high a counting rate per flux unit as the AGN within LASS sensitivity range of 1-20 keV.

Fig. 8-1. Maps containing the positions of four Cataclysmic Variable binary systems and the allowed X-ray positions from the HEAO-MC (diamonds). The X-ray error boxes are from the HEAO-LASS ("1H"; Wood et al. 1984) and the GSFC (HEAO A-2) Survey ("H"; Marshall et al. 1979).

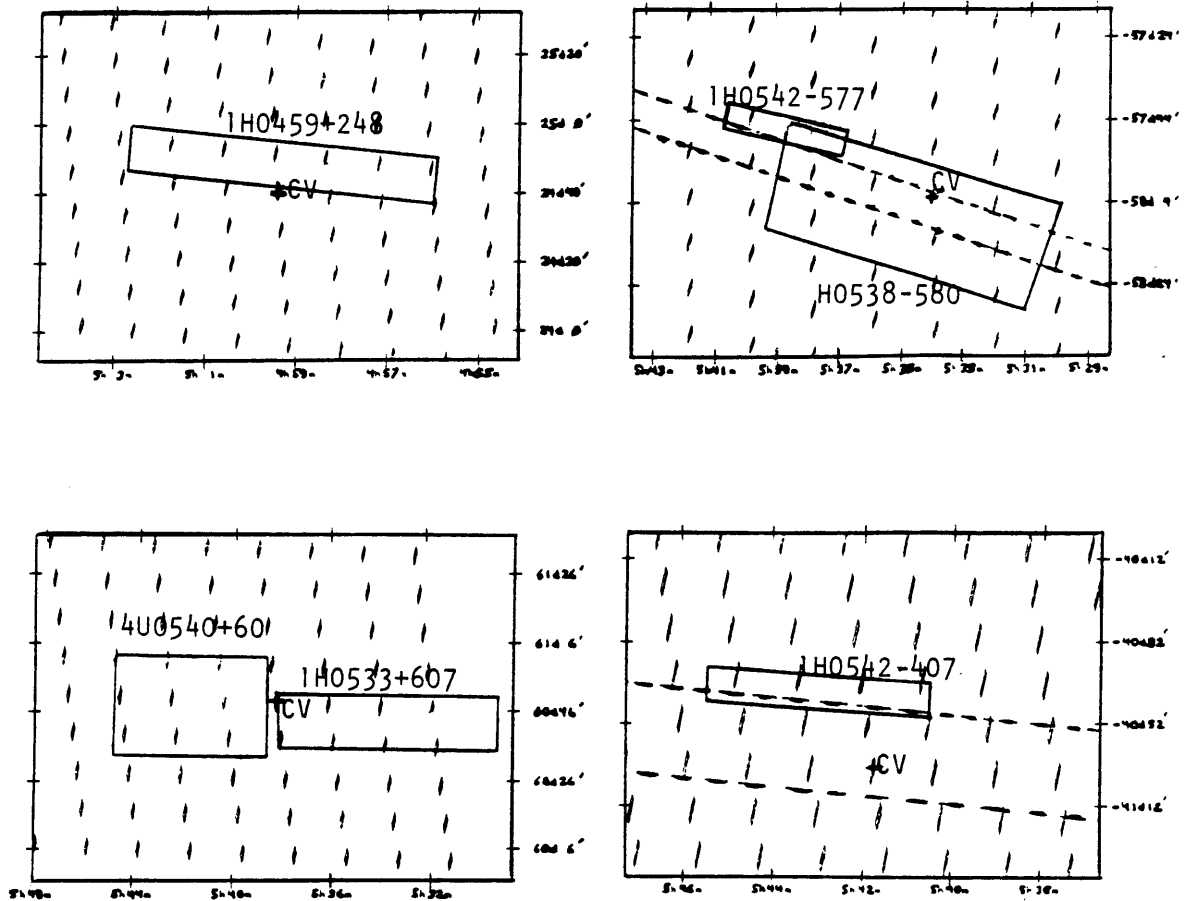Fig. 8-2. The optical spectra of the two northern Cataclysmic Variables. Both spectra were obtained at the McGraw-Hill Observatory; H0459+247 was observed on (UT) April 2, 1984, while H0538+608 was observed on (UT) April 1, 1984.
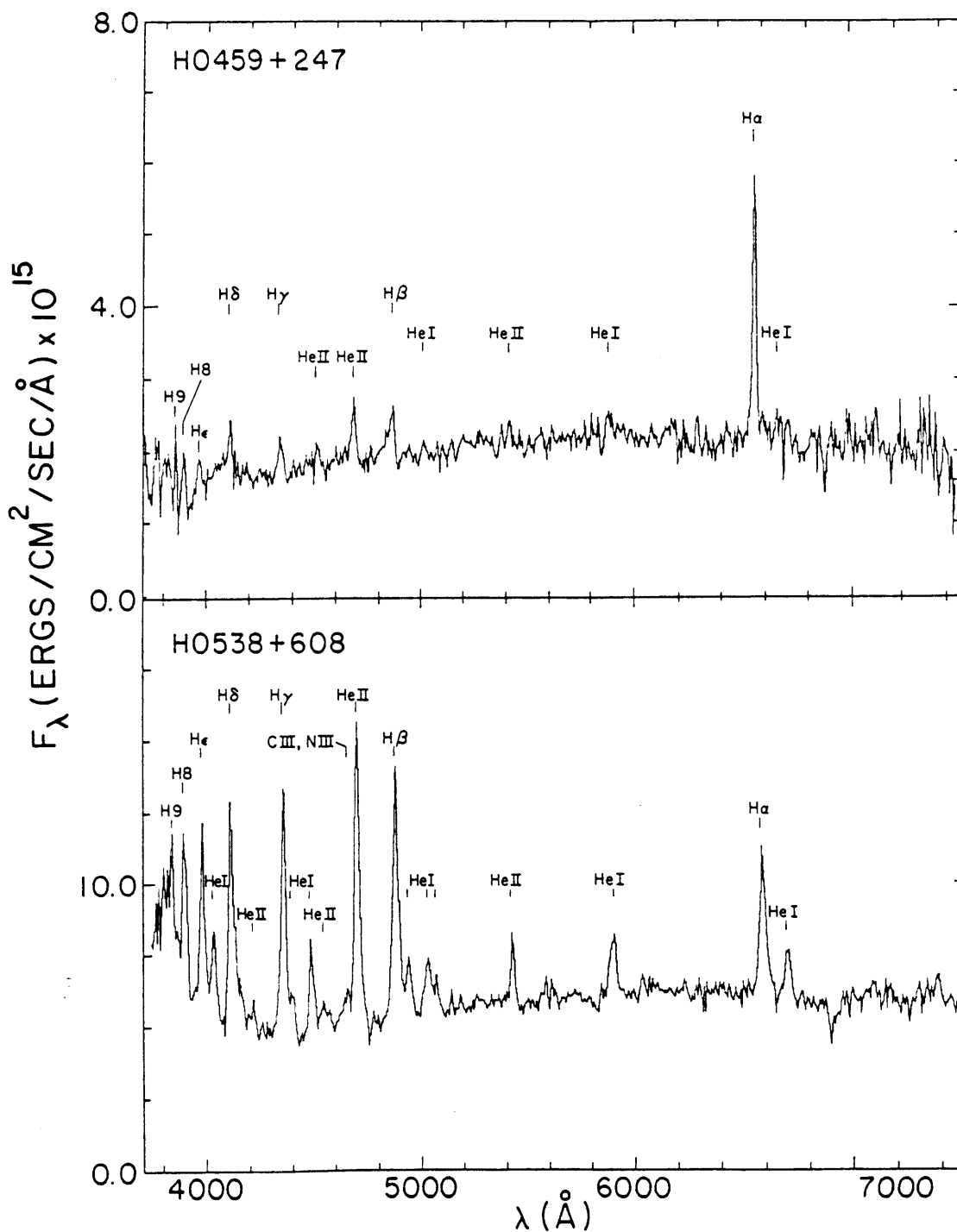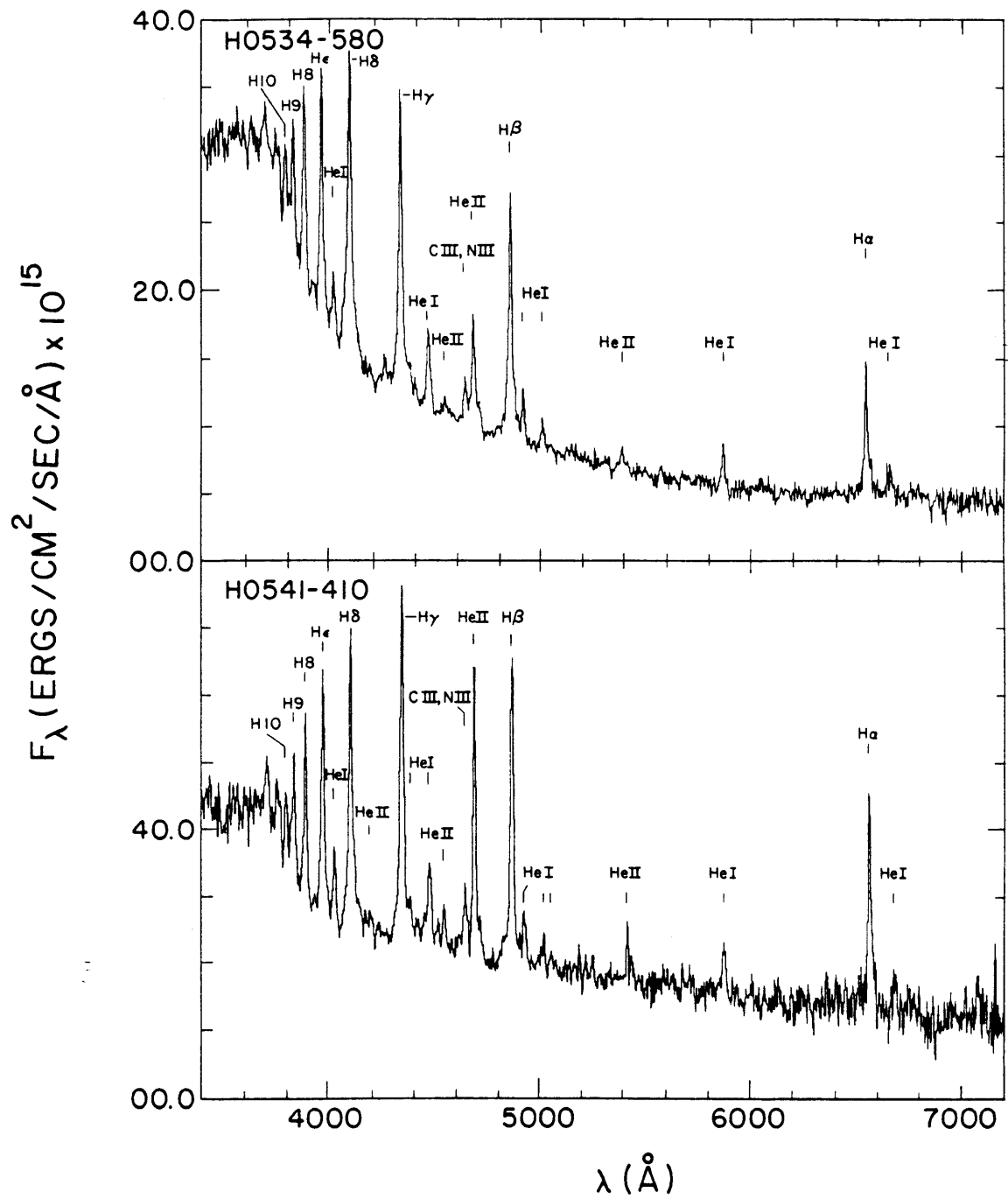
Fig. 8-3. The optical spectra of the two southern Cataclysmic Variables. H0534-581 was observed at the AAT on February 8, 1984, while H0542-411 was observed at the AAT on October 19, 1984.

There are four questions to be addressed regarding the optical

emission properties of CV's. These are:

(1) the periods (if any) of photometric or spectroscopic modulations,

(2) the type and frequency of outbursts,

(3) the equivalent widths and flux ratios of selected emission lines, and

(4) the maximum polarization exhibited during an orbital cycle.

It is possible to answer some, but not all of these questions. The

available information is discussed below.

HO459+247 (CV)

The discovery of this object was assisted by a serendipitous detec-

tion on the very edge of an Einstein IPC field in an observation of the

radio source 3C133 by Prof. Claude Canizares of M.I.T. A UV object was

observed several arcmin from the vignetted IPC position, and its spectrum

is shown in Figure 8-2. Hydrogen and helium emission are observed,

although several of the helium features are very weak. The key to the

spectrum is that all of the weak ($\sim 3\sigma$) features are emission lines at

the wavelengths of HeI and HeII, which are the typical features exhibited

by Cataclysmic Variables. The HeII lines are generally stronger than

HeI, and the flux of HeII $\lambda4686$ is larger that the flux of $H\beta$. These

high-excitation characteristics are observed in several CV's which are

know to be X-ray sources. The spectrum of HO459+247 is similar to that

of the recurrent nova T Pyx (Williams 1983).

The relative contributions of the continuum and the emission lines

in CV spectra vary considerably. Patterson (1984) has shown that the

equivalent widths of the emission lines correlate (inversely) with the

time of the orbital period, and that the latter quantity is correlated to the spectral type of the secondary star (weak lines = long periods = early-type secondaries).

The only photometric observation of this CV was a sequence of color measurements. Several attempts to monitor the source were impeded by poor weather conditions. A period $\geqslant$ 4 h is expected, based on the equivalent width of Hβ (Patterson 1984). Many of the X-ray selected CV's which have comparatively weak emission lines and strong HeII λ4686, relative to Hβ, are "intermediate polar" types, such as H2252-035 (Griffiths et al. 1980; Patterson and Price 1983) and 4U1849-31 (Steiner et al. 1981).

The MC detects the object in the sum of two celestial scans, with significances of 2.7 σ by MC1 and 4.4 σ by MC2 in the range of 1-13 keV.

H0538+608 (Magnetic, AM Her Type CV)

This object is a magnetic (AM Her type) variable. A recent measurement (March, 1985) of variable, circular polarization, reaching a maximum of 10% of the broad-band optical flux (Tapia, private communication), establishes the magnetic character of this system (see Angel 1978). The spectrum (Figure 8-2) displays the classic CV emission lines, with broadened hydrogen lines and very strong HeII λ4686. The strength of the HeII lines coupled with the photometric characteristics of the source had created a strong anticipation that this object was a magnetic type of CV.

H0538+608 was first measured with a photometer as a UV candidate object, and the 10 sec integrations in the B band revealed flickering-type variations that were far above the deviations expected for counting

statistics. The full amplitude of the flickering was about 20% of the mean count rate of the source at that timescale (10 sec). Efforts to monitor the object have been restricted (poor weather, again) to a single, 5-hour series of MASCOT CCD (see Section 4-3) observations taken on Dec. 15, 1983 by Dr. Jeffrey McClintock of M.I.T. and analyzed by the author. The light curve is shown in Figure 8-4, along with the results of a minimum χ^2 search for a frequency that may characterize the observed modulations. For each trial frequency within the range of 0.25 - 1.0 hour^{-1} (with increments of .02 hour^{-1}), the minimum reduced χ^2 values were computed for a sine/cosine series with a variable number of harmonic terms.

Specifically, the data was modeled by the function:

$$C + \sum_n (A_n \sin n\omega t + B_n \cos n\omega t)$$

where ω is the periodic frequency being tested, t is the time of the observations, and n is the harmonic order, n = 1,2,3, etc.). For each trial frequency (ω), the coefficients (C, A_n, and B_n) were computed to minimize χ^2. Figure 8-4 shows a plot of the minimum χ^2 values as a function of the trial frequency for the case, n = 3.

The best fit is for a period of 2.95 $\pm$ 0.10 hours with a full amplitude of 0.9 magnitudes, and the period does not change if a different number of harmonic terms is chosen. The reduced χ^2 values are very large because the variations along the light curve are statistically significant. These are short-timescale variations that would not be expected to affect the determination of the period.

This result is similar in timescale and amplitude to the behavior of many AM Her type systems (see Patterson 1984). However, the 2.95 hour modulation can only be regarded as a tentative orbital period, since less

Fig. 8-4. The optical light curve (CCD counts vs. hours of UT) for
H0538+607. The AM Her type Cataclysmic Variable was observed with the
MASCOT CCD instrument using a broad-band ($\lambda\lambda$ 4000-6400 Å) filter on
Dec. 15, 1983. Below the light curve is a harmonic analysis of the
modulations, indicating a minimum reduced χ^2 value at a period of 2.95
hours. This period is tentatively interpreted as the orbital period of
the binary system, although a confirmation is required.

HOURS (UT), 12/15/83
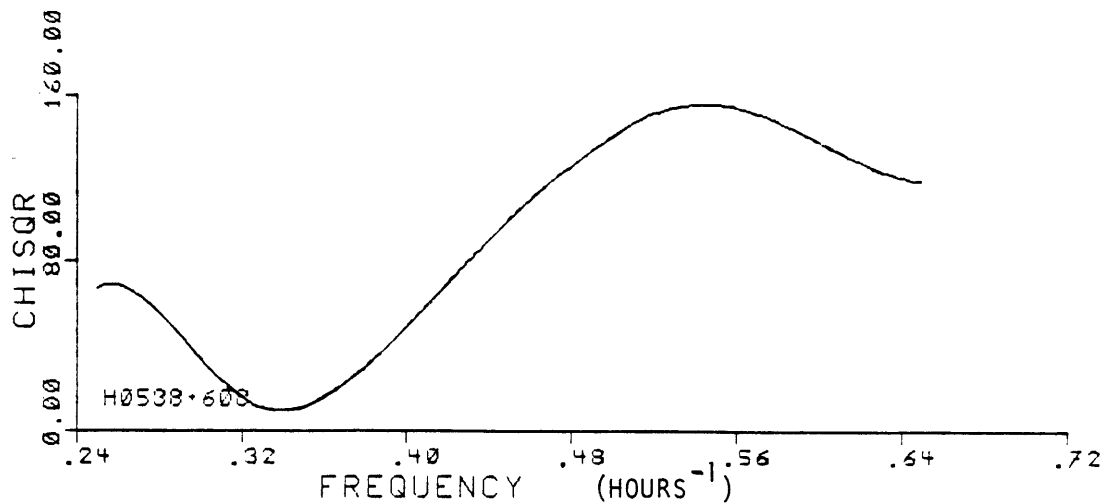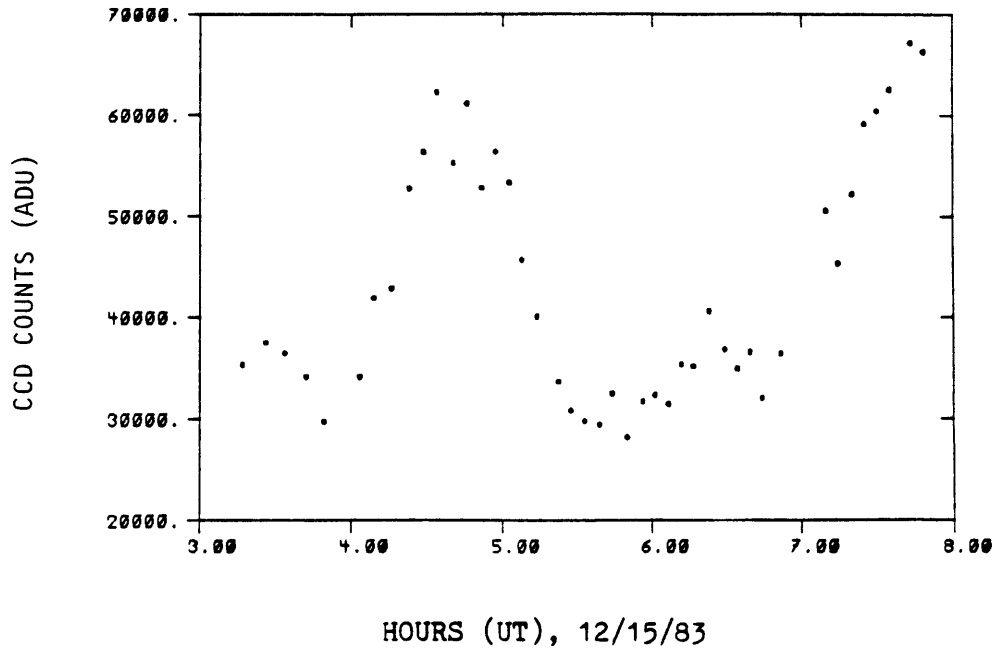
than two complete cycles have been observed. Nevertheless, it is an encouraging result, and a confirmation will be sought. The light curve ranges between visual magnitudes 14.4-15.5, and this is one of the brighter AM Her type objects known.

H0538+608 was detected by both Uhuru and the LASS, and the CV is within an MC error diamond with significances of 3.5 σ for MC1 and 4.4 σ for MC2, for two celestial scans in the range of 2.5 to 13.0 keV. AM Her type objects are known to be strong emitters of X-rays, and this identification is very probable.

H0534-581 (CV)

This CV is another bright (V = 14.8) member of its class. The spectrum (Fig. 8-3) displays an impressive set of emission lines. The hydrogen lines are broadened, the line flux peaks at $H\delta$, and the continuum of high-order Balmer emission is very strong. HeII $\lambda4686$ is not as strong compared to the other three CV's, but the HeII / $H\beta$ flux ratio is still far above average in this case (see Williams 1983).

The MC detections of this X-ray source are very significant (3.5 σ in MC1 and 5.2 σ in MC2 in the range of 2.5 - 13.0 keV for the sum of 3 celestial scans), and the position of the CV is consistent with the MC results. The CV is near the center of the HEAO A-2 error box for this source (see Fig. 8-1), and the CV is also within the LASS line of position in the analysis by the MC group (dashed lines; see Section 3-4). The cataloged LASS position misses the object significantly. Nevertheless, the ID is regarded as very probable.

This object has been photometrically monitored by Dr. Ian Tuohy and Mr. David Buckley, the MC collaborators at Mt. Stromlo Observatory. They

report frequent surges in the optical flux of the CV, but no periodic behavior has yet been observed.

H0542-411 (CV)

This object was discovered during the AAT observations of October, 1984. The spectrum (Fig. 8-3) is another dramatic diplay of H and He emission lines. Again, HeII λ4686 is very strong, and the H lines have broad wings. In many respects the spectrum of H0542-411 is similar to that of H0538+607 (the AM Her type CV), although an AM Her type classification cannot be made without polarimetry measurements of the object.

The photometric behavior of H0542-411 is unknown at this time. Observations by our Australian collaborators have been planned, but they, too, have been hampered by poor weather conditions.

This CV is within 2 arcsec of a faint K star on the plane of the sky, and a considerable effort was required to measure the CV spectrum without contamination from the other star. It will be necessary to conduct photometric observations with the inclusion of the K star in the measuring aperture.

The X-ray source was detected by the LASS, but by none of the other survey instruments. The MC detection is consistent with the position of the CV (2.4 σ by MC1 and 4.0 σ by MC2 for the sum of two celestial scans in the range of 0.9 - 5.5 keV). It is very probable that the CV is the identification of the X-ray source.

Table 8-1: A Summary of the Four Cataclysmic Variables

		H0459+247	H0538+608	H0534-581	H0542-411
Other X-ray		1H0459+248	1H0533+607 4U0540+60	1H0542-577 H0538-580	1H0542-407
Position R.A. (1950) Dec.		04 59 24.1 24 41 06	05 38 15.9 60 50 03	05 34 03.2 -58 03 31	05 41 44.5 -41 03 12
ID Status		A	A	A	A
Photometry	V B-V U-B	15.55 +0.80 -0.60	14.62 +0.54 -0.81	14.83 -0.31 -1.22	15.25 +0.09 -0.82
X-ray Flux (units 10^{-11} erg/cm²-s)		3.0	5.3	3.8	2.0

Spectra

	H0459+247	H0538+608	H0534-581	H0542-411
Line Flux Hβ (units 10^{-13} erg/cm²-s)	0.21	2.99	2.33	1.95
Equiv. Width (Å)	11.2	56.3	51.8	59.0
Relative Flux (Hβ ≡ 1.0) Hα	4.15	0.65	0.45	0.74
Hγ	0.63:	0.75	1.13	1.01
Hδ	0.94:	0.86	1.36	0.90
HeII λ4686	1.01	0.96	0.38	0.75
HeII λ4511	0.38:	0.10	...	0.11
HeII λ5411	0.30:	0.16	0.03	0.11
HeI λ4471	0.22:	0.25	0.21	0.25
HeI λ5876	0.41:	0.22	0.11	0.11

8-3. Discussion

There were 10 CV's listed as suggested identifications in the LASS catalog (Wood et al. 1984). The total number is brought to 16 with the additions of five discoveries and one cataloged CV (TT Ari). Since the early days of the optical studies of X-ray sources, HeII λ4686 has been recognized as an indicator of X-ray emission (e.g. McClintock et al. 1975). The average value of the flux ratios of HeII λ4686 to Hβ for the four CV objects is about 0.8, while the average ratio among 69 CV's surveyed by Williams (1983) was about 0.15. The X-ray sources that are being investigated are among the fainter half of the survey. However, for Cataclysmic Variables, the faint survey sources select some of the brightest and most energetic examples that can be observed.

There is little chance that any of these objects are spurious identifications. The density of CV's (brighter than V = 16.2) on the celestial sphere is 3.3×10^{-3} deg^{-2} (Green et al. 1982). This leads to an expectation of 0.016 CV's within the MC error diamonds for all of the 108 sources investigated. With respect to the four objects shown in this chapter, the number of "chance" CV's is even less, because the diamonds are in fact much smaller than the maximum size and these CV's are much more energetic than the average examples (as indicated by the strength of the HeII lines).

The four discovered Cataclysmic Variables are bright at both optical and X-ray wavelengths, and this establishes their importance for detailed study. Dr. Ian Tuohy and the author (with Dr. Jeffrey McClintock) have proposed to EXOSAT (the European X-ray Satellite) for simultaneous X-ray/optical observation of the four objects. The proposals have been accepted, and the northern CV's will be monitored by photometry, high-

resolution spectroscopy, and polarimetry, while EXOSAT conducts pointed observations of ~10 hours in duration. The optical and X-ray light curves, the radial velocity measurements of H and HeII emissions, and a temporal record of the optical polarization should all contribute to a detailed geometrical description of the emitting regions and their behavior during the course of the binary orbit. Only a few CV's have been studied with correlated observations (e.g. Biermann et al. 1984), and it is hoped that new observations will help clarify the properties that are intrinsic to the various types of X-ray emitting CV's.

IX. SUMMARY AND CONCLUSIONS

Conclusions are given under two general topics:

(1) the research program and systematic concerns,

(2) the types of objects being identified as sources of the HEAO-1

survey. The important optical properties of the individual objects have

been summarized in each of the discussion sections that follow the

presentations of the optical spectra.

The Program

It must be noted that this was not a controlled experiment. Factors

such as the choice of telescopes and the quality of the different batches

of Kodak photographic plates significantly influenced the procedures.

Furthermore, several identifications were gained from UV candidates that

were located on the second or third scan of the photographic plates,

while several unsuccessful investigations listed in Table 5-1 have had

only one thorough inspection of the Schmidt plate. Nevertheless, there

are several inescapable conclusions regarding the research program and

the results.

(1) The search procedures do produce identifications for the faint

HEAO-1 X-ray sources; candidates originated from each of the three steps

that were implemented to find them. Among the "probable" or "very

probable" identifications, 11 objects were previously known and

classified, 5 others were studied because they were bright stars or

galaxies, and the remaining 21 were UV objects (in 4 cases, noticed with

the assistance of the Einstein IPC or radio detections).

(2) Many of the proposed identifications are objects that were previously unknown. The X-ray detections are a signal of high-energy emission, and the optical identifications permit meaningful analysis of the individual objects and permit further studies of class properties. These advantages characterize all of the non-optical surveys, to some degree. This study demonstrates that the process can continue for the fainter population of sources detected by the HEAO-1 instruments.

(3) The identifications gained from LASS/MC sources that were not detected by other survey experiments provides evidence of support for the reality of the faint detections of the LASS catalog. The rate of finding "probable" or "very probable" identifications is 44% for sources detected by only the LASS and the MC, which is higher than the 36% rate for all the sources investigated (excluding the two IPC-assisted cases).

(4) The areas of the LASS error boxes appear to be systematically underestimated by a factor ~ 2, if most of the "probable" and "very probable" identifications are correct. The rms deviation between the candidate position and the center of the NRL error box is 2.0 half-widths of the error boxes in the azimuth (narrow) dimension and 1.1 half-widths in the elevation (long) direction. The error boxes are calculated at the 90% confidence level (Wood et al. 1984), but they must be expanded by the above factors in order to contain 90% of the probable identifications.

(5) Within a galactic latitude of $\pm 20^{\circ}$, the percentage of probable (or

better) identifications drops from about 50% to about 25%, with an
increasing reliance on cataloged objects, such as Be stars and RS CVn
stars. The crowded optical fields, the differential loss of UV photons
(reddening) due to increased interstellar extinction, and the tendency
for the apparent magnitudes of the optical counterparts to be fainter
near the galactic plane, may all contribute to the difficulty at low
latitudes. The use of wide-field objective prism photography may
producehere UV observations were unsuccessful; however, realistically,
some of the work will require X-ray images of the fields, and even then
the prospects of securing the identifications are not certain.

The Sources

(1) The unidentified HEAO-1 sources at high galactic latitude contain
many uncataloged active galactic nuclei (Seyfert galaxies, QSO's and BL
Lac objects). The broad-line AGN discovered in this research show
stronger FeII emission than is typical of those objects. They may also
have β_{ox} values that are lower than average. The latter can be under-
stood if the brighter AGN are discovered first, by the many objective
prism surveys which are capable of observing objects at 14th magnitude
and brighter. However, the frequency of the strong FeII-emitters is
somewhat puzzling. The HEAO-1 survey continues to discover nearby BL Lac
objects. If all of the tentatively classified BL Lac types (Table 5-1)
are confirmed, then the ratio of BL Lac objects to low-redshift Seyfert 1
and QSO's among the newly discovered AGN is ~ 5/18, which is very similar
to the identified portion of the LASS catalog (~ 14/54). BL Lac types

can easily escape notice, and it is very unlikely that many would be found if not for the effort to identify X-ray and radio sources. Finally the HEAO-1 survey will select the few exceptional QSO's that have flat X-ray spectra and high ratios of X-ray to optical luminosity.

(2) The more active examples of X-ray emitting cataclysmic variable systems, and RS CVn type stars continue to be discovered as faint sources of the HEAO-1 survey. At least one of the cataclysmic variables is a magnetic (AM Her type) object, and polarization measurements will soon determine whether any of the others are AM Her types as well.

(3) There are also a small number of clusters or groups of galaxies being identified as X-ray sources. The new identifications are likely to be "poor" clusters or clusters in the galactic plane, because those with more obvious optical morphologies are probably well-studied by both optical and X-ray investigators (see Forman and Jones 1982). The active elliptical galaxy that is listed in Table 5-1 may be related to the "poor" cluster type. A complete description of this case requires further observations (optical and radio imaging), but the galaxy already shows many characteristics that are similar to the cD and D galaxies at the centers of such clusters. This case will be a very interesting study, whether or not the faint galaxies "near" the elliptical have redshifts that indicate cluster membership.

(4) There is a low probability of spurious identifications caused by chance occurrences of the optical candidates in or near the allowed X-ray positions. The sum of the expectation values for "chance" Seyfert 1

(V<16)), QSO's (V<17), BL Lac Objects, and Cataclysmic Variables (V<16.2)

within any of 40 MC diamonds of the maximum (1' x 4') size near all of

the 108 program sources is 0.65. This implies that the large majority of

the 37 "A" and "B" status identifications are correct. Two "B" status

identifications have been subsequently confirmed by X-ray imaging

observations.

(5) The program will contribute additional results from many

"unsuccessful" observations of candidates. The research frequently

encounters faint blue stars, white dwarfs, and normal galaxies that

appear as HII regions, all of which inevitably (by chance) lie in or near

the MC diamonds. Many of these objects are observed with the 3.9 m AAT,

where a high-quality spectrum is quickly obtained. There is no basis for

proposing that any of these are X-ray sources. The identifications of

serendipitous Einstein detections at high latitudes have been completed

with no contributions from these three classes of objects. However, in

each case there is an ongoing effort in optical astronomy to physically

model the objects and compute the emission spectra. For example, theore-

ticians are developing non-LTE models for the surface emissions of hot

subdwarfs and they require accurate measurements of the equivalent widths

of H and He absorption lines, which this research program can supply.

Two of the HII type (starburst) galaxies observed with the AAT have

absolute magnitudes, M_V < 20, which is rare for this type of galaxy.

These "serendiptious" discoveries will be compiled and reported as time

is available.

APPENDIX

Many spectral measurements and luminosity results are given throughout the latter chapters of this work. The definitions and equations governing these measures are specified in this section.

A-1. The Measurement of Spectral Features

All of the optical spectra are plotted as a flux density (erg cm^{-2} s^{-1} Å^{-1}) versus wavelength (Å). The flux of an emission line, F_e, is defined as the integrated flux density that is above the level of the continuous emission ("continuum") within the wavelength range that contains the emission feature. Since flux-calibrated spectra are in the form of quantized (average) flux densities, f_i, per constant wavelength interval, $d\lambda$, a summation symbol is used rather than an integral sign.

$$\underline{\text{line flux:}} \quad F_e = d\lambda \sum_i (f_i - f_{ci}),$$

where f_{ci} is the flux density of the continuum at wavelength i, and the summation is carried over the range in i that contains the emission line.

When defining the continuum values, it is essential to adopt a "global" perspective of the spectrum. For example it is important to realize that the AGN spectra with very broad emission lines may not reach the continuum level anywhere between Hγ ($\lambda_o 4340$) and the strongest OIII line ($\lambda_o 5007$). In this report, the local values of the continua (f_{ci}) were computed from linear interpolations between the calculated averages within specified continua ranges on either side of the feature being measured.

The equivalent width, W, is a measure of the strength of a spectral feature relative to the local strength of the continuum. It is a range in wavelength (units are $\overset{\circ}{A}$) at the flux density of the local continuum that would contain an amount of flux that is equal to the the line flux, F_e (as above). Equivalent widths are also measured for absorption features, using the same equation for F_e and generally ignoring the minus sign.

<u>Equivalent width</u>: $W = F_e/f_{ic}$.

Line widths are often of interest for both the emission and absorption features of an optical spectrum. The observed width of a feature, $\Delta\lambda'$, is generally results from a convolution of the instrumental width, $\Delta\lambda_{sp}$, and the "true" width, $\Delta\lambda$. The instrumental width is usually measured from the observed emission lines of comparison lamps that are used to calibrate the wavelength scale. The deconvolution is calculated by assuming that the factors add in quadrature:

<u>"True" Line Width</u>: $\Delta\lambda = (\Delta\lambda'^2 - \Delta\lambda_{sp}^2)^{1/2}$.

The full width at zero intensity (FWZI) is the Doppler velocity that would be required to shift a spectral element across the entire baseline of the "true" width of a spectral feature. For FWZI $\ll$ c, where c is the speed of light:

<u>Full Width at Zero Intensity</u>: $FWZI = c\ \Delta\lambda/\lambda_o$,

where $\Delta\lambda$ is the full width of the spectral feature and λ_o is the observed center of the spectral feature.

An analogous measurement can be made of the full width at half-maximum, FWHM, by measuring the line width at a point half-way between the continuum and the peak of an emission line (or the minimum of an absorption line).

The redshift, z, of a spectral feature is calculated very simply:

$$\underline{\text{Redshift:}} \quad z = (\lambda' - \lambda_o)/\lambda_o,$$

where λ' is the observed wavelength of a feature that is "normally" found at a wavelength of λ_o when both the emitter and the observer are in the same rest frame.

A-2. Spectral Continuum Measurements

To compare an object's optical brightness with its X-ray brightness, many authors calculate a spectral index, which is the exponent of a power-law function that would connect any two measures of flux density. The particular spectral index often calculated in studies of nearby AGN is β_{ox}, which connects the flux densities (e.g. erg cm^{-2} s^{-1} $\overset{\circ}{A}^{-1}$) between the measured values at 2 keV (f_x) and at 4000 $\overset{\circ}{A}$ (f_{opt}), both measured at

the redshifted wavelengths in the observer's rest frame. The assumed photon spectrum is

$$f(E) = k \, E^{-\beta},$$

where E is the photon energy and k is a constant. A simultaneous solution for both measured flux densities leads to the expression:

Optical/X-ray <u>spectral index</u> (β_{ox}): $\beta_{ox} = 0.356 \log (f_{opt}/f_x)$.

The value of f_{opt} is obtained (or extrapolated) from the optical spectrum at a wavelength of $\lambda = 4000 \times (1+z)$ Å, with an estimated correction for absorption by interstellar material in the Galaxy. The spectral flux density must be absolutely calibrated, and light loss due to cirrus clouds or poor seeing conditions may be "restored" if photometric measurements of the objects are available, by scaling the spectrum by a constant factor that produces an agreement between the photometric magnitudes and the integrated spectral flux densities, using the normalization of Allen (1976). The extinction correction is:

$$f_{opt} = f(4000 \, (1+z)) \times 10^{(A_\lambda/2.5)},$$

where A_λ is the extinction (in magnitudes) at $\lambda = 4000 \times (1+z)$ Å. The extinction can be written as:

$$A_\lambda = A_v + E(\lambda - V).$$

The value of A_v can be estimated from the galactic latitude, b, using (Schmidt 1968) $\qquad A_v = 0.18 \csc b.$

The values of $E(\lambda - V)$ are given by Bless and Savage (1972). For low redshifts, $A_\lambda \sim 1.38 \, A_v$.

In this work the value of f_x is calculated from the LASS count rate (counts cm^{-2} s^{-1}; Wood et al. 1984) for a given source by assuming a value for the X-ray spectral index, α_x. The X-ray spectral index is assumed to be valid only for the range of 2 to 10 keV. For AGN, as explained in Section 6-1, the adopted flux normalization for a LASS count rate, R, is:

$$F_x = R \times 5 \times 10^{-9} \text{ ergs } cm^{-2} s^{-1}.$$

If it is assumed that the X-ray flux density is governed by

$$f_x = k \ E^{-\alpha},$$

then F_x is simply the integral of f_x over the range of 2-10 keV, and

$$k = F_x \ (1-\alpha) \ E^{(1-\alpha)} \bigg|_{E=2}^{10}.$$

The choice of α permits the evaluation of the constant, k. The equation for f_x is:

$$f_x = f(E = 2 \text{ keV}/(1+z)) = k \ (2/(1+z))^{-\alpha}.$$

Choose α, solve for k, and then calculate f_x. The use of the 2-10 keV flux measures to calculate the flux density at 2 KeV is not sensitive to interstellar absorption effects unless the galactic latitude is very low. A superior measurement of β_{ox} would fit the X-ray spectral index and interstellar column density for each individual AGN before the flux at 2 keV is determined, but that is not possible for LASS/MC X-ray sources.

REFERENCES

Allen, C. W. 1976, Astrophysical Quantities (3rd ed.; London: Athlone Press).

Angel, J. R. P. 1978, Ann. Rev. Astron. Astrophys., 16, 487.

Angel, J. R. P., and Stockman, H. S. 1980, Ann. Rev. Astron. Astrophys., 8, 321.

Arp, H. 1983, Ap. J., 271, 479.

Atwood, B., Ingerson, T., Lasker, B. M., and Osmer, P. S. 1979, P.A.S.P., 91, 120.

Bahcall, J. N. 1971, Astron. J., 76, 283.

Bahcall, J. N., and Peebles, P. J. E. 1969, Ap. J. (Letters), 156, L7.

Baity, W. A. et al. 1981, Ap. J., 244, 429.

Baldwin, J. A., Phillips, M. M., and Terlevich, R. 1981, P.A.S.P., 93, 5.

Balick, B., and Heckman, T. M. 1982, Ann. Rev. Astron. Astrophys., 20, 431.

Balzano, V. A. 1983, Ap. J., 268, 602.

Barbieri, C., Cristian, S., Omizzolo, S., Romano, G. 1984, European Southern Observatory Scientific Preprint no. 339.

Becker, R. H., Boldt, E. A., Holt, S. S., Serlemitsos, P. J., and White, N. E. 1980, Ap. J. (Letters), 237, L177.

Bennett, A. S. 1962, M.N.R.A.S., 125, 75.

Bessell, M. S. 1985, P.A.S.P., in prep.

Biermann, P. et al. 1981, Ap. J. (Letters), 247, L53.

Biermann, P. et al. 1984, Steward Observatory, University of Arizona Preprint no. 561.

Birks, J. B. 1964, The Theory and Practice of Scintillation Counting (New York: The MacMillan Company).

Blades, J. C., Hunstead, R. W., and Murdoch, H. S. 1981, M.N.R.A.S., 194, 669.

Bless, R. C., and Savage, B. D. 1972, Ap. J., 171, 293.

Boksenberg, A., Carswell, R. F., Allen, D. A., Fosbury, R. A. E., Penston, M. V., and Sargent, W. L. W. 1977, M.N.R.A.S., 178, 451.

Boksenberg, A., Daniziger, I. J., Fosbury, A. E., and Goss, W. M. 1980, Ap. J. (Letters), 242, L145.

Boksenberg, A., and Sargent, W. L. W. 1978, Ap. J., 220, 42.

Bolton, C. T. 1975, Ap. J., 200, 269.

Bowyer, C. S., Byram, E. T., Chubb, T. A., and Friedmann, H. 1964, Science, 146, 912.

Bradt, H. V., Doxsey, R. E., Jernigan, J. G. 1979, X-Ray Astronomy, ed. W. A. Baity, L. E. Peterson (Oxford: Pergamon), p. 3.

Bradt, H., Garmire, G., Oda, M., Spada, G., and Sreekantan, B. V. 1968, Space Science Reviews, 8, 471.

Bradt, H. V. D., and McClintock, J. E. 1983, Ann. Rev. Astron. Astrophys., 21, 13.

Bradt, H. V., Naranan, S., Rappaport, S., and Spada, G. 1968, Ap. J., 157, 1005.

Bridle, A. H., Perley, R. A. 1984, Ann. Rev. Astron. Astrophys., 22, 319.

Brown, R. L., and Gould, R. J. 1970, Phys. Rev. D., 1, 2252.

Canizares, C. R., McClintock, J. E., and Grindlay, J. E. 1980, Ap. J. (Letters), 236, L55.

Canizares, C. R., McClintock, J. E., and Ricker, G. R. 1978, Ap. J. (Letters), 226, L1.

Canizares, C. R., and Winkler, P. F. 1981, Ap. J. (Letters), 246, L33.

Chanan, G. A., Margon, B., and Downes, R. A. 1981, Ap. J. (Letters), 243, L5.

Charles, P. A., Longair, M. S., and Sanford, P. W. 1975, M.N.R.A.S., 170, 17p.

Clark, G. W. 1965, Phys. Rev. Letters, 14, 91.

Clark, G. W. 1982, Bull. A.A.S., 14, 943.

Cooke, B. A., Elvis, M., Maccacaro, T., Ward, M. J., Fosbury, R. A. E., and Penston, M. V. 1976, M.N.R.A.S., 177, 121p.

Cowley, A. P., Crampton, D., Hutchings, J. B., Remillard, R., and Penfold, J. E. 1983, Ap. J., 272, 118.

Davidson, K. 1972, Ap. J., 171, 213.

Davidson, K., and Netzer, H. 1979, Rev. Mod. Phys., 51, 715.

Dower, R. G., Griffiths, R. E., Bradt, H. V., Doxsey, R. E., and
Johnston, M. D. 1980, Ap. J., 235, 355.

Doxsey, R., Bradt, H., McClintock, J., Petro, L., Remillard, R.,
Ricker, G., Schwartz, D., and Wood, K. 1983, Ap. J. (Letters),
264, L43.

Doxsey, R., Grindlay, J., Griffiths, R., Bradt, H., Johnston, M.,
Leach, R., Schwartz, D., and Schwarz, J. 1979, Ap. J. (Letters),
228, L67.

Duus, A., and Newell, B. 1977, Ap. J. Suppl., 35, 209.

Eardley, D. M., and Lightman, A. P. 1976, Nature, 262, 196.

Elvis, M., Maccacaro, T., Wilson, A. S., Ward, M. J., Penston, M. V.,
Fosbury, R. A. E., and Perola, G. C. 1978, M.N.R.A.S., 183, 129.

Fireman, E. L. 1974, Ap. J., 187, 57.

Forman, W., and Jones, C. 1982, Ann. Rev. Astron. Astrophys., 20, 547.

Forman, W., Jones, C., Cominsky, L., Julien, P., Murray, S., Peters, G.,
Tananbaum, H., and Giacconi, R. 1978, Ap. J. Suppl., 38, 357.

Friedman, H., Byram, E. T., and Chubb, T. A. 1967, Science, 156, 374.

Garcia, M., Baliunas, S. L., Conroy, M., Johnston, M. D., Ralph, E.,
Roberts, W., Schwartz, D. A., and Tonry, J. 1980, Ap. J. (Letters),
240, L107.

Giacconi, R., Gursky, H., Paolini, F. R., and Rossi, B. B. 1962,
Phys. Rev. Letters, 9, 439.

Graham, J. A. 1982, P.A.S.P., 94, 244.

Green, R. F., Ferguson, D. H., Liebert, J., and Schmidt, M. 1982,
P.A.S.P., 94, 560.

Griffiths, R. E., Briel, U., Schwartz, D. A., Schwarz, J., Doxsey, R. E.,
and Johnston, M. D. 1979(a), M.N.R.A.S., 188, 813.

Griffiths, R. E., Doxsey, R. E., Johnston, M. D., Schwartz, D. A.,
Schwarz, J., and Blades, J. C. 1979(b), Ap. J. (Letters), 230, L21.

Griffiths, R. E., Gursky, H., Schwartz, D. A., Schwarz, J., Bradt, H.,
Doxsey, R. E., Charles, P. A., Thorstensen, J. R. 1978, Nature,
276, 247.

Griffiths, R. E., Lamb, D. Q., Ward, M. J., Wilson, A. S., Charles, P. A., Thorstensen, J., McHardy, I. M., and Lawrence, A. 1980, M.N.R.A.S., 193, 25p.

Griffiths, R. E., Tapia, S., Briel, U., and Chaisson, L. 1979(c), Ap. J., 234, 810.

Griffiths, R. E., Ward, M. J., Blades, J. C., Wilson, A. S., Chisson, L., and Johnston, M. D. 1979(d), Ap. J. (Letters), 232, L27.

Grindlay, J. E., McClintock, J. E., Canizares, C., van Paridijs, J., Cominsky, L., Li, F. K., and Lewin, W. H. G.1978, Nature, 274, 567.

Grindlay, J. E., Steiner, J. E., Forman, W. R., Canizares, C. R., and McClintock, J. E. 1980, Ap. J. (Letters), 239, L43.

Gull, T. R., York, D. G., Snow, T. P., and Henize, K. G. 1976, Ap. J., 206, 260.

Gursky, H., Giacconi, R., Gorenstein, P., Waters, J. R., Oda, M., Bradt, H., Garmire, G., and Sreekantan, B. V. 1966, Ap. J., 146, 310.

Gursky, H., and Schwartz, D. A. 1977, Ann. Rev. Astron. Astrophys., 15, 541.

Gursky, H., et al. 1978, Ap. J., 223, 973.

Haschick, A. D., and Burke, B. F. 1975, Ap. J. (Letters), 200, L137.

Hatchett, S., Buff, J., and McCray, R. 1976, Ap. J., 206, 847.

Heckman, T. M. 1980, Astron. Astrophys., 83, 152.

Holt, S. S., and McCray, R. 1982, Ann. Rev. Astron. Astrophys., 20, 323.

Houck, J. R., Schneider, D. P., Danielson, G. E., Beichman, C. A., Lonsdale, C. J., Neugebauer, G., and Soifer, B. T. 1985, Ap. J. (Letters), 290, L5.

Huchra, J., and Sargent, W. 1973, Ap. J., 186, 433.

Hutchings, J. B., Crampton, D., and Cowley, A. P. 1983, Ap. J. (Letters), 275, L43.

Jauncey, D. L. 1975, Ann. Rev. Astron. Astrophys., 13, 23.

Johnston, M. D., Bradt, H. V., Doxsey, R. E., Griffiths, R. E., Schwartz, D. A., and Schwarz, J. 1979, Ap. J. (Letters), 230, L11.

Johnston, M. D., Bradt, H. V., Doxsey, R. E., Gursky, H., Schwartz, D.
    A., Schwarz, J., and van Paradijs, J. 1978, Ap. J. (Letters), 225,
    L59.

Johnston, M. D., Bradt, H. V., Doxsey, R. E., Margon, B., Marshall, F.
    E., and Schwartz, D. A. 1981, Ap. J., 245, 799.

Joss, P. C., and Rappaport, S. A. 1984, Ann. Rev. Astron. Astrophys.,
    22, 537.

Kallman, T. R., and McCray, R. 1982, Ap. J. Suppl., 50, 263.

Kellermann, K. I., and Pauliny-Toth, I. I. K. 1981, Ann. Rev. Astron.
    Astrophys., 19, 373.

Kerr, F. J. 1969, Ann. Rev. Astron. Astrophys., 7, 39.

Khachikian, E. Y., and Weedman, D. W. 1974, Ap. J., 192, 581.

Klebesadel, R. W., Strong, I. B., and Olson, R. A. 1973, Ap. J.
    (Letters), 182, L85.

Kleinmann, S. G., Gillett, F. C., and Joyce, R. R. 1981, Ap. J.,
    19, 441.

Koski, A. T. 1978, Ap. J., 223, 56.

Kriss, G. A., and Canizares, C. R. 1982, Ap. J., 261, 51.

Kriss, G. A., and Canizares, C. R., and Ricker, G. R. 1980, Ap. J., 242,
    492.

Kuhr, H., Liebert, J. W., Strittmatter, P. A., Schmidt, G. D., and
    McCray, C. 1983, Ap. J. (Letters), 275, L33.

Lamb, D. Q., and Masters, A. R. 1978, Ap. J. (Letters), 234, L117.

Landolt, A. U. 1983, Astron. J., 88, 439.

Lang, F. L. et al. 1981, Ap. J. (Letters), 246, L21.

Lawrence, A., and Elvis, M. 1982, Ap. J., 256, 410.

Lawrence, A., Pye, J. P., and Elvis, M. 1977, M.N.R.A.S., 181, 93p.

Levine, A. M. et al. 1984, Ap. J. Suppl., 54, 581.

Lewin, W. H. G., and Joss, P. C. 1981, Space Sci. Rev., 28, 3.

Lovelace, R. V. E. 1976, Nature, 262, 649.

Maccacaro, T., Perola, G. C., and Elvis, M. 1982, Ap. J., 257, 47.

Maccagni, D., and Tarenghi, M. 1981, Ap. J., 243, 42.

Madejski, G. M., and Schwartz, D. A. 1983, Ap. J., 275, 467.

Malkan, M. A. 1983, Ap. J., 268, 582.

Malkan, M. A., and Sargent, W. L. W. 1982, Ap. J., 254, 22.

Margon, B. 1984, Ann. Rev. Astron. Astrophys., 22, 507.

Margon, B., and Jacoby, G. H. 1984, Ap. J. (Letters), 286, L31.

Markert, T. H. et al. 1979, Ap. J. Suppl., 39, 948.

Marscher, A. P., and Broderick, J. J. 1981, Ap. J., 249, 406.

Marshall, F. E., Boldt, E. A., Holt, S. S., Mushotzky, R. F., Pravdo, S.
     H., Rothschild, R. E., and Serlemitsos, P. J. 1979, Ap. J. Suppl.,
     40, 657.

Marshall, F. J., Clark, G. W. 1984, Ap. J., 287, 633.

Mason, K. O., Cordova, F. A., Middleditch, J., Reichert, G. A.,
     Bowyer, S., Murdin, P., and Clark, D. 1983, P.A.S.P., 95, 370.

McClintock, J. E., Canizares, C., Li, F., and Grindlay, J. E. 1980,
     Ap. J. (Letters), 235, L81.

McClintock, J. E., Canizares, C. R., and Tarter, C. B. 1975, Ap. J. 198,
     641.

McClintock, J. E., Petro, L. D., Remillard, R. A., and Ricker, G. R.
     1983, Ap. J. (Letters), 266, L27.

McHardy, I. M., Lawrence, A., Pye, J. P., and Pounds, K. A. 1981,
     M.N.R.A.S., 197, 893.

McNally, D. 1971, Highlights of Astronomy (vol. 2; Dordrecht-Holland:
     D. Reidel Publishing Company), p. 339.

Moore, R. L., and Stockman, H. S. 1981, Ap. J., 243, 60.

Morrison, R., and McCammon, D. 1983, Ap. J., 270, 119.

Mufson, S. L. et al. 1984, Ap. J., 285, 571.

Mushotzky, R. F. 1982, Ap. J., 256, 92.

Mushotzky, R. F., Boldt, E. A., Holt, S. S., Pravdo, S. H.,
     Serlemitsos, P. J., Swank, J. H., and Rothschild, R. H. 1978,
     Ap. J. (Letters), 226, L65.

Mushotzky, R. F., Boldt, E. A., Holt, S. S., and Serlemitsos, P. J. 1979, Ap. J. (Letters), 232, L17.

Mushotzky, R. F., Holt, S. S., and Serlemitsos, P. J. 1978, Ap. J. (Letters), 225, L115.

Mushotzky, R. F., Marshall, F. E., Boldt, E. A., Holt, S. S., and Serlemitsos, P. J. 1980, Ap. J., 235, 377.

Neugebauer, G. et al. 1984, Ap. J. (Letters), 278, L1.

Nugent, J. J. et al. 1983, Ap. J., 51, 1.

Oda, M. 1965, Appl. Opt., 4, 143.

Ogelman, H., Beuermann, K., and Krautter, J. 1984, Ap. J. (Letters), 287, L31.

Oke, J. B. 1974, Ap. J. Suppl., 27, 21.

Oke, J. B., and Sargent, W. L. W. 1968, Ap. J., 151, 807.

Osterbrock, D. E. 1977, Ap. J., 215, 733.

Osterbrock, D. E. 1984, Q.J.R.A.S., 25, 1.

Patterson, J. 1984, Ap. J. Suppl., 54, 443.

Patterson, J., and Price, C. M. 1981, Ap. J. (Letters), 243, L83.

Petre, R., Mushotzky, R. F., Krolik, J. H., and Holt, S. S. 1984, Ap. J., 280, 499.

Petro, L., Bradt, H., Kelley, R., Horne, K., and Gomer, R. 1981, Ap. J. (Letters), 251, L7.

Phillips, M. M. 1977, Ap. J., 215, 746.

Phillips, M. M. 1978, Ap. J. Suppl., 38, 187.

Phillips, M. M., Charles, P. A., and Baldwin, J. A. 1983, Ap. J., 266, 485.

Piccinotti, G., Mushotzky, R. F., Boldt, E. A., Holt, S. S., Marshall, F. E., Serlemitsos, P. J., and Shafer, R. A. 1982, Ap. J., 253, 485.

Pilkington, J. D. H., and Scott, P. F. 1965, Mem. Roy. Astron. Soc., 69, 183.

Pravdo, S. H., and Marshall, F. E. 1984, Ap. J., 281, 570.

Pravdo, S. H., and Serlemitsos, P. J. 1981, Ap. J., 246, 484.

Pringle, J. E. 1981, Ann. Rev. Astron. Astrophys., 19, 137.

Raymond, J. C. 1984, Ann. Rev. Astron. Astrophys., 22, 75.

Raymond, J. C., and Smith, B. W. 1977, Ap. J. Suppl., 35, 419.

Rees, M. J. 1978, Nature, 275, 516.

Rees, M. J. 1984, Ann. Rev. Astron. Astrophys., 22, 471.

Reichert, G. A., Mason, K. O., Thorstensen, J. R., and Bowyer, S. 1982,
    Ap. J., 260, 437.

Remillard, R. A., and Canizares, C. R. 1984, Ap. J., 278, 761.

Ricker, G. R., Bautz, M. W., Dewey, D., and Meyer, S. S. 1981,
    Solid State Imagers for Astronomy, Proc. Soc. Photo-Opt
    Instrum. Eng., 290, 190.

Ricketts, M. J. 1978, M.N.R.A.S., 183, 51p.

Rieke, G. H. 1978, Ap. J., 226, 550.

Robinson, E. L. 1976, Ann. Rev. Astron. Astrophys., 14, 119.

Rossi, B., and Staub, H. 1949, Ionization Chambers and Counters
    (New York: McGraw-Hill).

Rothschild, R. E., et al. 1981, Ap. J., 250, 723.

Rybicki, G. B., and Lightman, A. P. 1979, Radiative Processes in
    Astrophysics (New York: Wiley).

Schmelz, J. T., Feigelson, E. D., and Schwartz, D. A. 1984, Bull. Amer.
    Astron. Soc., 16, 472.

Schmidt, M. 1968, Ap. J., 151, 393.

Schmidt, M., and Green, R. F. 1983, Ap. J., 269, 352.

Schwartz, D. A., Bradt, H., Buckley, D., Patterson, J., Remillard, R.,
    Roberts, W., and Tuohy, I. 1985, Proc. of COSPAR meeting, X-ray
    Astronomy, J. Bleeker and P. A. J. deKorte, eds. (Oxford:
    Pergammon Press), in press.

Schwartz, D. A., Doxsey, R. E., Griffiths, R. E., Johnston, M. D.,
    and Schwarz, J. 1979, Ap. J. (Letters), 229, L53.

Schwartz, D. A., Garcia, M., Ralph, E., Doxsey, R. E., Johnston,
    M. D., Lawrence, A., McHardy, and I. M., Pye, J. P. 1981,
    M.N.R.A.S., 196, 95.

Schwartz, D. A., Gursky, H., Schwarz, J., Bradt, H. V. , and Doxsey, R.
    E. 1978, Nature, 275, 517.

Schwartz, D. A., and Ku, W. H. M. 1983, Ap. J., 266, 459.

Schwartz, D. A., Schwarz, J., Gursky, H., Bradt, H., and Doxsey, R. E.
    1978, Proc. AIAA 16th Aerospace Science Conference, p. 78.

Schwartz, D. A. et al. 1980, Ap. J. (Letters), 238, L53.

Seaton, M. J. 1979, M.N.R.A.S., 187, 73p.

Shapiro, S. L., and Lightman, A. P. 1976, Ap. J., 204, 555.

Shectman, S. A., and Hiltner, W. A. 1976, P.A.S.P., 88, 960.

Simkin, S. M., Su, H. J., and Schwarz, M. P. 1980, Ap. J., 237, 404.

Skinner, G. K. 1980, Nature, 288, 141.

Soifer, B. T. et al. 1984, Ap. J. (Letters), 283, L1.

Staubert, R., Kendziorra, E., Pietsch, W., Reppin, C., Trumper, J.,
    and Voges, W. 1978, Ap. J. (Letters), 225, L113.

Stein, W. A., O'Dell, S. L., and Strittmatter, P. A. 1976, Ann. Rev.
    Astron. Astrophys., 14, 173.

Stein, W. A., and Weedman, D. A. 1976, Ap. J., 205, 44.

Steiner, J. E. 1981, Ap. J., 250, 469.

Steiner, J. E., Schwartz, D. A., Jablonski, F. J., Busko, I. C.,
    Watson, M. G., Pye, J. P., and McHardy, I. M. 1981, Ap. J.
    (Letters), 249, L21.

Steinle, H., Voges, W., Pietsch, W., Reppin, C., Trumper, J.,
    Kendziorra, E., and Staubert, R. 1982, Astron. Astrophys.,
    107, 350.

Stocke, J. T., Liebert, J., Gioia, I. M., Griffiths, R. E., Maccacaro,
    T., Danziger, I. J., Kunth, D., and Lub, J. 1983, Ap. J., 273, 458.

Stocke, J. T., Liebert, J., Maccacaro, T., Griffiths, R. E., and Steiner,
    J. E. 1982, Ap. J., 252, 69.

Stone, R. P. S. 1977, Ap. J., 218, 767.

Strittmatter, P. A., Serkowski, K., Carswell, R., Stein, W. A.,
    Merrill, K. M., and Burbridge, E. M. 1972, Ap. J. (Letters),
    175, L7.

Strittmatter, P. A., and Williams, R. E. 1976, Ann. Rev. Astron. Astrophys., 14, 307.

Swanenburg, B. N. et al. 1981, Ap. J. (Letters), 243, L69.

Tananbaum, H., Peters, G., Forman, W., Giacconi, R., Jones, C., and Avni, Y. 1978, Ap. J., 223, 74.

Thorstensen, J. R., Charles, P., Bowyer, S., Briel, U. G., Doxsey, R. E., Griffiths, R., and Schwartz, D., 1979, Ap. J. (Letters), 233, L57.

Toor, A., and Seward, F. D. 1974, Astron. J., 79, 995.

Tucker, W. H. 1975, Radiation Processes in Astrophysics (Cambridge: The MIT Press).

Tucker, W. H. 1983, Ap. J., 271, 531.

Tuohy, I. R., Mason, K. O., Garmire, G. P., and Lamb, F. K. 1981, Ap. J., 245, 183.

Ulmer, M. P., Brown, R. L., Schwartz, D. A., Patterson, J., and Cruddace, R. G. 1983, Ap. J. (Letters), 270, L1.

Ulrich, M. H., Kinman, T. D., Lynds, C. R., Rieke, G. H., and Ekers, R. D. 1975, Ap. J., 198, 261.

Uomoto, A. 1984, Ap. J., 284, 497.

Urry, C. M., Mushotzky, R. F. 1982, Ap. J., 253, 38.

Urry, C. M., Mushotzky, R. F., Kondo, Y., Hackney, K. R. H., and Hackney, R. L. 1982, Ap. J., 261, 12.

Vaiana, G. S. et al. 1981, Ap. J., 244, 163.

Wall, J. V., Shimmins, A. J., and Merkelijn, J. K. 1971, Aust. J. Phys. Ap. Suppl., 19, 68.

Walter, F. M., Bowyer, S., Mason, K. O., Clarke, J. T., Henry, J. P., Halpern, J., and Grindlay, J. E. 1982, Ap. J. (Letters), 253, L67.

Walter, F. M., Cash, W., Charles, P. A., and Bowyer, C. S. 1980, Ap. J., 236, 212.

Warwick, R. S. et al. 1981, M.N.R.A.S., 197, 865.

Weedman, S. 1977, Ann. Rev. Astron. Astrophys., 15, 69.

Weisskopf, M. C., Silver, E. H., Kestenbaum, H. L., Long, K. S., and Novick, R. 1978, Ap. J. (Letters), 220, L117.

Weistrop, D., Shaffer, D. B., Mushotzky, R. F., Reitsema, H. J., and Smith, B. A. 1981, Ap. J., 249, 3.

Weistrop, D., Shaffer, D. B., Reitsema, H. J., and Smith, B. A. 1983, Ap. J., 271, 471.

Weistrop, D., Smith, B. A., and Reitsema, H. J. 1979, Ap. J., 233, 504.

Weymann, R. J., Carswell, R. F., and Smith, M. G. 1981, Ann. Rev. Astron. Astrophys., 19, 41.

Weymann, R. J., Williams, R. E., Beaver, E. A., and Miller, J. S. 1977, Ap. J., 213, 619.

White, N. E., Fabian, A. C., and Mushotzky, R. F. 1983, ESLAB Preprint 83/64.

White, N. E., and Holt, S. S. 1982, Ap. J., 257, 318.

Wickramasinghe, D. T., Visvanathan, N., and Tuohy, I. R. 1984, Ap. J., 286, 328.

Wilkes, B. J. 1985, Ap. J. (Letters), 288, L1.

Williams, G. 1983, Ap. J., 53, 523.

Willis, A. J. et al. 1980, Ap. J., 237, 596.

Winkler, P. F., Canizares, C. R., Clark, G. W., Markert, T. H., Kalata, K., Schnopper, H. W. 1981, Ap. J. (Letters), 246, L27.

Wood, K. et al. 1984, Ap. J. Suppl., 56, 507.

Worrall, D. M., Boldt, E. A., Holt, S. S., Mushotzky, R. F., and Serlemitsos, P. J. 1981, Ap. J., 243, 53.

Wright, A. E., Savage, A., and Bolton, J. G. 1977, Aust. J. of Phys. Ap. Suppl., 41, 1.

Wyckoff, S., Wehinger, P. A., and Gehren, T. 1981, Ap. J., 247, 750.

Zamorani, G. et al. 1981, Ap. J., 245, 357.

Zuckermman, B., and Palmer, P. 1974, Ann. Rev. Astron. Astrophys., 12, 279.

RONALD ALAN REMILLARD .

Personal Data

Permanent Address: 157 West Brookline St. #3, Boston, MA 02118
Date of Birth: April 13, 1952
Place of Birth: Woonsocket, Rhode Island

Education:

Mass. Inst. of Technology	S.M. Physics, 1981
Univ. of Calif., Berkeley	A.B. Physics/Astron. 1976
Univ. of Calif., Berkeley	A.B. Philosophy 1974

Present Position:

1983- present   Graduate student, M.I.T.

Past Positions:

1981-1983   Research staff, M.I.T. Center for Space Research
1977-1981   Graduate Student - Research Assistant, M.I.T.

Publications:

"Optical Sudies of the Seyfert 2 X-ray Galaxy NGC 2110", J. E.
McClintock, J. van Paradijs, R. A. Remillard, C. R. Canizares, A. T.
Koski, and P. Veron., Ap. J. 233, 809 (1979).

"The Discovery of an O Subdwarf in the Globular Cluster NGC 6712", R. A.
Remillard, C. R. Canizares, and J. E. McClintock, Ap. J. 240, 109
(1980).

"The X-ray and Optical Outburst of Aquila X-1 (4U1908+00)", P. A.
Charles, J. R. Thorstensen, S. Bowyer, G. W. Clark, F. K. Li, J. van
Paradijs, R. A. Remillard, S. S. Holt, L. J. Kaluzienski, V. T.
Junkkarinen, R. C. Puetter, H. E. Smith, G. S. Pollard, P. W.
Sanford, S. Tapia, and F. J. Vrba, Ap. J. 237, 154 (1980).

"A UBV Photometric Study of the 5.2 Hour X-ray Binary 4U2129+47", J. E.
McClintock, R. A. Remillard, and B. Margon, Ap. J. 243, 900 (1981).

"H0323+022: A Puzzling High-Latitude X-ray/Optical/Radio Source" R. E.
Doxsey, H. Bradt, J. E. McClintock, L. Petro, R. A. Remillard, G.
R. Ricker, D. A. Schwartz, and K. Wood, Ap. J. (Letters) 264, 143
(1983).

"The 1980 Outburst of 4U0115+63 (V635 Cas)", G. A. Kriss, L. R. Cominsky, R. A. Remillard, G. Williams, and J. R. Thorstensen, Ap. J. 266, 806 (1983).

"Periodic Variability of the X-ray Nova A0620-00 in Quiescence", J. E. McClintock, L. D. Petro, R. A. Remillard, and G. R. Ricker, Ap. J. (Letters) 266, 806 (1983).

"Discovery of a Massive Unseen Star in LMC X-3", A. P. Cowley, D. Crampton, J. B. Hutchings, R. A. Remillard, and J. E. Penfold, Ap. J. 272, 118 (1983).

"SAS-3 Observations of Cygnus X-1: The Intensity Dips", R. A. Remillard and C. R, Canizares, Ap. J. 278, 761 (1984).

"An Optical Reddening Study to Determine the Distance to Cygnus X-2", J. E. McClintock, L. D. Petro, G. Hammerschlag-Hensberge, C. R. Proffitt, and R. A. Remillard, Ap. J. 283, 794 (1984).

"A Comparison of the Continuum Spectra of Four Comets", R. A. Remillard and D. C. Jewitt, (submitted to Icarus March, 1985).

"The Discovery of Eight Bright Active Galactic Nuclei Observed with the HEAO-1 Scanning Modulation Collimator", R. A. Remillard, H. V. Bradt, D. Buckley, W. Roberts, D. A. Schwartz, I. R. Tuohy, and K. Wood, (submitted to the Astrophysical Journal April, 1985).

Talks

"Discovery of a Hot Subdwarf in the Globular Cluster NGC 6712", Bull. Amer. Astron. Soc. 11, 473 (1979).

"Identification of Southern X-ray Sources with the HEAO-1 Scanning Modulation Collimator", Bull. Amer. Astron. Soc. 14, 891 (1983).